Front. Mech. Eng. 2023, 18(4): 53
https://doi.org/10.1007/s11465-023-0769-8

REVIEW ARTICLE

Nanoparticle-enhanced coolants in machining: mechanism, application, and prospects

Shuguo HU[a], Changhe LI (✉)[a], Zongming ZHOU[b], Bo LIU[c], Yanbin ZHANG[a], Min YANG[a], Benkai LI[a], Teng GAO[a], Mingzheng LIU[a], Xin CUI[a], Xiaoming WANG[a], Wenhao XU[a], Y. S. DAMBATTA[a,d], Runze LI[e], Shubham SHARMA[a,f]

[a] *School of Mechanical and Automotive Engineering, Qingdao University of Technology, Qingdao 266520, China*
[b] *Hanneng (Qingdao) Lubrication Technology Co., Ltd., Qingdao 266100, China*
[c] *Sichuan New Aviation TA Technology Co., Ltd., Shifang 618400, China*
[d] *Mechanical Engineering Department, Ahmadu Bello University, Zaria 810106, Nigeria*
[e] *Massachusetts Institute of Technology, Cambridge, MA 02139, USA*
[f] *Department of Mechanical Engineering, IK Gujral Punjab Technical University, Punjab 144603, India*

✉ *Corresponding author. E-mail: sy_lichanghe@163.com (Changhe LI)*

ABSTRACT Nanoparticle-enhanced coolants (NPECs) are increasingly used in minimum quantity lubrication (MQL) machining as a green lubricant to replace conventional cutting fluids to meet the urgent need for carbon emissions and achieve sustainable manufacturing. However, the thermophysical properties of NPEC during processing remain unclear, making it difficult to provide precise guidance and selection principles for industrial applications. Therefore, this paper reviews the action mechanism, processing properties, and future development directions of NPEC. First, the laws of influence of nano-enhanced phases and base fluids on the processing performance are revealed, and the dispersion stabilization mechanism of NPEC in the preparation process is elaborated. Then, the unique molecular structure and physical properties of NPECs are combined to elucidate their unique mechanisms of heat transfer, penetration, and anti-friction effects. Furthermore, the effect of NPECs is investigated on the basis of their excellent lubricating and cooling properties by comprehensively and quantitatively evaluating the material removal characteristics during machining in turning, milling, and grinding applications. Results showed that turning of Ti–6Al–4V with multi-walled carbon nanotube NPECs with a volume fraction of 0.2% resulted in a 34% reduction in tool wear, an average decrease in cutting force of 28%, and a 7% decrease in surface roughness *Ra*, compared with the conventional flood process. Finally, research gaps and future directions for further applications of NPECs in the industry are presented.

KEYWORDS nanoparticle-enhanced coolant, minimum quantity lubrication, biolubricant, thermophysical properties, turning, milling, grinding

1 Introduction

With the rapid development of manufacturing in today's world, the mechanical properties of core components have become increasingly stringent requirements in aerospace, military, medical, and infrastructure fields. New materials with high strength, toughness, high-temperature resistance, and other characteristics have emerged to meet the needs of the core component use [1–3]. However, in addition to the excellent properties of these materials, an element with poor processability also exists. Therefore, these materials, such as titanium alloys, nickel-based alloys, and high-strength steels, are called difficult-to-machine materials.

In the metal cutting process, choosing the right cutting fluid can improve the cooling and lubrication performance, further reduce the friction in the machining process, and thus improve tool life, machining efficiency, and surface quality. Currently, the common approach of using cutting fluid in the machining process is still flooding, and the use of flooding cutting fluid accounts for 7%–18% of the total cost of the machining process [4–6]. Moreover, traditional flooded metalworking fluids are usually made from nonrenewable mineral oils and

Received August 11, 2023; accepted October 1, 2023

scarce water resources. Mineral oils are toxic and nondegradable, and the splashing of cutting fluids during the machining process generates and triggers a variety of respiratory illnesses, which pose a threat to the health of workers. Simultaneously, the use of metalworking fluids easily causes environmental pollution; thus, the subsequent processing requirements have become strict. However, this approach is not in line with the current green manufacturing concept of sustainable development. The sustainable transformation and upgrading of the traditional manufacturing industry is imminent [7,8]. Dry machining in the 1990s has gained increasing attention. Dry machining refers to the absence of the use of cutting fluid; as a clean and environmentally friendly process, the use of cutting fluid, which reduces the cost of processing, has been gradually promoted. However, this machining process is characterized by high demands on machine rigidity and accuracy as well as machining parameters, and the lack of cutting fluid leads to severe friction at the tool–workpiece interface and heat buildup, which does not ensure geometric tolerances and surface integrity of the part [9]. Near dry machining, minimum quantity lubrication (MQL) is a green cooling lubrication method in which a small amount of lubricating medium is atomized by a gas at a certain pressure into micron-sized droplets delivered to the tool–workpiece contact interface [10–12]. MQL is between the dry and flood types; compared to flooding, the droplets flow faster and more efficiently under high-pressure gas, which reduces costs, and dry machining provides some cooling and lubrication, which improves machining quality [13–18]. In addition, the lubricating medium is typically a vegetable oil that has nontoxic, renewable, and biodegradable advantages, hence the name biolubricant. However, numerous studies have revealed that biolubricants suffer from insufficient cooling capacity due to their poor extreme pressure properties, such as high viscosity. Particularly in the case of difficult-to-machine materials, the high temperatures and pressures generated in the cutting zone make it impossible for biolubricants to meet the heat transfer and antiwear properties of machining, thereby limiting their application [19,20]. Nanoparticle-enhanced coolants (NPECs) have been widely used as new cooling and lubricating media in electronic microchannels, engines, spacecraft, nuclear energy, and solar energy [21]. NPECs are obtained by adding nano-enhanced phases to base oils (vegetable oils) via certain ultrasonic vibration, mechanical mixing, and the addition of dispersants. Thus, NPEC is an efficient and clean cooling and lubrication method that overcomes the insufficient heat exchange capacity and poor extreme pressure performance of MQL technology. Figure 1 shows the development route of the NPEC.

The presence of nano-enhanced phases not only efficiently enhances the heat transfer properties but also reduces the tribological behavior of the tool–workpiece interface. Therefore, the heat source is effectively limited during machining, heat is further reduced, and surface quality is substantially improved. NPECs have considerable application potential in new industrialized green cutting technologies. Based on a Web of Science literature search and a metrological analysis of the literature in this field from 2013 to 2022, the results show that the number of publications on NPECs is increasing annually (Fig. 1). Some representative review papers that argue in terms of mechanism, device, technology, and application are available in these publications. For example, Sharma et al. [22] compared the effectiveness of the application of conventional cutting fluids and NPECs. They later reviewed the effect of using NPECs in MQL-related methods for commonly used materials in turning, milling, drilling, and grinding [23]. Sidik et al. [24], Said et al. [25], and Singh et al. [17] provided further summaries. Sen et al. [26] demonstrated the advanced performance of ecofriendly NPEC cutting fluids. Wickramasinghe et al. [27] focused on the sustainable application of vegetable oil-based NPEC in machining process optimization, whereas Wang et al. [28] reviewed the application of vegetable oil-based NPEC trace lubrication in turning. Chinchanikar et al. [29] examined the thermophysical properties and applications of NPECs. Kulkarni and Chinchanikar [30] assessed the research progress of NPECs for machining nickel-based high-temperature alloys with minimal lubrication. Baldin et al. [31], Zhang et al. [32], Liu et al. [33], and Cui et al. [34] have also made remarkable contributions. These scholars have reviewed MQL versus conventional flooding and NPEC trace lubrication machining performance. However, the thermophysical properties of NPECs, such as infiltration, film formation, cooling, and lubrication occurrences during processing, as well as the effects of molecular structures and physicochemical properties, remain unclear. This phenomenon limits the ability of technicians to parameterize the NPEC micro-lubricated cutting process and restricts the development of this highly promising field of clean and precision manufacturing. This paper reveals the stabilization mechanism of NPEC and the advanced film-forming and heat-transfer mechanisms based on the technical understanding of NPEC to fill this literature gap and provide a scientific foundation. Comprehensive quantitative assessments of material removal characteristics during machining in turning, milling, and grinding applications and investigations on the effect of NPEC are also conducted. This article is committed to providing a scientific basis and theoretical foundation for the further development of this technology and promoting its practical industrial application. Figure 2 shows the research roadmap of the article.

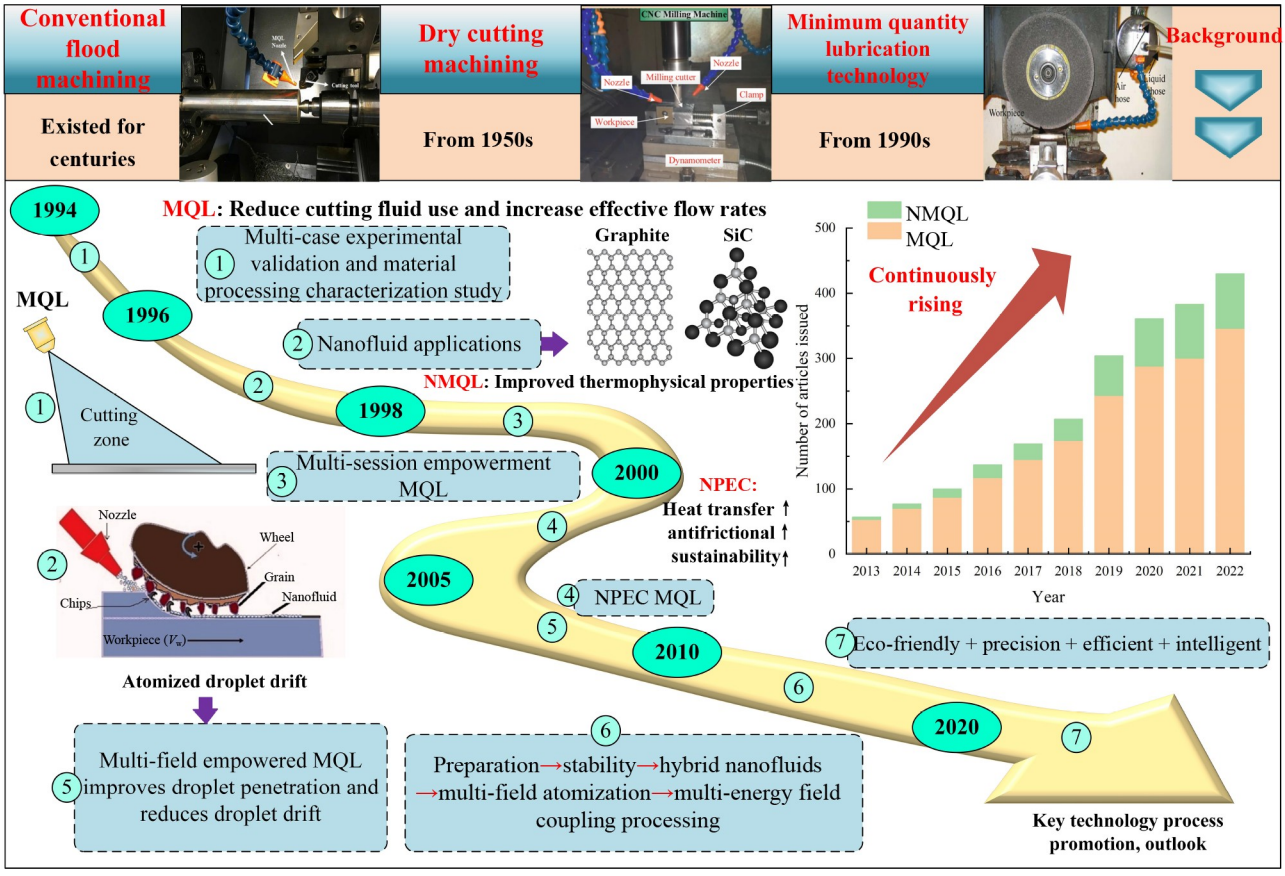

Fig. 1 Development history of nanoparticle-enhanced coolants (NPECs). MQL: minimum quantity lubrication; NMQL: nanofluid minimum quantity lubrication.

2 Nanoparticle-enhanced coolants

The performance of NPECs during machining is influenced by the physical properties of the nano-enhanced phase, the type of base fluid, the preparation method, and the dispersion stabilization. This section briefly reviews the commonly used base fluids and nano-enhanced phases for MQL, reveals the mechanism of action of the molecular structure cooling and lubricating properties of vegetable oils and nano-enhanced phases, and examines the commonly used NPEC preparation methods. The main challenge of NPECs lies in their poor stability. This section concludes by describing the kinetic behavior and dispersion-stabilizing mechanism of nano-enhanced phases in NPECs.

2.1 Base fluids

In the preparation of NPECs, water and oil are excellent base fluids for dispersing nano-enhanced phases. However, a large difference in the effect of the two base fluids is observed in the process. Oil-based NPECs have the advantage of ensuring lubrication, whereas water-based NPECs increase the availability of machinists because water is readily available and inexpensive. Kumar et al. [35] found that the use of water-based alumina NPEC can replace conventional cutting fluids in the micromachining of Ti–6Al–4V. Mao et al. [36] analyzed water- and oil-based fluids using NPEC and found that water-based fluids have poorer lubrication properties than oil-based fluids but demonstrate superior cooling. In addition, water-based NPECs are unsuitable for machining rusty parts. However, water-based NPECs alone cannot meet the lubrication requirements of strong friction interfaces [37]. Najiha et al. [38] showed that the cutting of aluminum alloy materials can be achieved using water-based NPECs. Compared with traditional oil-based trace lubrication, water-based NPECs have excellent heat dissipation performance but technical drawbacks of insufficient lubrication.

NPEC oil-based fluids typically contain vegetable, mixed vegetable, and mineral oils. Traditional mineral oil-based cutting fluids are widely used. However, the toxicity of the oil mist emitted due to elevated temperatures in the machining process has a considerable impact on the ecological environment and the health of workers. The application of vegetable oil cutting fluids in MQL did not reduce the machining quality compared with that of mineral oil cutting fluids [39]. Yıldırım et al. [40] investigated the machining performance of vegetable

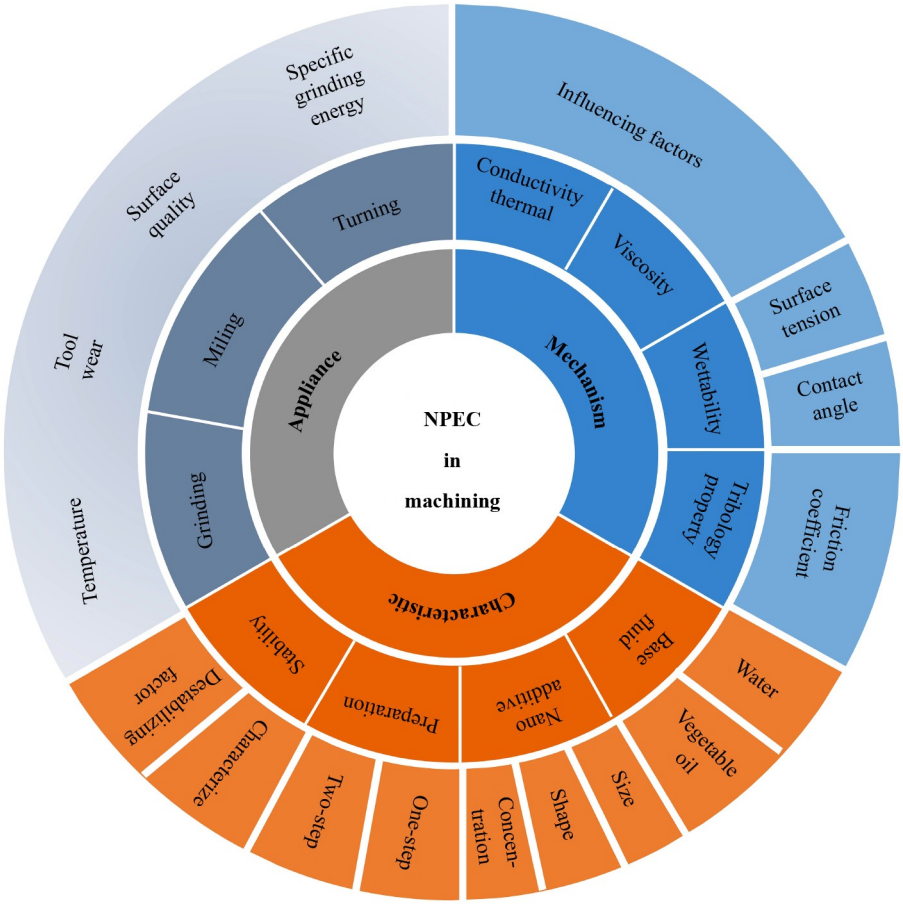

Fig. 2 Article logic.

oil-based biolubricants compared with conventional mineral oil micro-lubrication for milling high-temperature nickel-based alloys and found that vegetable oil-based cutting fluids have higher tool life and lower cutting forces than mineral oils. In addition, from the perspective of environmental protection, vegetable oil is considered an environmentally friendly biolubricant due to its degradability and sustainable processing [41]. As a renewable resource, the application of vegetable oil in machining avoids the negative impact on the environment and is an important direction for sustainable development [42].

Sustainable cutting fluids, such as vegetable oils and water, are often referred to as biolubricants. As biolubricants, vegetable oils can simultaneously be lubricating, degradable, and environmentally friendly. These oils have all the necessary properties of a lubricant, including a high viscosity index, low volatility, and good lubricity. As cooling media in MQL, vegetable oils can reduce cutting fluid consumption by more than 90% and have made progress in their application in general material cutting [43–45]. Xavior and Adithan [46] used coconut oil, emulsion, and pure cutting oil immiscible with water as cutting fluids for cutting operations on AISI 304 steel using carbide tools. The results of the study showed that coconut oil performed better than the two other cutting fluids in reducing tool wear and improving surface finish, mainly due to its thermal and oxidative stability. Khan et al. [47] conducted an experimental study on the turning performance of an AISI 9310 material using vegetable oil-based cutting fluid as the MQL base fluid. The results showed a direct relationship between the cutting speed, feed rate, and cutting temperature. Compared with dry and wet machining, the use of vegetable oil MQL-assisted machining reduced surface roughness, tool wear, and cutting temperature. This reduction is mainly attributed to the decrease in wear and damage to the tool tip and the favorable chip–tool interactions due to the application of MQL, which eliminates the formation of traces of uniformly built-up edges (BUEs).

However, Table 1 [48] shows considerable differences in lubrication properties among vegetable oils and large performance gaps in machining. For example, Ojolo et al. [49] investigated the effect of vegetable oils (i.e., peanut, palm kernel oil, shear butter, and coconut oil) on cutting forces during the machining of mild steel, copper, and aluminum. The experimental results showed that palm kernel and peanut oils were the best choices for reducing cutting forces. Wang et al. [48] used the nickel-based

Table 1 Machinability of common vegetable oils when grinding nickel-based alloys [48], reproduced with permission from Elsevier

Base oil	Friction coefficient	Specific grinding energy/(J·mm^{-3})	G-ratio
Pure soybean oil	0.41	91.02	26.50
Pure peanut oil	0.45	98.62	22.92
Pure maize oil	0.34	80.90	29.15
Pure rapeseed oil	0.39	80.94	29.13
Pure palm oil	0.33	78.85	28.63
Pure castor oil	0.30	73.47	26.89
Pure sunflower oil	0.36	86.54	28.19

alloy GH4169 as the workpiece material and seven vegetable oils as the base oils to experimentally evaluate the tribological properties of the grinding wheel–workpiece interface. The lubricating properties of these vegetable oils were generally evaluated in terms of abrasive force, specific abrasive energy, coefficient of friction (COF), abrasive ratio, and surface morphology. Based on the experimental results, the lubricating properties were ranked as follows: corn oil < canola oil < soybean oil < sunflower oil < peanut oil < palm oil < castor oil.

The differences in processing properties between different vegetable oils are due to their molecular structures, as shown in Fig. 3. Singh et al. [50] observed the effect of the molecular structure of vegetable oils on their tribological properties through microanalysis. They found that the type of fatty acid affects the tribological properties and that sunflower oil is prone to autoxidation due to its high content of polyunsaturated fatty acids (linolenic and linoleic acids). By contrast, rapeseed and olive oils with high a content of monounsaturated (oleic) fatty acids are less susceptible to oxidation. Therefore, the poor oxidative stability of sunflower oil leads to reduced tribological properties compared with the two other types of vegetable oils. In addition, Dong et al. [51] and Liu et al. [39] found that when vegetable oils were processed as MQL base oils, their fatty acid contents affected the processing performance. Zhang et al. [32] systematically summarized the main parameters affecting the properties of vegetable oils. Natural vegetable oils comprise a variety of saturated and unsaturated fatty acids, which can be classified according to the length of the carbon chain, number of C=C, and polar groups. Among them, oils containing large amounts of unsaturated fatty acids (soybean, rapeseed, sunflower, and sesame oils) exhibit a good balance between cooling and lubrication. However, their strength and the susceptibility of the C=C bonds to oxidation result in poor thermal stability. By contrast, oils with high saturated fatty acid contents have higher viscosities and superior lubricating properties. The absence of C=C bonds results in large load-carrying capacities in the cutting zone. However, high viscosity is not conducive to effective heat transfer and dissipation, which can cause heat buildup in the cutting zone and affect machined surface quality. In addition, polar atoms or groups, which can produce strong physical adsorption, create a saponification effect with the metal surface and form a chemical oil film to improve the machining performance.

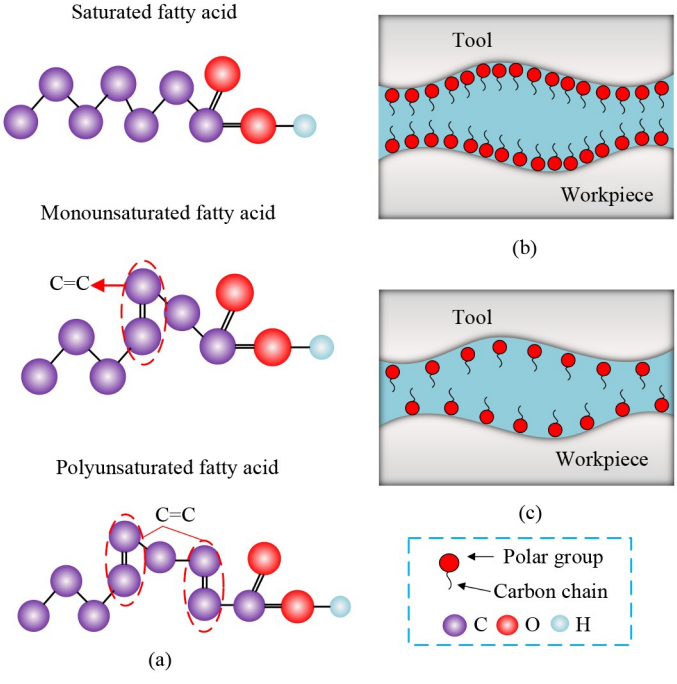

Fig. 3 Lubrication structure diagram: (a) three-dimensional fatty acid structure, (b) saturated fatty acid processing, and (c) unsaturated fatty acid processing.

However, the easy oxidization property of vegetable oils limits their application in the industry. Scholars have attempted to improve the shortcomings of single vegetable oils by blending them to achieve a balance between cooling and lubricating properties. Guo et al. [52] used castor oil blended with six vegetable oils (1:1) for grinding and machining the nickel-based alloy GH4169. Their experimental results showed that the combined lubricating properties of the soybean–castor oil blend were better than those of castor oil and exhibited the best lubricating properties, reducing the specific tangential and specific normal grinding forces by 27.03% and 23.15%, respectively, and obtaining the best surface quality compared with castor oil. In another study, they also analyzed the mixed vegetable oil at a volume ratio of 1:2 and found that the mixed base oil has relatively less ricinoleic and unsaturated fatty acid components and relatively more saturated fatty acid components, and the oil film formed during the grinding process is relatively dense, which provides superior antiwear performance [53]. Jia et al. [54] conducted similar experiments and showed that soybean–castor blended base oil provided the best lubrication and that the addition of soybean oil improved the fluidity, atomization, heat exchange, and wetting properties of castor oil.

The addition of extreme pressure additives is also another way to improve the antioxidant properties of vegetable oils. Ozcelik et al. [55] conducted comparative experiments by adding different ratios of extreme pressure additives to sunflower oil, rapeseed oil, and traditional cutting fluids. The best surface quality was obtained for canola oil and 8% extreme pressure additive during processing. Sani et al. [56] added phosphorus and ammonia particles to vegetable oil to configure a new cutting fluid and compared it with conventional cutting fluids. Their experimental results showed that the new vegetable oil cutting fluid has superior tribological properties. Padmini et al. [57] added MoS_2 as an extreme pressure additive to three vegetable-based oils (coconut, sesame, and rapeseed) for turning AISI 1040 steel and compared their properties. They found that coconut oil had the best processing performance with the addition of MoS_2 nano-enhanced phases, and tool wear was reduced by 31.58% compared with canola oil. The nano-enhanced phase can be used as an extreme-pressure anti-wear agent due to its good extreme-pressure antiwear and green and environmentally friendly characteristics. Thus, this agent is an ideal substitute for traditional extreme-pressure antiwear agents. Therefore, the addition of chemical extreme pressure additives according to the processing needs is an option.

Overall, the selection of a suitable lubricant base oil should be preceded by an evaluation of the cooling and lubrication needs of the processing conditions. Oil-based NPECs are mainly used to regulate interfacial friction, whereas water-based NPECs are the opposite. Thus, the base oils of oil-based biolubricants should prioritize environmentally friendly and renewable plant-based lubricants. Vegetable oil biolubricants are easy to oxidize due to their fatty acids and polar groups, which improves the lubricity of the process. However, the modification of vegetable oils can help improve their shortcomings; for example, a combination of characteristics of vegetable oil blends and the addition of extreme pressure additives can enhance the physical properties of vegetable oil biolubricants.

2.2 Nano-enhanced phases

Biolubricants have exceptional lubricating film-forming properties, but the grinding process for difficult-to-machine materials can easily lead to lubricating film failure, and the performance of biolubricants can be substantially limited [58]. Thus, the nano-enhanced phase is an effective way to solve the above difficulties, and the incorporation of this phase considerably improves the extreme-pressure performance of pure vegetable oils. Therefore, the synergistic effect of the two can be effectively utilized. The surface effect of nano-enhanced phases is shown in Fig. 4. In addition, nano-enhanced phases can reduce the degree of friction in the cutting zone, uniformly withstand compressive forces, improve heat dissipation, and reduce stress concentrations. When milling TC4 steel using graphene-based NPEC, Li et al. [59] demonstrated that graphene (GNP) flakes enhanced the cooling and lubricating properties of the fluid film formed in the cutting region. When turning Ti–6Al–4V with a textured carbide tool, Singh et al. [50] found that GNP NPEC reduced COF by 39%. During the milling of Al6061-T6, the application of an enhanced coolant based on MoS_2 [60] and SiO_2 [61] nano-enhanced phases improves the tribological properties of the tool–workpiece–chip and reduces the cutting forces and temperatures due to the nano-enhanced phase rolling action, leading to superior surface quality of the workpiece. Paturi et al. [62] found that after turning Inconel 718, the surface quality of the workpiece was improved by approximately 35% with the addition of 0.5 wt.% of tungsten disulfide (WS_2) NPEC compared with pure MQL (PMQL). Yıldırım et al. [63,64] increased tool life by 105.9% compared with dry cutting after machining nickel-based high-temperature alloys using hexagonal boron nitride (HBN) NPEC with a mass fraction of 0.5 wt.%. The effect of NPECs is influenced by the type, size, shape, and concentration of the nano-enhanced phases. Scholars have conducted numerous experimental studies on the above variables.

1) Shapes

Minor differences in the roles of different shapes of nano-enhanced phases are observed. Table 2 shows the commonly used nano-enhanced phases. Stratiform structure nano-enhanced phases produce laminar exfoliation

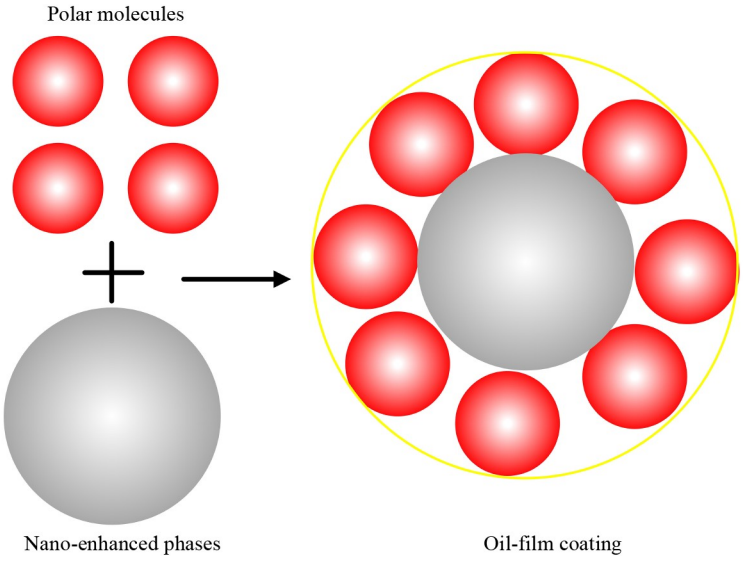

Fig. 4 Schematic of nano-enhanced phases surface effect.

Table 2 Commonly used nano-enhanced phases for machining

Categories	Nano-enhanced phases
Spherical nano-enhanced phases	Al_2O_3, SiO_2, ZrO_2, SiC, ND
Threadiness nano-enhanced phases	CuO_2, MnO_2, TiO_2, ZnO, CNTs
Stratiform nano-enhanced phases	CBN, GNP, MoO_3, HBN, MoS_2

Notes: CBN, cubic boron nitride; ND, diamond.

during friction, extrusion, and shear. For stratiform nano-enhanced phases, Tevet et al. [65] conducted tribological characterization of nano-enhanced phases with different structures and found their rolling, sliding, and exfoliation behaviors under boundary lubrication conditions. This characterization can improve the machined surface quality and reduce cutting forces and temperatures. HBN has weak van der Waals forces between the molecular layers due to its structure, which reduces friction by sliding through these molecular layers against each other during machining [66]. In addition, GNPs have the advantages of high thermal conductivity and strength, making them the most promising material for cooling and lubrication. However, GNP is restricted by its high price. For spherical nano-enhanced phases, Musavi et al. [67] found that spherical copper oxide NPEC in A286 high-temperature alloy turning machining has superior lubrication performance, which resulted in improved surface quality because the spherical nano-enhanced phases remained in a steady state during the process. Therefore, the friction and wear behavior of the tool–workpiece–chip interface could be improved by increasing the sphericity of the nano-enhanced phases. In addition, nano-enhanced phases provide rolling and surface repair and increase lubricant viscosity. Kao and Lin [68] investigated TiO_2 nanoparticle-reinforced coolant and found that the near-spherical nano-enhanced phase reduced rolling resistance. Therefore, spherical nano-enhanced phases are suitable for tribological and lubrication applications and are highly desirable for mechanical manufacturing processes. Threadiness nano-enhanced phases are also widely used in NPECs due to their excellent thermal conductivity, which can markedly reduce the temperature during processing. However, the unavoidable agglomeration of NPECs during their use reduces their tribological properties in the machining region.

2) Size

NPECs are colloids of particles that are at least less than 100 nm in dimension with a base solvent, and the nano-enhanced phases offer the following advantages over conventional oil emulsion suspensions used for heat dissipation. i) High specific surface area yields effective heat transfer performance. ii) Brownian motion in the NPEC allows for a more stable dispersion of the nano-enhanced phases with less clogging compared with conventional fluid particles. iii) Wettability, concentration, and thermal conductivity can be adjusted by varying the concentrations of NPECs [69]. Small nano-enhanced phases have been previously proposed to provide a smooth surface under NPEC trace lubrication conditions [70]. However, some scholars have discovered experimental phenomena that contradict these conclusions. Dubey et al. [71] used two different particle sizes in the formulation of NPECs for turning and machining AISI 304 steel. Their experimental results showed that the experimental values of surface roughness obtained for the 40 nm diameter were lower for the 40- and 30-nm diameter Al_2O_3 NPEC conditions. Khajehzadeh et al. [72] investigated the turning of AISI 4140 hardened steel with TiO_2 NPEC and showed that the average reduction in tool back face wear decreased from 46.2% to 34.8% as the size of the nano-enhanced phases increased from 10 to 50 nm. Similarly, Lee et al. [73] investigated the machining

performance of NPEC airflow-assisted electrostatic atomization lubricated titanium alloy micro-grinding. The results showed that large nanodiamond particles (80 nm) were highly favorable for obtaining low surface roughness values to fully explore the mapping relationship between the cutting and grinding properties and nano-enhanced phases. Nano-enhanced phases with large sizes can be selected in conjunction with high-viscosity vegetable oil biolubricants to address the unfavorable size effect of nano-enhanced phases in NPEC MQL processing and reduce this effect [74].

Therefore, the mechanism of action of different sizes of nano-enhanced phases at the friction interface is also different, and the scale of the roughness peak at the friction interface should be considered. In the case of a large cutting dosage, the large size of the nano-enhanced phases should be first considered when reducing the machining process parameters, such as the cutting force. Meanwhile, in the case of finishing, the use of small nano-enhanced phases is recommended when ensuring the surface integrity of the parts and tool life. Simultaneously, combining different sizes of nano-enhanced phases with base oils of corresponding viscosities can improve the machining quality.

3) Concentration

Nano-enhanced phases lead to superior results in vegetable oil biolubricants; however, the gain effect is also affected by the concentration. Mao et al. [36] found that the lubrication and cooling properties in the abrasive zone improved as the concentration of nano-enhanced phases increased. Talib et al. [75] found that HBN particles provided a lubricating film in Fig. 5, which reduced friction and prevented wear. However, the remaining particles in the rough valleys restricted the movement of nearby particles as the HBN concentration increased, resulting in large forces that led to frictional wear. Additional damage areas are formed when 0.1 and 0.5 wt.% HBN particles slide along the contact surface, which leads to abrasive wear. Thus, 0.05 wt.% HBN particles are the optimal concentration. Agglomeration occurs when the concentration of NPEC exceeds certain conditions, subsequently affecting the stability of the NPEC and leading to deterioration of the processing quality.

Pal et al. [76] prepared NPEC with different concentrations (0.5, 1.0, and 1.5 wt.%) by mixing Al_2O_3 nano-enhanced phases with sunflower oil. The results showed that compared with the flood condition, the optimal concentration of 1.5 wt.% reduced thrust, torque, surface roughness, and drill tip temperature by 44%, 67%, 56%, and 26%, respectively, at the 30th hole. In addition, different concentrations lead to viscosity variations of the NPEC. The thin lubrication film formed by low viscosity cannot withstand the stress from the extra loading of particles, which increases friction and damages the sliding surfaces [77]. Sen et al. [78] found that the maximum viscosity was reached at 3% Al_2O_3 concentration with superior lubricating properties. However, the nano-enhanced phases can agglomerate and affect the thermal conductivity of the Al_2O_3 nano-enhanced phases in palm oil. The concentration of the nano-enhanced phases has a direct relationship with the contact angle, which decreases sharply with increasing NPEC concentration when the wetting area increases. However, the contact angle also increases further when a certain concentration is exceeded because the excess nano-enhanced phases aggregate and then deposit after losing dynamic stability. Therefore, the wettability of the NPEC decreases with excessive concentration, and the surface quality of the workpiece deteriorates [79].

The results of numerous studies have shown that optimal concentration values exist and produce optimal effects with the application of different nano-enhanced phase processes. Modulation of the NPEC performance can be achieved by optimizing the concentration of the nano-enhanced phases. Overall, the shape, size, and concentration of the nano-enhanced phases will affect the machining performance. The good or poor machining performance is the result of their joint action, and no complete parameter is available for the nano-enhanced phases. Therefore, future exploration should further optimize the parameters of the nano-enhanced phases to provide a complete parameter for the processing of different workpiece materials.

2.3 Preparation

The preparation of the NPEC is the most important step in the experimental study, that is, “combining” the base fluid with the nano-enhanced phases. The preparation

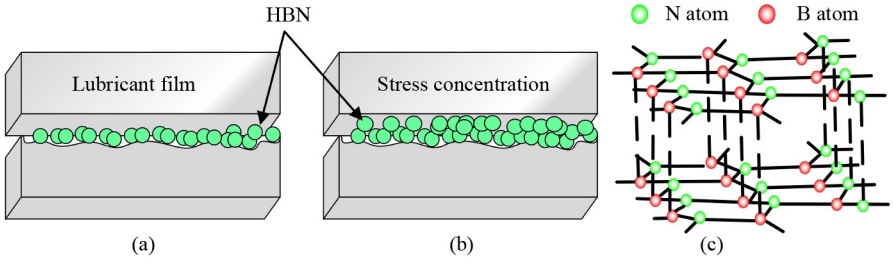

Fig. 5 (a) Lubricating film, (b) frictional wear, (c) molecular structure of the hexagonal boron nitride (HBN).

stage is crucial for enhancing the thermophysical properties of NPECs. Therefore, fine preparation is required to avoid chemical changes, agglomeration, and the inhomogeneous suspension of nano-enhanced phases. The two main methods of synthesizing NPECs are as follows: one-step and two-step.

Physical (e.g., vapor deposition, laser ablation, and ultrasound-assisted submerged arc) and chemical (via reducing agents) methods are commonly used in a one-step process. Simultaneous preparation and dispersion of nano-enhanced phases in the base fluid prevent oxidation of the nano-enhanced phases, disperse them homogeneously, enhance stability, and avoid storage, drying, and NPEC transportation in the process, which reduces agglomeration and thus improves stability [80].

The two-step preparation involves the preparation and dispersion of nano-enhanced phases into the base fluid [81]. First, nano-enhanced phases are prepared via vapor deposition, chemical reduction, or mechanical milling and then dispersed into the base liquid via the mechanical dispersion method, ultrasonication, and addition of dispersants [82–85]. The mechanical dispersion method distributes nano-enhanced phases in the liquid medium using external mechanical energy such as shear or collision force, ball milling, mechanical stirring, and other methods. The ultrasonic dispersion method places the NPEC directly in the ultrasonic field and uses ultrasonic waves of suitable frequency to facilitate the movement of the nano-enhanced phases. This approach overcomes the mutual attraction between the nano-enhanced phases and destroys the equilibrium between the original particles as well as between the particles and molecules of the substrate, dispersing the nano-enhanced phases into the substrate liquid. Mechanical dispersion and sonication disrupt the original kinetic behavior of the nano-enhanced phases (van der Waals and Brownian forces) and reduce the interactions between the nano-enhanced phases. The addition of the dispersant increases the repulsive force between the nano-enhanced phases; a greater repulsive force between the particles than the attractive force prevents the agglomeration between the nano-enhanced phases to improve stability. Figure 6 shows the two-step method used to prepare NPECs.

Overall, the one- and two-step methods have advantages and disadvantages. The one-step method has the advantage of good dispersion and high suspension stability but suffers from the limitations of high cost and difficulty in controlling the size of nano-enhanced phases. Thus, this method is only applicable to low-pressure base fluids. The two-step method is the most cost-effective method for obtaining superior particle size control and is suitable for mass production. However, these steps are highly complex and require additional time and experimental equipment. In specific applications, choosing the appropriate preparation method according to different experimental requirements and the use of NPEC conditions is necessary. Thus, a two-step method should be used in the field of machining to prepare NPECs.

2.4 Stability

NPECs are complex mixtures of nano-enhanced phases and biolubricants. They tend to aggregate due to their high surface activity, and the lack of suspension stability leads to increased cluster formation and deposition rates. Agglomeration causes the nano-enhanced phases to settle and clog the nozzles, thus reducing the thermophysical properties of the NPEC. The stability of NPEC depends on the properties of the nano-enhanced phases, the type of base fluid, the preparation method, and the subsequent treatment [86]. Therefore, the stability of NPECs should be carefully considered.

2.4.1 Destabilizing factors

Microscopically, NPECs belong to the liquid–solid two-phase system. Thus, a distinct phase interface exists between the liquid molecules and the nano-enhanced phases, and a buoyant force of the base liquid is observed on the particles. Brownian motion of nano-enhanced phases refers to the irregular way in which microscopic particles move in liquids or gases due to the thermal motion of molecules [87]. The nano-enhanced phases are small and light; thus, their Brownian motion is fast, enabling their distribution over a large area in a short time. The nano-enhanced phases in the base fluid are in

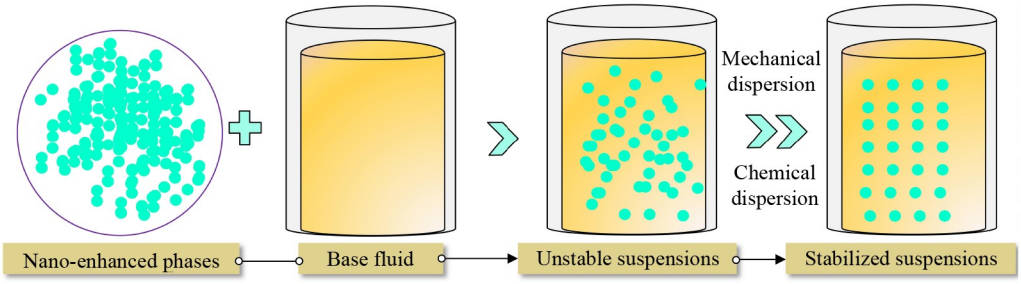

Fig. 6 Two-step preparation.

irregular motion and are thus subjected to Brownian forces. Van der Waals force potential exists for mutual attraction. Numerous atoms between neighboring particles are attracted to each other due to their large percentages on the surface of nano-enhanced phases; therefore, van der Waals forces emerge between particles. This force varies according to the distance between two particles; it usually increases as the distance decreases and is directly related to the geometry, size, and surface properties of the particles. Van der Waals gravity and electric double-layer repulsion depend on the size of the nano-enhanced phases. Numerous atoms are present on the particle surface when the particle size is small [21], which increases the density of active sites. Agglomeration occurs when van der Waals attraction exceeds electric double-layer repulsion. Several researchers have reported that NPECs are less stable at high particle concentrations [88,89]. The increase in particle concentration results in large particle cluster sizes, which is due to low interparticle distances and increased van der Waals gravity, directly affecting the settling velocity. In addition, the nano-enhanced phases have gravity. Under the joint action of these forces, the metal particles are prone to collision, agglomeration, and settlement. Therefore, NPECs should reduce the frequency and efficiency of collision to minimize the impact of agglomerates and maintain good stability.

2.4.2 Stability strategies

NPECs are usually treated using physical or chemical methods to achieve stability. Physical methods aim to disperse the nano-enhanced phases in the liquid medium using external mechanical energy, such as shear or collision force, which destroys the original kinetic behavior of the nano-enhanced phases and reduces the interaction between nano-enhanced phases. Chemical methods change the surface properties of suspended nano-enhanced phases and inhibit the formation of particle clusters to obtain a stable suspension.

Commonly used physical stabilization methods include mechanical mixing and ultrasonic treatment. The device is shown in Fig. 7. Mechanical stirrers are important tools for promoting NPEC stability. Mansour et al. [90] homogeneously dispersed TiO_2 nano-enhanced phases in base oil using a magnetic stirring process. However, the stabilization time of NPECs obtained by mechanical stirring is short. Ultrasonication is one of the methods

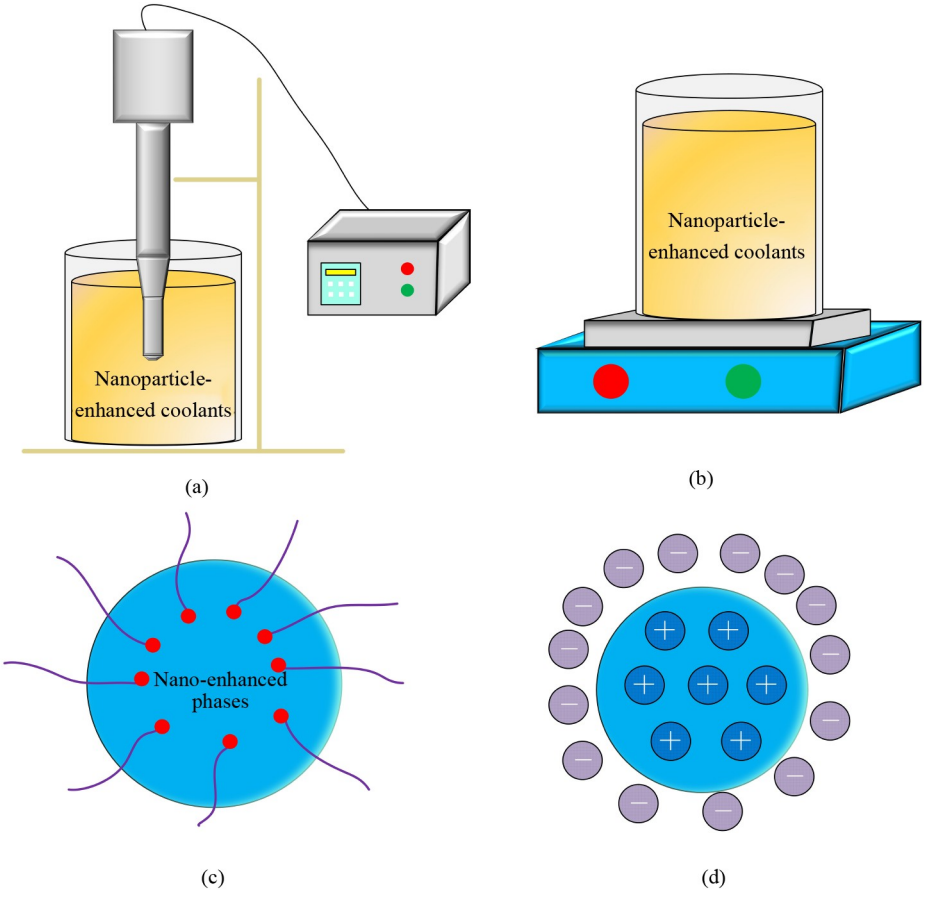

Fig. 7 Physical and chemical stabilization of nanoparticle-enhanced coolant device: (a) ultrasonication, (b) mechanical stirrer, (c) steric stabilization, and (d) electrosteric stabilization.

used to improve the stability of NPECs and shows better stability than magnetic stirring. Ultrasonication places the NPEC directly into the ultrasonic field and uses ultrasonic waves of suitable frequency to facilitate the movement of nano-enhanced phases. Therefore, this method overcomes the mutual attraction between the nano-enhanced phases and destroys the balance between the original particles as well as between the particles and molecules of the base liquid, dispersing the nano-enhanced phases into the base liquid. Nguyen et al. [91] reported the effectiveness of sonication for the production of monodispersed Al_2O_3 by ultrasonication at 30% amplitude for 500 s. The size of the nano-enhanced phase clusters was reduced from 230 to 130 nm. Sadeghi et al. [92] also used ultrasonication and found that the cluster size of nano-enhanced phases decreased with increasing ultrasonication time within 150 min. Stability was verified using ζ potential and dynamic light scattering. In addition, sonication improves stability; however, excessive sonication leads to shortening of the carbon nanotube (CNT) length, and optimized sonication is necessary to prevent such defects [93]. Elsheikh et al. [94] added CuO nano-enhanced phases to rice bran vegetable oil at a volume concentration of 1 vol.% and stirred the mixture under a magnetic stirrer for 4 min. The prepared solution was then sonicated for 2 h using an ultrasonic generator to ensure uniform dispersion. Therefore, the results reveal the optimal ultrasonic treatment time for each NPEC. However, no accurate range of treatment times exists for enhanced coolants of different nano-enhanced phases to obtain NPECs with the desired optimum properties. Multiple physical methods can be used to synergize the treatment to disperse the NPEC and obtain improved processing properties.

The influence of the nature of the nano-enhanced phases (hydrophilic or hydrophobic) should be considered during the selection of the base fluid, which is either polar or nonpolar. Hydrophilic nano-enhanced phases such as metal oxide particles (CuO, SiO_2, and Al_2O_3) are readily dispersed in polar solvents such as water, whereas hydrophobic nano-enhanced phases (CNT, GNP) are readily dispersed in nonpolar base fluids. In these cases, the use of additional stabilizers is no longer necessary because the stability can be sufficiently improved using physical methods. However, different chemical stabilization techniques are required to form stable NPECs by mixing hydrophilic nano-enhanced phases in nonpolar solvents or hydrophobic nano-enhanced phases in polar solvents. Figure 7 shows the chemical stabilization methods, which include electrostatic stabilization (surfactants and covalent surface functional groups) and spatial stabilization (ionic polymers or ionic liquids).

The electrostatic stabilization technique is mainly based on providing a surface charge to the particles. Ion adsorption creates a double electric layer around the nano-enhanced phases, and electrostatic stabilization is achieved when electrostatic repulsive forces play a dominant role and balance the van der Waals attraction between two similarly charged particles. Surfactants with different charges are added to the NPEC suspension to improve electrostatic stability [95]. Table 3 shows common surfactants, where the amphoteric surfactant includes cationic and anionic hydrophilic groups that can form cations and anions based on the pH of the medium. Mao et al. [96] found that NPEC containing sodium dodecylbenzene sulfonate (SDBS) surfactant prevented the aggregation of nano-enhanced phases and significantly improved the cutting performance. However, supersaturated adsorption on the surface of nano-enhanced phases occurred when the SDBS concentration exceeded 0.5 wt.%, at which point the suspension stability of the NPEC deteriorated with increasing SDBS concentration [67]. Behera et al. [97] investigated the diffusion behavior of Al_2O_3 NPEC with different surfactants on WC tools and Inconel 718 workpieces. Their results showed that the optimum wetting behavior was observed when nonionic surfactant was added to NPEC, and the lowest COF, tool wear, and radius of chip curl were obtained in Inconel 718 machining. Shukla et al. [98] investigated the effect of MoO_3 NPEC mixed with six different surfactants on the properties of turned AISI 304 steel. The optimum mixing ratio and volumetric concentration were obtained from ζ-potential and thermal conductivity tests, respectively. The results showed that SPAN20 surfactant provided the best processing performance at a mixing ratio of 3:2 and 0.45 vol.%. The average cutting force and tool wear were significantly reduced by 32.05% and 53%, respectively, with a minimum surface roughness of 1.21 μm. Şirin et al. [99] used sodium dodecyl sulfate (SDS) and gum arabic (GA) as surfactants added to a hybrid NPEC to improve the homogeneity by decreasing the surface tension, thus enhancing the thermal conductivity.

However, the exact type of surfactant to be added has not been specifically demonstrated, while most surfactants (SDBS, SDS, GA, cetyltrimethylammonium bromide (CTAB), and polyvinylpyrrolidone) are organic

Table 3 Surfactants commonly used in machining

Type	Surfactant
Nonionic	Alkylphenol ethoxylates, octyl phenol ethoxylate, polyvinylpyrrolidone
Cationic	Sodium dodecyl sulfate, sodium dodecylbenzene sulfonate, sodium oleate
Anionic	Gum arabica, dodecyl trimethyl ammonium bromide, cetyltrimethylammonium bromide, cetyltrimethylammonium chloride
Hermaphroditic	Lecithin, hydroxy sulfobetaine

in nature and have some biodegradability issues. These surfactants may deteriorate over time due to biological activity and operating conditions. Therefore, the stability of surfactants may be a major challenge when considering long-term applications. Spatial stabilization of NPECs can be achieved using nonionic surfactants and polymers. This stabilization technique involves noncovalent functionalization [100]. Spatial stabilization can stabilize NPECs with high particle concentrations, but electrostatic stabilization cannot. Furthermore, this stabilizing effect cannot be predicted using the ζ-potential method because the polymer does not affect the charge of the nano-enhanced phases. Currently existing limitations include the sensitivity of spatial stability to temperature changes, stabilizer concentrations, and absorption spectra.

Overall, the plant-based oil, molecular movement, and external factors of NPECs affect their stability. The selection and preparation methods for NPEC should consider their application properties and stability. A broad study of hybrid stabilization methods, that is, a combination of different physical and chemical methods, is needed to improve the stability of NPECs under different operating conditions. The above methods of stability enhancement can help improve the availability of NPECs in additional applications.

3 Thermophysical properties

NPECs are widely used in machining applications due to their excellent cooling and lubricating properties. In the last decade, exponential growth in scientific research on NPECs has been observed. However, the properties of NPECs vary depending on their production, particle size, dispersion, and concentration [101]. The presence of nano-enhanced phases modifies the thermal conductivity, viscosity, and wettability of the base fluid and can produce a lubricating film at the processing interface [102]. This lubricant film acts differently at the machining interface. In some cases, the nano-enhanced phases fill microcracks and pores, act by rolling between surfaces, and cause the surface to be polished during the formation process, thus improving surface integrity [61, 103–105]. This section focuses on the thermophysical properties of NPECs, such as their thermal conductivity, viscosity, wettability, and tribological properties.

3.1 Thermal conductivity

NPECs are widely used because of their excellent thermal properties, and their thermal conductivity reflects the heat transfer capability of NPECs in machining. Previous studies found that the addition of nano-enhanced phases to the base fluid can further improve heat transfer because solid media typically have better heat transfer properties than liquids. Titanium alloys are commonly used in the manufacture of aerospace structural components; however, they have become a current research hotspot due to their high strength and low thermal conductivity. One study found that at 0.1 wt.% volume fraction of GNP, the addition of GNP can further reduce the grinding temperature by approximately 21.1% compared with biolubricants [106]. The results show that nano-enhanced phases are crucial in difficult-to-machine materials. The excellent lubricating properties of NPECs can reduce the degree of friction and temperature in the cutting zone. The main heat transfer mechanism of NPECs in the cutting zone can be analyzed from two perspectives. i) A thermal boundary layer, including laminar and turbulent thermal boundary layers, is formed during heat transfer in the cutting zone, and the laminar thermal boundary layer mainly serves for heat transfer. NPECs may cause thermal damage to the workpiece due to heat accumulation in the turbulent layer and lowering its viscosity facilitates heat transfer, as shown in Fig. 8. ii) Mao et al. [96] proposed four stages of boiling heat transfer in a lubricating medium as a function of temperature: non-boiling heat transfer, nucleation boiling, transition boiling, and stable film boiling. In the nucleation boiling region, the heat transfer coefficient increases rapidly with temperature and reaches a maximum when the critical heat flow density is reached. An extremely high surface temperature can lead to liquid film boiling and bubble generation, which further accelerates the heat transfer. As shown in Fig. 8, the binding of nano-enhanced phases results in the formation of an adsorption layer around them, and the presence of this layer reduces the thermal resistance between the interior of the droplets, which, in turn, facilitates heat transfer [107]. In addition, the nano-enhanced phases in the NPEC have irregular diffusion and Brownian motion, and they will adsorb the surrounding biolubricant to form a fluid adsorption layer, which can eliminate part of the heat in contact with the workpiece and enhance the heat transfer between the workpiece and the NPEC.

Therefore, the study of the thermal conductivity of NPECs is of considerable importance for processing performance. The nature of the base fluid, concentration of nano-enhanced phases, particle size, shape, and temperature affect the thermal conductivity of NPECs. The transient hot-wire technique is highly accurate and stable and is commonly used to measure the thermal conductivity of NPECs.

3.1.1 Effect of temperature and concentration

The addition of nano-enhanced phases to the base fluid increases the thermal conductivity of the NPEC. Furthermore, increasing the solid concentration and temperature of the nano-enhanced phases similarly affects the thermal conductivity of NPECs. Figure 9 [50,108–110]

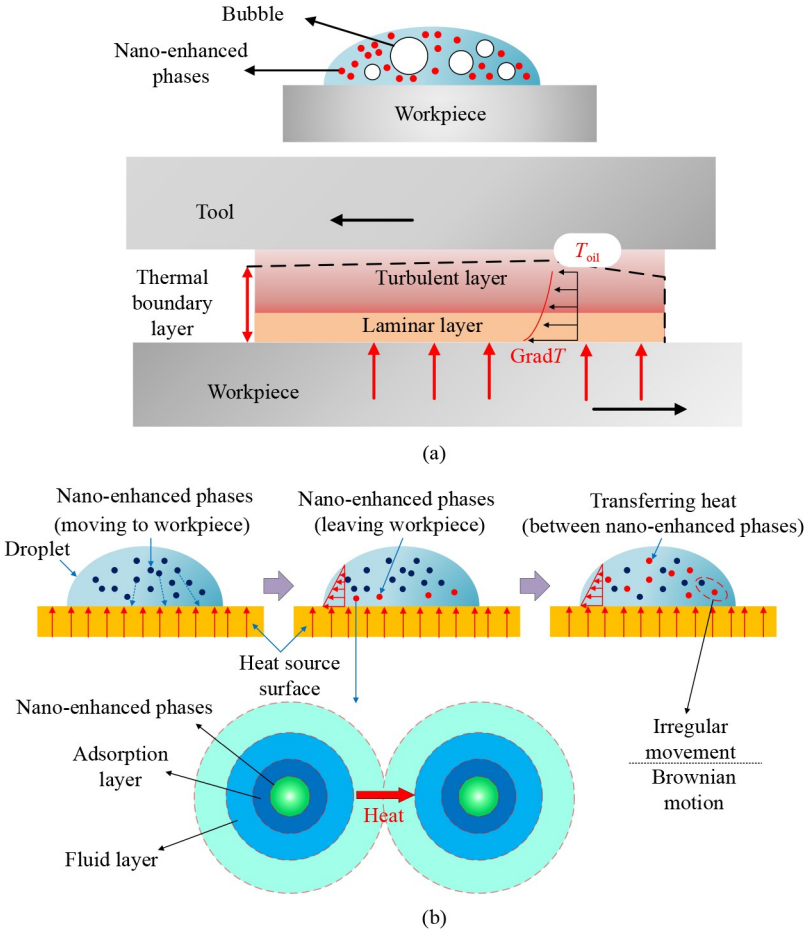

Fig. 8 Heat transfer mechanism of nanoparticle-enhanced coolants: (a) boiling heat transfer, (b) heat transfer motion of nano-enhanced phases.

shows the variation of NPECs with temperature and thermal conductivity. Ramya et al. [111] investigated the relationship between the thermal conductivity and temperature of enhanced coolants containing ZnO nano-enhanced phases and found that the thermal conductivity increases with temperature. This finding was also demonstrated by Duangtongsuk and Wongwises [112] in their experimental study of the thermal conductivity of TiO_2 NPECs with volume concentrations of 0.2–2 vol.%. Figure 9(a) shows the thermal conductivity variation of six concentrations of GNP nanosheets as a function of test temperature, where the NPEC thermal conductivity further increases with temperature, regardless of the concentration [108]. Kole and Dey [113] explored the effect of temperature and nano-enhanced phase concentration on thermal conductivity. The results showed that 2.5 vol.% of CuO nano-enhanced phases increased the thermal conductivity of the base fluid by 10.4% at room temperature and 11.9% at 80 °C. Saeedinia et al. [114] investigated the thermal conductivity of CuO NPECs with particle weight fractions of 0.2–2 wt.% at different temperatures. The results showed that the thermal conductivity increased with the addition of nano-enhanced phases to the base fluid and further increased with particle concentration. The best thermal conductivity was observed at a volume fraction of 2% with an increase of 6.2%. As shown in Fig. 9(c), the thermal conductivity of all three NPECs was enhanced as the GNP concentration increased from 0 to 2.5 wt.%. The 0.5, 1, 1.5, 2, and 2.5 wt.% concentrations of GNP resulted in 3.6%, 7.2%, 10.8%, 14.4%, and 18% enhancements in the thermal conductivity of the base canola oil [50]. Wang et al. [115] investigated the effect of temperature and solid concentration on the thermal conductivity of graphite NPEC. They found that the addition of graphite with a volume fraction of 1.36 vol.% to the base fluid increased the thermal conductivity by 36%.

First, the thermal conductivity increases with concentration and temperature, probably because the NPEC reduces the agglomeration of nano-enhanced phases with increasing temperature, thus raising the homogeneity of NPEC in the mixture and the thermal conductivity. Second, the thermal conductivity of the nano-enhanced phases is substantially larger than that of the base fluid, leading to an increase in the thermal conductivity with the nano-enhanced phases. In addition, the random motion of

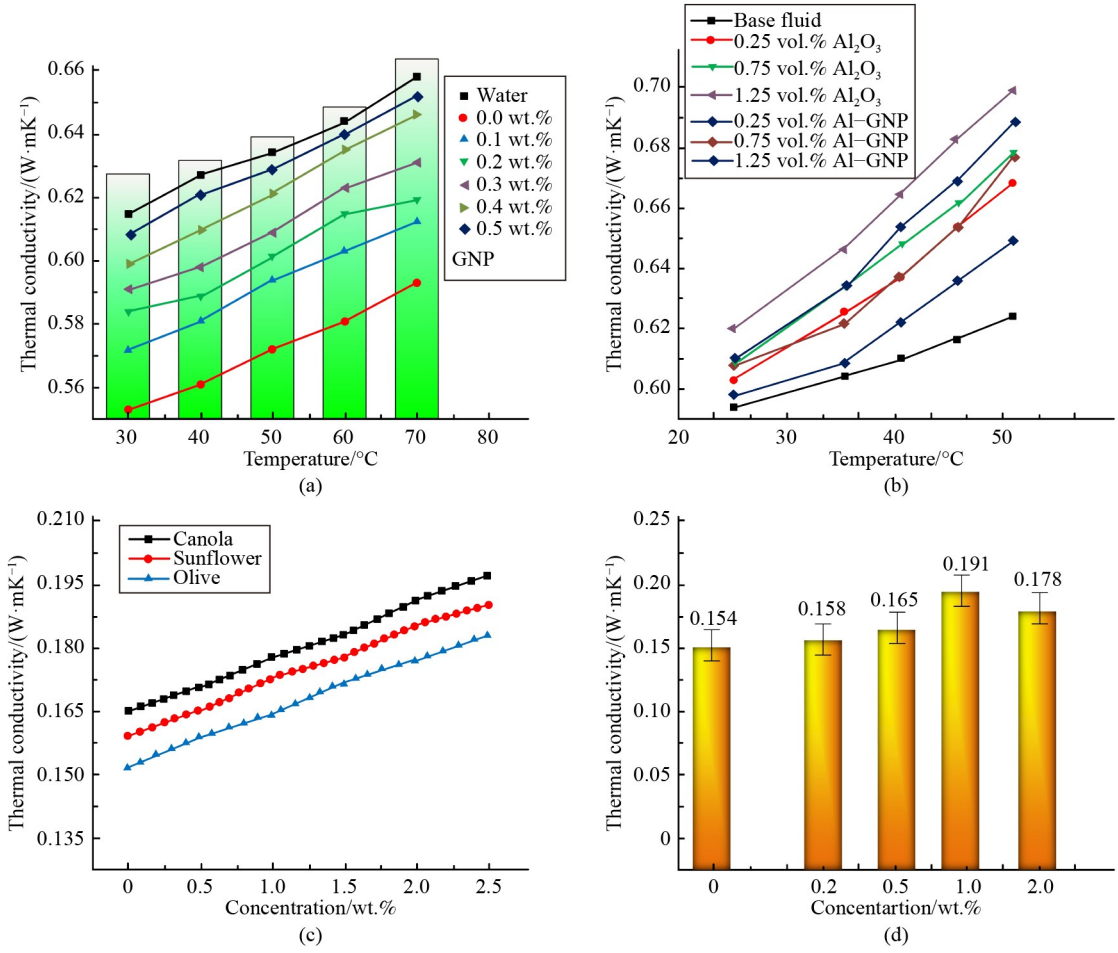

Fig. 9 Thermal conductivity as a function of temperature and concentration: (a) variation of graphene (GNP) nanoparticle-enhanced coolants (NPECs) thermal conductivity with temperature; (b) variation of thermal conductivity of Al_2O_3 and Al–GNP NPEC with temperature [109]; (c) variation of GNP thermal conductivity with concentration in three different base oils [50]; (d) variation of thermal conductivity of GNP with concentration [110]. Reproduced with permissions from Refs. [50,109,110] from Elsevier.

the nano-enhanced phases increases with temperature; therefore, energy is rapidly transferred inside the fluid. The Brownian motion and aggregation of the nano-enhanced phases are affected by temperature changes and show variations in the thermal conductivity of the NPEC.

3.1.2 Influence of other factors

In addition to temperature and nano-enhanced phase concentration as factors influencing the thermal conductivity of NPECs, the size, shape, and type of nano-enhanced phases also affect the thermal conductivity of NPECs.

1) Size

The size of the nano-enhanced phases also affects the thermal conductivity of NPECs [116]. Researchers investigated the effect of particle size variation (5–100 nm) on the thermal conductivity of synthesized NPECs. Sharifpur et al. [117] prepared Al_2O_3 NPECs of various sizes (31, 55, and 134 nm diameter) and found that a low diameter leads to a superior degree of thermal conductivity enhancement. Teng et al. [118] dispersed nano-enhanced phases of different nominal diameters (20, 50, and 100 nm) into NPECs of four different concentrations (0.5, 1, 1.5, and 2 wt.%). The results show a correlation between small-sized nano-enhanced phases and high temperatures; a small diameter leads to improved thermal conductivity. This phenomenon is attributed to the enhancement of Brownian diffusion at small nano-enhanced phase sizes [119]. Xie et al. [120] measured the thermal conductivity of four different particle sizes of NPECs. The current study found that instead of high thermal conductivity due to the small particle size, the thermal conductivity is a result of the combined effect of Brownian diffusion and its surface area.

Therefore, the size of the nano-enhanced phases affects the thermal conductivity of the NPEC. Small nano-enhanced phases lead to high surface areas and weak van der Waals forces, resulting in low agglomeration and improved stability. This phenomenon increases the

thermal conductivity of the NPEC; however, its size should not be too small. The results suggest that the diameters of nano-enhanced phases between 20 and 40 nm are optimal for thermal conductivity.

2) Shapes

The shape of nano-enhanced phases is a crucial parameter that affects the thermal conductivity of NPECs because the surface area to volume ratio (A/V) of these phases affects the thermal conductivity of NPECs. Wei et al. [121] found that NPECs with rod-like particles exhibit superior thermal conductivity due to their larger A/V compared with spherical nano-enhanced phases. Maheshwary et al. [122] investigated the thermal conductivity of NPECs with various nano-enhanced phase shapes (spherical, cylindrical, and cubic). Regarding the three types of nano-enhanced phases, cubic has the best heat transfer performance due to high A/V. Spherical nano-enhanced phases exhibit poor performance; however, their low fabrication cost and excellent tribological properties promote further applications in heat transfer.

3) Types

Different types of nano-enhanced phases may affect the thermal conductivity of NPECs. However, this parameter is not the only one that determines the thermal conductivity of NPECs [123–125]. The results show that TiO_2 NPECs exhibit high thermal conductivity based on the thermal conductivities of Al_2O_3, TiO_2, WO_3, and Fe NPECs [126]. Pang et al. [127] synthesized Al_2O_3 and SiO_2 NPEC with volume fraction of 0.005–0.5 vol.% in methanol. The results show that the thermal conductivity in SiO_2 NPEC is higher than that in other NPECs, probably because the agglomeration of Al_2O_3 nano-enhanced phase affects the stability, further influencing the thermal conductivity. Five types of NPECs were synthesized by adding nano-enhanced phases (TiO_2, ZnO, Al_2O_3, SiO_2, and MgO) to the ethylene glycol (EG)-based fluid, and the thermal conductivity was measured. Xie et al. [128] found that the thermal conductivity of the NPEC not only depended on the intrinsic thermal conductivity of the nano-enhanced phases but also necessitated considering a combination of influencing factors.

Overall, excellent thermal conductivity was obtained using exceptionally small sizes (average size of 20–40 nm) and relatively large surface areas and volume ratios in the nano-enhanced phases. In addition, the dispersion of nano-enhanced phases ($ZnO/GNP/Al_2O_3/CuO/TiO_2/MoS_2/SiO_2/Fe$) in the base fluid (water/vegetable oil) with approximately 1–5 wt.% increased the thermal conductivity of NPECs by 10%–30%. Incorporation of nano-enhanced phases improves the thermal conductivity of NPECs. However, their importance for sustainability and human health should be considered when using these phases for machining.

3.2 Viscosity

Viscosity is the flow resistance of the fluid. It is another important factor in the application of NPECs in heat transfer applications and has a direct effect on pressure loss and pumping power. Viscosity has a direct effect on the internal COF and influences the formation of the lubricant film. High-viscosity cutting fluids can form a lubricating film on high-temperature friction surfaces, increasing the load-carrying capacity and further improving the lubrication effect. As shown in Fig. 10, the different viscosity values of each vegetable oil are mainly due to its fatty acid molecular structure. At high viscosity, the friction conditions between the tool and the workpiece and those between the tool and the chip are improved. This trend is particularly evident in castor oil, which has a substantially higher viscosity than other base oils. Therefore, castor oil has a low COF [52]. The incorporation of nano-enhanced phases further increases the viscosity of the biolubricant and improves its lubricating properties. Cui et al. [129] investigated the tribological properties of GNP NPECs at the wheel–workpiece interface through frictional wear tests. GNP nano-enhanced phases have a large specific surface area, which improves the viscosity and lubrication properties of the

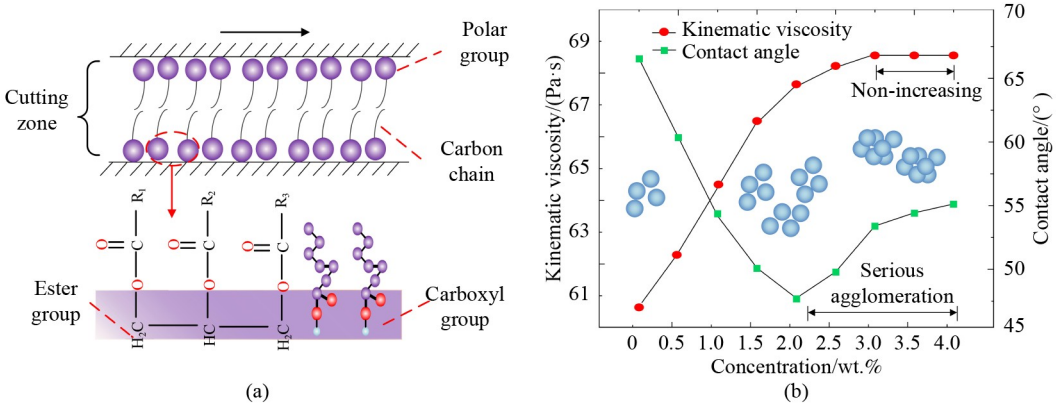

Fig. 10 (a) Vegetable oil cutting zone lubrication performance, (b) performance with different concentrations.

NPECs. Zhang et al. [130] suggested that the weak intermolecular shear strength of layered nano-enhanced phases in MoS_2 also reduces the friction in the cutting zone. The extreme pressure in the cutting zone extrudes the nano-enhanced phases out of the film to enhance the extreme pressure properties of the biolubricant [131]. As shown in Fig. 10(b), nano-enhanced phases with an appropriate volume fraction help in lubrication. However, as the concentration increases, aggregation occurs due to the strong van der Waals gravity of the molecules. The agglomerated nano-enhanced phases eventually lead to the cessation of oil droplet viscosity [132]. This phenomenon can be explained by the aggregation of nano-enhanced phases, which causes some degree of precipitation. In addition, the decrease in the number of effective active nano-enhanced phases in the droplets is unsuitable for mechanical processing.

Therefore, studying the viscosity of NPECs for processing performance is crucial. Various parameters affect the effective viscosity of NPECs, such as the viscosity of the base fluid, concentration of nano-enhanced phases, particle size, shape, and temperature. A piston rheometer, rotational rheometer, and capillary viscometer were used to determine the viscosity of the NPECs.

3.2.1 Effect of temperature and concentration

The temperature and solid concentration of NPECs are two important factors that affect viscosity. Many studies have shown that the addition of nano-enhanced phases increases the viscosity of the base fluid. In addition, the agglomeration behavior increases with the concentration of nano-enhanced phases, increasing the fluid viscosity [133]. Saeedi et al. [134] synthesized CeO_2 nano-enhanced phases in an EG to investigate the effect of nano-enhanced phase volume fractions (0.05–1.2 vol.%) on NPEC viscosity. Their results showed that viscosity was enhanced with an increase in the volume fraction. The viscosity of the 1.2 vol.% NPEC increased by 95% compared with that of the base fluid. Krishnakumar et al. [135] synthesized Al_2O_3-EG NPECs with volume fractions ranging from 0.1 to 1 vol.% and found that the viscosity increased with the volume fraction of NPECs.

Duangtongsuk and Wongwises [136] experimentally investigated the dynamic viscosity of NPECs. In this study, TiO_2 nano-enhanced phases dispersed in water with a volume concentration of 0.2–2 vol.% and a temperature range of 15–35 °C were used. The results show that the viscosity of the NPEC increases with particle concentration and decreases with increasing temperature of the NPEC [137]. Singh et al. [50] investigated the effect of temperature on the viscosity of GNP NPECs. Figure 11 [50,104,138,139] shows the relationship between the viscosity of NPECs and the temperature and concentration. As shown in Fig. 11(a), the dynamic viscosity decreases with the increase in temperature [104]. Soltani and Akbari [139] investigated the effect of temperature change on the dynamic viscosity of multi-walled carbon nanotube (MWCNT)–MgO hybrid NPECs. Increasing the temperature from 25 to 50 °C leads to a decrease in the dynamic viscosity of the NPEC by approximately 77%. Figure 11(c) shows the increase in viscosity of the NPEC with the addition of HBN, graphite, and MoS_2 [138]. This increase is proportional to the increase in nano-enhanced phases, which is attributed to the increase in the thickness of the fluid layer between the friction pair. Figure 11(d) shows the dynamic viscosity of MWCNT–MgO hybrid NPECs as a function of the nano-enhanced phase volume fraction at different temperatures. The viscosity of the hybrid NPEC increases with the nano-enhanced phase volume fraction at different temperatures with a similar trend [139].

Therefore, the viscosity of the NPEC decreases with increasing temperature, probably due to the effect of Brownian diffusion motion, particle cluster formation, and drag caused by the sliding motion of nano-enhanced phases and the underlying fluid, and the interaction between fluid molecules decreases with increasing temperature. Therefore, the temperature increases and the viscosity of the NPEC decreases. In addition, the formation of particle clusters and the high number of nano-enhanced phases impede the intermolecular motion when the concentration increases, thereby increasing the viscosity of the NPEC.

3.2.2 Influence of other factors

1) Size

The size of the nano-enhanced phases is an important parameter that affects the viscosity of NPECs. Several researchers have investigated the viscosity of NPECs based on the size of the nano-enhanced phases and have reported inconsistent and opposite results [141–147]. Hu et al. [142] synthesized NPECs with Al_2O_3 and ZnO nano-enhanced phases with particle sizes ranging from 20 to 100 nm. The viscosity of Al_2O_3 NPECs increased with particle size at a volume concentration of 7.5 vol.%. However, the trend was reversed after the particle size reached 50 nm at the same concentration. The viscosity increases with particle size at volume fractions higher than 7.5 vol.%. The viscosity of the ZnO NPEC tends to increase with particle size. The viscosity enhancement is negligible at low volume concentrations of the ZnO nano-enhanced phases. Minakov et al. [143] investigated the size effect of nano-enhanced phases on the viscosity of NPECs. The authors reported that the viscosity of all types of NPECs decreased with increasing particle size. Nithiyanantham et al. [145] studied the effect of SiO_2 particle size on the viscosity of NPECs. The results show

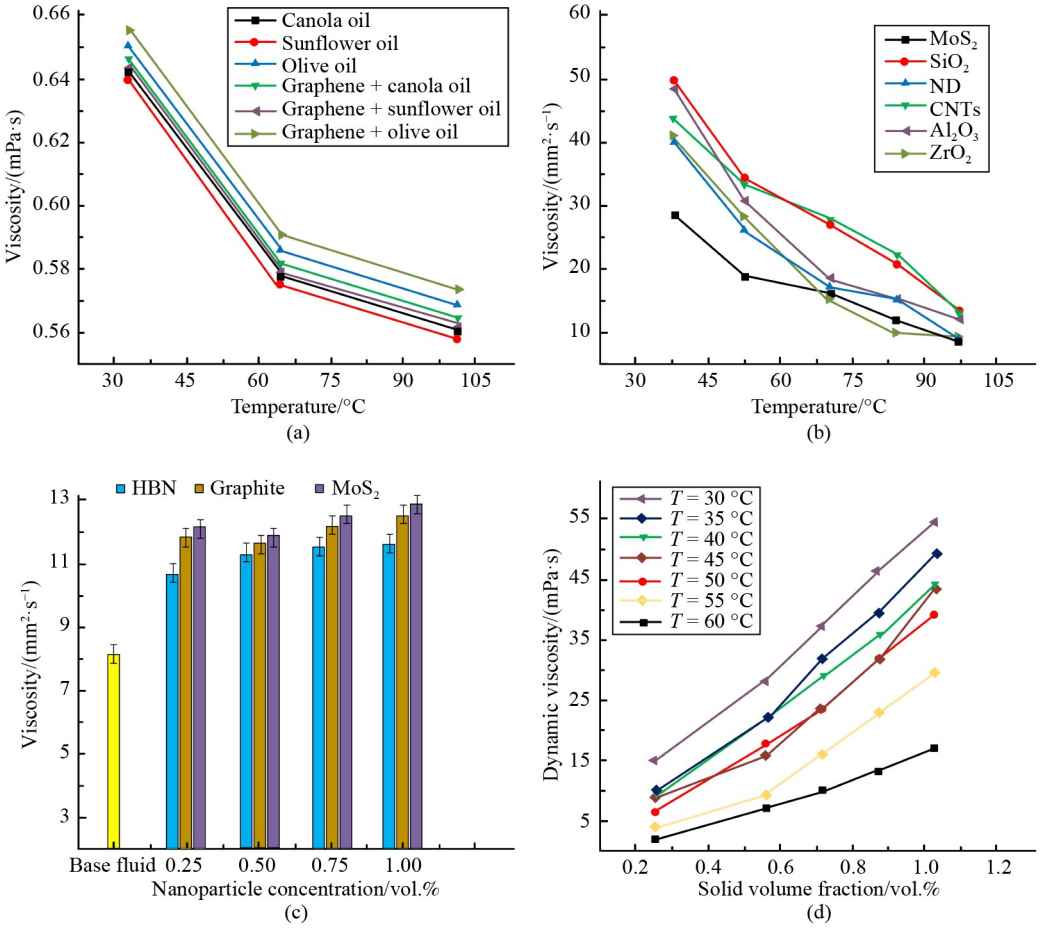

Fig. 11 Viscosity as a function of temperature and concentration. (a) Variation of graphene nanoparticle-enhanced coolant (NPEC) viscosity with temperature [50]; (b) variation of viscosity with temperature for six NPECs [104]; (c) viscosity variation with concentration for three different NPECs [138]; (d) variation of MWCNT–MgO hybrid NPECs viscosity with solid volume fraction [139]. CNTs: carbon nanotubes; HBN: hexagonal boron nitride; MWCNT: multi-walled carbon nanotube; ND: diamond. Reproduced with permissions from Refs. [50,104,138,139] from Elsevier.

that the viscosity increase is high at low particle sizes due to small interparticle distances and high van der Waals forces between the two molecules [148–150]. By contrast, Li et al. [151] investigated the size effect of nano-enhanced phases on the viscosity of NPECs and found that the viscosity increased significantly with particle size. In another study, Abdelhalim et al. [147] reached similar conclusions.

2) Shapes and types

Timofeeva et al. [152] investigated the effect of particle shape on the viscosity of Al_2O_3 NPECs. Various shapes of nano-enhanced phases were considered in the experimental study, and the results showed that NPECs with cylindrical and lamellar nano-enhanced phases exhibited higher viscosity than other shapes, mainly due to their surface-based volume ratio effects [153,154]. Studies on the effect of the particle shape of SiO_2 and ZnO on the viscosity of NPECs revealed that the particle shape does not vary disproportionately [154]. The factors affecting the viscosity of NPECs require further systematic studies before conclusions can be drawn. Cui et al. [129] found that the effect of nano-enhanced phases on the viscosity of base oil varied by comparing four types of nano-enhanced phases (HBN, GNP, MoS_2, and MoO_3) with pure base oil (palm oil), and the viscosity of the four NPECs was higher than that of pure oil. HBN NPECs showed the lowest viscosity (72.4 mPa·s), which was 9.5% higher than the viscosity of pure oil (66.1 mPa·s). By contrast, GNP NPECs had the highest viscosity (82.2 mPa·s), which was 24.4% higher than the viscosity of pure oil.

Overall, the temperature concentration of the NPEC, as well as the size, shape, and type of the particles, affect its viscosity, thus yielding effects. In the process of selecting nano-enhanced phases, the type of base fluid and nano-enhanced phases should be balanced to obtain optimal processing performance. In addition, the viscosity of the NPEC increases with particle size, probably due to the intermolecular van der Waals forces, which increase fluid resistance, leading to an increase in viscosity.

3.3 Wetting performance

Surface tension has a crucial effect on the NPEC trace lubrication wetting of the tool–workpiece interface. It is an important parameter that affects droplet breakup and tearing, and the state of the droplets on the workpiece determines the wetting effect. Surface tension typically has a significant effect on the boiling heat transfer process, wetting behavior, and spray characteristics of NPECs. Bertolini et al. [155] measured the surface tension of NPECs and found that the addition of nano-enhanced phases to the base fluid decreases the surface tension. In addition, surface tension determines the boiling point, bubble departure field, and interfacial equilibrium of the fluid [156]. Zhang et al. [157] discussed the effect of base oil viscosity and surface tension on friction and found that vegetable oils with high viscosity and low surface tension exhibited excellent cooling lubrication properties. A negative correlation between surface tension and heat transfer coefficient was observed for NPECs. The superior heat transfer coefficient of NPECs may be attributed to the formation of additional bubbles and their expansion due to weak binding. Therefore, the presence of additional bubbles and high boiling point heat transfer activity helps obtain superior performance, such as lowering the temperature in the grinding zone, avoiding burns on the workpiece, and improving the machining quality of the workpiece [104]. Jia et al. [158] reported that lowering the surface tension of the liquid facilitates the improvement of the atomization characteristics. Therefore, lubricant use and migration permeability can be further improved.

Adhesion between the liquid and solid causes droplet distribution onto the surface. The viscosity of the liquid prevents the droplet from contacting the surface. When a drop of liquid (cutting fluid) rests on a solid surface to form an interface, the angular profile between the droplet and the contacting surface is called the wetting (contact) angle. Small contact angles are considered to have superior wetting properties [103]. By contrast, when the contact angle is large, the droplet wetting capability is poor. With the addition of nano-enhanced phases, the contact angle gradually decreases and the wetting performance improves. Li et al. [104] obtained the contact angles of various NPECs on nickel-based workpieces, as shown in Table 4. They observed additional bubbles on the surface of the workpiece containing NPEC, indicating a high boiling heat transfer coefficient. A high heat transfer coefficient indicates that the NPEC has a high heat-carrying capacity, which may be a good option for effective cooling and lubrication during machining. Zhang et al. [159] found that the contact angle significantly affects the surface quality of the workpiece. A small contact angle leads to a low surface roughness of the workpiece, resulting in good cooling and lubrication. A small contact angle results in a large penetration area of the NPEC, which significantly affects the lubrication and cooling performance [130].

Table 4 NPEC contact angles on a Ni-based workpiece

Nanoparticle-enhanced coolants	Contact angle/(°)
SiO_2	49.2
PCD	43.5
CNT	47.5
MoS_2	46.0
Al_2O_3	45.5
ZrO_2	41.5

Notes: PCD, polycrystalline diamond; CNT, carbon nanotube.

A strong relationship exists between boiling heat transfer and wettability, especially during bubble formation, expansion, separation, and movement. The low surface tension of the NPEC suggests a weak binding force for bubble formation and expansion. The presence of additional bubbles and high boiling point heat transfer activity helps in obtaining excellent properties, such as lowered temperature in the grinding zone, prevention of workpiece burning, and improvement of the workpiece machining quality [104]. In addition, according to the theory of thermal convection, the droplets during thermal convection can be divided into the thermal boundary layer and the main flow zone. The thickness of the thermal boundary layer remains constant. However, the fluid in the main flow zone moves quickly from the cut zone before absorbing sufficient heat. In other words, the fluid in the main flow region does not provide satisfactory heat exchange. As shown in Fig. 12 [157], when the surface tension decreases, the thermal boundary layer expands and the proportion of abrasive fluid in the main flow region decreases. This result explains the high cooling efficiency of MQL droplets with small contact angles.

Thus, the effectiveness of cooling lubrication depends on the wetting properties of NPECs. Surface tension influences the boiling heat transfer process, and contact angle provides an inverse measure of wettability. When the contact angle decreases, the area of the thermal boundary and the fluid involved in heat transfer both increase. Meanwhile, the high thermal conductivity and heat transfer coefficient of the NPEC indicate improved heat dissipation performance. NPECs can effectively improve the heat transfer efficiency and reduce the thermal load introduced to the tool–workpiece interface during the cutting process. In addition, CNT NPECs with high heat transfer coefficients and significant cooling and lubrication capabilities may be a superior choice for the machining of MQL cemented carbides (high-temperature alloys).

3.4 Tribological properties

Friction plays a vital role in machining. A considerable

amount of heat is generated due to the presence of friction between the tool and the chip and between the tool and the workpiece, which affects the tool life and the surface quality of the workpiece [160–163]. Therefore, understanding the tribological behavior of the chip–tool–workpiece interface during machining is crucial [164]. Several factors influence the COF in the machining interface, such as type of machining, material, geometry, and tool wear, as well as lubrication and cooling conditions [165]. Adding coolant to the machining process can reduce the cutting temperature. In addition, scholars have proven that the addition of nano-enhanced phases in the base fluid can effectively reduce the machining temperature, friction, and wear based on the original [166,167]. As shown in Fig. 13 [168], scholars have proposed that NPECs have four effects of cooling and lubrication in machining.

Sikdar et al. [169] stated that the addition of solid lubricants to the cutting fluid helps fill the concave and convex surface gaps and promotes sliding on the friction subsurface. Spherical or quasi-spherical nano-enhanced phases can form a ball-bearing effect on the friction surface. In this case, sliding friction is transformed into rolling friction with a low COF. Nano-enhanced phases in NPECs improve tribological performance by eliminating direct tool–workpiece contact and filling surface gaps to reduce frictional wear [61,170–172]. Ouyang et al. [173] evaluated the performance of wear tests containing 0.5 wt.% GNP and 0.7 wt.% MWCNTs in castor oil and wear traces obtained by scanning electron microscopy, energy dispersive spectroscopy, and Raman spectroscopy on steel plates and balls. The results of the wear analysis of steel balls and plates were highly consistent, indicating that graphene CNTs reduced the COF and surface wear by 26% and 48%, respectively, at low speeds and under loaded conditions. Samuel et al. [174] observed that the nanolayer increases with the concentration of nano-enhanced phases, and wear on the surface decreases due to the nanolayer between the surfaces. This NPEC layer supports large loads; in the case of spherical particles, this layer induces a rolling effect, which reduces the COF and cutting forces [168]. Kumar et al. [35] verified the tribological performance tests of four water-based NPECs (HBN, Al_2O_3, MoS_2, and WS_2), and alumina NPECs showed optimum tribological performance. The COF was reduced by 53.89% compared with dry friction. HBN,

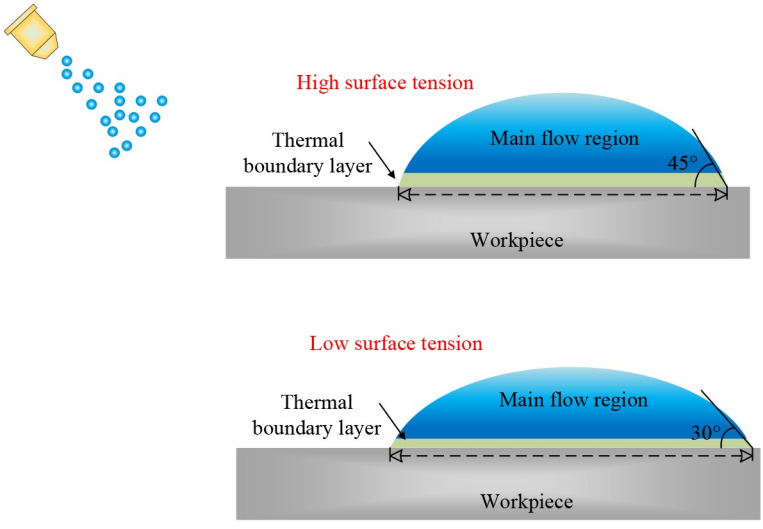

Fig. 12 Effect of wetting properties on heat transfer [157], reproduced with permission from Elsevier.

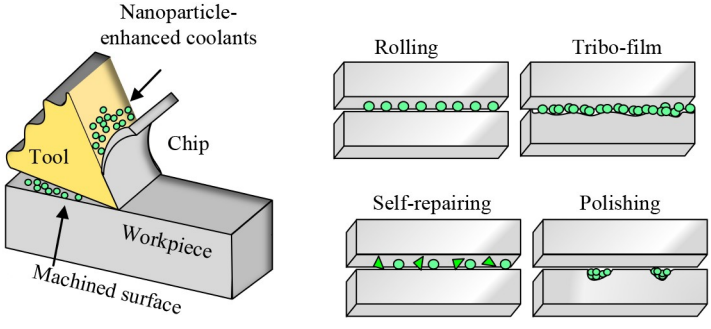

Fig. 13 Lubrication mechanism diagram [168], reproduced with permission from Elsevier.

MoS_2, and WS_2 NPECs may be due to the layered structure, where the layers are bonded together by weak van der Waals forces and the lubrication mechanism involves sliding of the layers.

As indicated in the studies of Gulzar et al. [175] and Ali et al. [176], Al_2O_3 and TiO_2 nano-enhanced phases can form a friction film that protects the machined material from crack propagation and reduces the surface roughness by filling the surface grooves and bumps. Meanwhile, Peña-Parás et al. [177] demonstrated that TiO_2-filled surface grooves reduced friction due to their hemispherical shape and small size. However, airflow variations in MQL applications can affect the formation of protective films. High pressure transports the NPEC close to the cutting edge and removes substantial heat [61]. Wang et al. [28] revealed that some nano-enhanced phases of solid lubricating materials, such as GNP, can form a smooth and dense friction film on the workpiece surface during the machining process, which helps further reduce friction and surface wear. Talib et al. [178] found that COF increased at concentrations higher than 0.05 wt.% of HBN because the agglomeration of nano-enhanced phases led to the deterioration of the tribological behavior of the NPEC, possibly due to the high hardness of HBN nano-enhanced phases, which made HBN an abrasive material at high concentrations. However, only some nano-enhanced phases can improve the processing performance of vegetable oil-based lubricants. Alves et al. [179] investigated the effect of adding nano-enhanced phases to vegetable oil-based lubricants and found that the addition of CuO nano-enhanced phases to sunflower and soybean oils increased the COF by approximately 20% and 7.5%, respectively. They found that the addition of oxide nano-enhanced phases to plant-based lubricants may deteriorate film formation. The authors explained that this phenomenon may be related to the third-body behavior of these oxides, which increases friction and reduces the electrical conductivity between the sample surfaces [180]. In addition, Azman et al. [181] revealed that an increase in the concentration of GNP and nano-enhanced phases in the cutting fluid proportionally increased the COF. In this case, the increase in the COF was caused by the substantial aggregation of high concentrations of GNP nano-enhanced phases. The augmented concentration of NPECs and the degree of chemical interaction between the particles and the newly formed surface increase the protective film between the tribological pairs, which improves the surface quality and reduces the COF [61].

In addition, some high hardness nano-enhanced phases can be considered as precision polishing materials. After polishing, the roughness of the friction pair decreases, the contact area increases, and the COF decreases. The compressive stresses on the contact surfaces are also reduced, thus increasing the load-bearing capacity of the lubricant, which is referred to as the polishing mechanism of nano-enhanced phases. Thus, the physicochemical properties of different nano-enhanced phases determine their role at the friction interface. With the combination of relatively low cutting zone friction and heat flux density, in terms of specific energy, NPEC conditions can reduce specific energy by 40%–42%, 25%–30%, and 17%–19% compared with dry cutting, flooded, and MQL, respectively [182]. Sayuti et al. [61] used NPEC produced from SiO_2 nano-enhanced phases ranging from 5 to 15 nm with nozzles located at 15°, 30°, 45°, and 60° in MQL applications during end milling and observed that the nano-enhanced phases acted as a polishing effect. In addition, the impregnation of sheared nano-enhanced phases in the surface pores shows shearing of the particles, surface peaks, and pore filling, leading to the formation of a thin protective film comprising sheared whole nano-enhanced phases. Such replicated conditions at the processing interface lead to the removal of surface roughness of the material, contributing to the increase in chemical bonding of the NPEC to the newly formed surface [131,183]. Rahman et al. [184] used nano-enhanced phases of Al_2O_3, MoS_2, and TiO_2 in vegetable oils of rapeseed oil and extra virgin olive at concentrations of 0.5, 2, and 4 vol.%, respectively, as a cutting fluid for turning Ti–6Al–4V ELI alloys. This study demonstrated improved surface integrity through the polishing effect induced by canola oil NPEC containing 0.5 vol.% by volume Al_2O_3 particles. The temperature is also reduced at the chip–tool–workpiece interface and at the COF due to the rolling mechanism of the existing spherical Al_2O_3 nano-enhanced phases in the friction film formed at the machining interface. In addition, NPECs containing 0.5 vol.% volumetric MoS_2 were effective in reducing the machining temperature, which may indicate a reduction in cutting forces and COF due to the rolling effect. Similarly, Al_2O_3 and TiO_2 nano-enhanced phases acted as a rolling mechanism between the interacting surfaces [185].

Cui et al. [129] found that the laminar structure allows the lubricant to effectively fill the pits on the surface of the workpiece and increase the surface smoothness, thus improving the lubrication performance, as shown in Fig. 14(a). The average value of the COF reaches its maximum (0.449) under palm oil lubrication conditions. As shown in Fig. 14(b), the COF of the GNP condition is 34.3% lower than that of the MQL condition of pure palm oil. The experimental results of the average COF proved that GNP nano-enhanced phases exhibit excellent anti-friction properties. This finding may be due to the hexagonal honeycomb structure of GNP molecules. Therefore, GNP NPECs exhibit the strongest lubrication stability and wear resistance. In addition, Singh et al. [109] observed that Al–GNP hybrid NPECs had the lowest COF at 1 vol.% nano-enhanced phase concentration. As shown in Fig. 14(c), the tool wear rate and COF of Al–GNP hybrid and Al_2O_3 NPECs were reduced with the

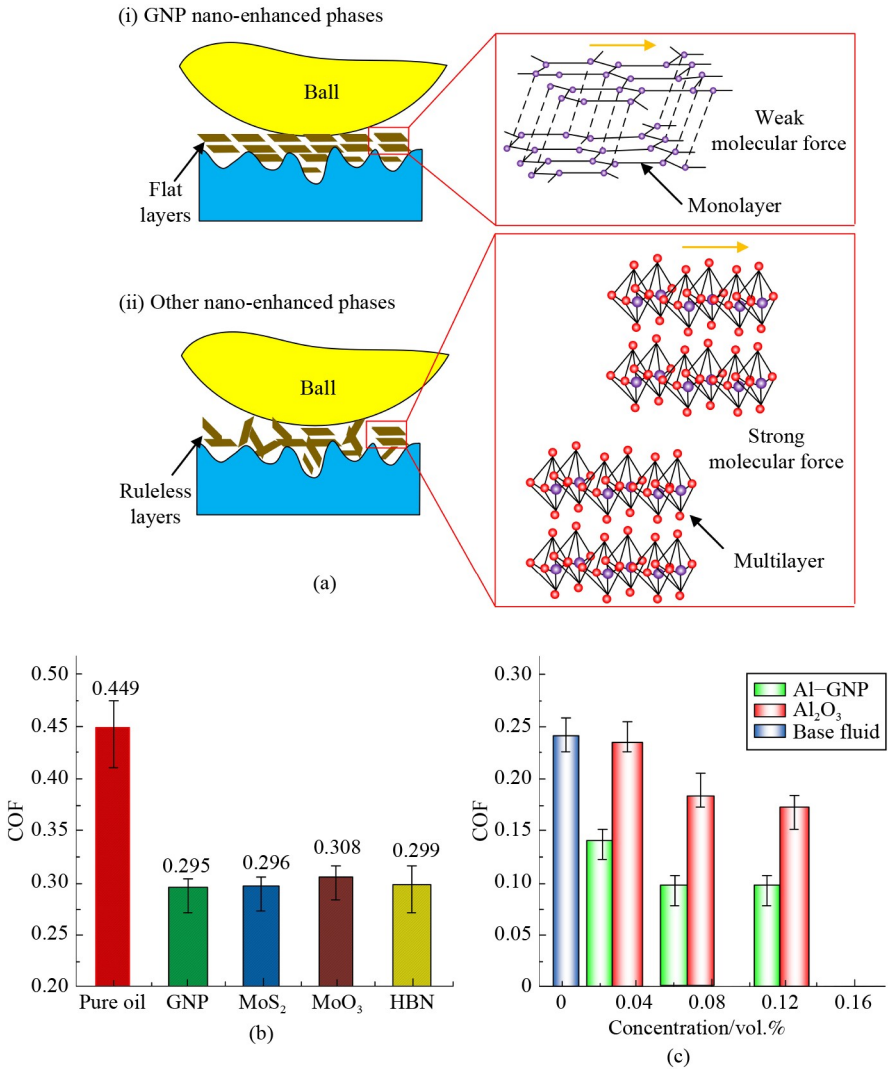

Fig. 14 (a) Macroscopic lubrication mechanism model of stratiform nano-enhanced phases; (b) effect of different types on the coefficient of friction (COF) [129], reproduced with permission from Elsevier; (c) effect of nano-enhanced phase concentration on COF [109], reproduced with permission from Springer Nature. GNP: graphene; HBN: hexagonal boron nitride.

increase of nano-enhanced phase concentration, respectively, compared with the base fluid. In addition, at 1 vol.% nano-enhanced phase concentration, the Al–GNP hybrid NPECs exhibited the best performance. An experimental study by Kalita et al. [186] revealed improved lubrication with increasing concentrations of MoS_2 nano-enhanced phases. The COF of soy-based NPECs (8 wt.%) was reduced by almost 14% compared with NPECs containing 2 wt.% nano-enhanced phases.

The application of NPEC markedly reduces friction at the interface, further decreasing the frictional heat source and the generation of cutting heat, subsequently reducing the cutting temperature. Simultaneously, the temperature reduces the thermal load of the friction interface and the thermal stress of the friction vice and suppresses the formation of residual tensile stress and microcracks. Thus, the surface quality of the workpiece is significantly improved. In addition, the reduction in friction reduces tangential force loads, stripping between interfering bumps at the interface of the friction pair and mechanical wear. NPECs provide excellent heat transfer, film-forming, wetting, antiwear, and friction reduction properties, improving machine efficiency and reliability. The analysis shows that the NPEC can easily penetrate the machining interface and increase the heat transfer capacity, facilitating its promotion in the MQL machining field.

4 Applications in machining

Titanium alloys [187], high-temperature alloys [188], high-strength steels [49], composite materials [189], and other difficult-to-machine materials [190,191] are widely used in numerous fields, such as medical, aerospace, and military applications, due to their excellent

physicochemical properties. However, these difficult-to-machine materials are characterized by their low thermal conductivity, fracture toughness, and poor machinability, which allows for a significant increase in temperature during machining to produce thermal damage [192]. NPECs have been used as a method to improve the machinability of difficult-to-machine materials. This section provides a comprehensive quantitative assessment of the material removal characteristics during machining for turning, milling, and grinding applications using machining temperature, tool wear, surface quality, and specific grinding energy as evaluation tools.

4.1 Turning

The workpiece in turning is rotated relative to the tool to continuously remove materials, with the cutting edge continually in contact with the workpiece during the process. However, the high temperatures generated in the cutting zone during this process result in chip adherence to the cutting edge of the tool, which leads to deterioration in the quality of the cut and affects tool life. Therefore, improving tool life and workpiece surface quality is crucial. As a new green machining method, the NPEC has a good cooling–lubricating superposition effect in machining.

Figure 15 shows a lubrication exclusion zone during continuous cutting, where the tool and chip have a certain contact length of continuous intense contact [193]. Therefore, continuous contact friction at high temperatures, pressures, and speeds can lead to workpiece surface adhesion and tool wear. In continuous cutting, NPEC wetting performance is a major consideration, and droplet wetting, diffusion, and transport are crucial. Numerous capillary tubes between the tool and the chip are widely recognized when the cutting fluid is wetting the cutting zone. In addition, capillary permeation has three stages: liquid-phase permeation, droplet evaporation, and gas-phase filling. After the three stages, the lubricant is adsorbed on the solid surface, forming a solid boundary lubrication layer. The boundary lubrication layer has a certain load-bearing capacity. Capillary interactions in the tool–chip contact zone directly affect friction on the front surface of the tool and subsequently influence the friction and shear angles. Therefore, heat generation is suppressed due to friction reduction [194].

4.1.1 Cutting temperature

When cutting heat during the removal of difficult-to-machine materials, considerable heat is generated during the cutting process and concentrated in the tool–workpiece contact area due to the low thermal conductivity, resulting in an increase in the cutting temperature [195,196]. The main source of cutting heat is the friction between the front face and the chip, followed by the friction between the rear face and the workpiece. High temperatures in the cutting zone can deteriorate the surface quality of the workpiece and cause its deformation [197]. Sharp temperature changes at the tool–workpiece interface are limited to a region of 1–2 mm on the surface [198]. NPEC not only reduces the use of cutting fluid but also fully immerses the cutting area and suppresses the generation of cutting heat.

Yi et al. [199] investigated the effect of MQL NPEC on the turning temperature of Ti–6Al–4V. During the turning process, the lowest temperature at the tool–chip interface (TCIT) was observed at a feed rate of 0.05 mm/r, an air pressure of 10^5 Pa, and graphene oxide concentration of 0.5 wt.%. The temperature at TCIT was reduced by 50.53 °C compared with the PMQL condition. In addition, a heat transfer model for the turning process using NPEC was created on the basis of the thermal conductivity and specific heat of graphene oxide NPEC as well as their heat transfer and friction coefficients. Comparing the simulation and experimental measurements, the simulation results were close to the experimental results, indicating the reliability of the thermal model. Singh et al. [200] investigated the effect of turning Ti–6Al–4V on the cutting temperature at different cutting speeds and found that the cutting temperature under NPEC micro-lubrication was 31%–42% lower than that under dry conditions. The temperature reduction achieved under NPEC trace lubrication is mainly due to the good thermal conductivity and lubrication properties of the tool–chip/tool–workpiece contact surfaces.

Gupta et al. [201] evaluated the performance of Al_2O_3, MoS_2, and GNP NPECs in turning Ti alloy (grade II)

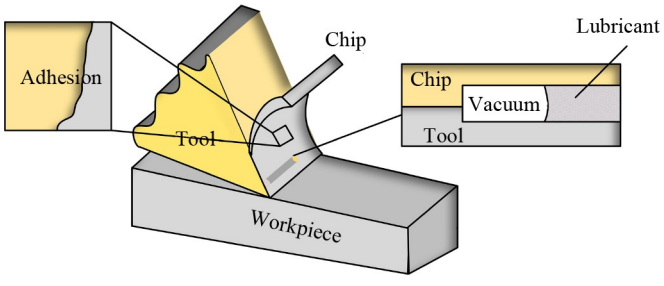

Fig. 15 Capillary infiltration.

using cubic boron nitride (CBN) tools. An increase in the cutting speed and feed rate increases local temperature. Cutting speed has a greater effect on cutting temperature than feed rate. GNP shows a lower cutting temperature than Al_2O_3 and MoS_2 NPEC. This finding is mainly due to the low viscosity and high thermal conductivity of GNP NPECs, which removes the heat released on the cutting zone. Meanwhile, NPEC improved the frictional properties of the chip–tool contact surface, and the enhanced wetted surface could promote improved heat removal [109]. Therefore, GNP NPECs are effective in reducing the cutting temperature. As shown in Fig. 16, the cutting temperature T varies in different environments and increases with V_c. NPEC provided effective heat dissipation when canola oil was combined with Al_2O_3, MoS_2, and TiO_2 (at low cutting speeds). However, Al_2O_3 nano-enhanced phases with olive oil exhibited superior heat dissipation at medium and high speeds. The lowest cutoff temperature of 875 °C was obtained for 0.5 wt.% MoS_2–canola oil NPEC, again confirming that the percentage of nano-enhanced phases has a considerable influence on the lubrication and cooling properties during machining [184].

4.1.2 Tool wear

Tool wear, which is described as the loss of material that occurs in the area where the tool and the work material are in contact, is the most basic indicator of tool life. An increase in cutting speed typically affects tool wear and tool life. Tool wear influences the workpiece surface integrity, efficiency, cutting force, energy consumption, and other indicators during machining. As shown in Fig. 17(a), ISO 3685 indicates that the degree of tool wear is determined by the depth/width of the crater on the front face of the tool, the wear on the back face of the tool (average or maximum), and the notch wear on the back face of the tool [202]. The reduction in cutting forces decreases the mechanical load during material removal, which effectively reduces tool wear. Simultaneously, the reduction in cutting temperature decreases the thermal softening of the workpiece, weakening the material adhesion and effectively reducing tool adhesion. The researchers compared the effect of NPEC on tool wear under different lubrication conditions. The flank wear (V_B) of Ti–6Al–4V was reduced by 47.37% and 31.58% under 0.1 wt.% MoS_2 NPEC and pure biolubricant MQL, respectively, compared with the results of dry cutting [203]. Biolubricant MQL increased tool life by 50%, whereas flake GNP NPEC increased it by 100% [204].

Jamil et al. [192] investigated the effect of low-temperature CO_2 and the MQL technique based on hybrid NPECs on Ti–6Al–4V turning. Figure 17(b) shows the variation of main flank wear at different rotational speeds, feed rates, and cooling environments. The machining time under low-temperature CO_2 was 236 s, whereas the tool failure machining time was 292 s for mixed NPECs. The lower COF under Al_2O_3–MWCNT NPECs compared with cryogenic cooling resulted in a longer tool life. Figure 17(c) shows that the highest V_B was measured in the dry and flooded cases at 83.9 and 65.3 µm, respectively. Variations in the graphite content exhibited insignificant differences, with an average V_B value of approximately 47 µm. By contrast, a 29% reduction in V_B was observed compared with the PMQL technique. In addition, no buildup was observed on the tool back face, and MQL with additional polytetrafluoroethylene (PTFE) particles significantly reduced tool wear [205]. By studying the wear behavior of the texture tool of Ti–6Al–4V, as shown in Fig. 17(d), T3 (NPEC) has the maximum tool life at all cutting speeds, followed by T2 (rapeseed oil MQL), and finally T1 (dry) [115]. Furthermore, Hegab et al. [206] found that the addition of 2 wt.% MWCNT NPECs reduced tool flank wear by 45%

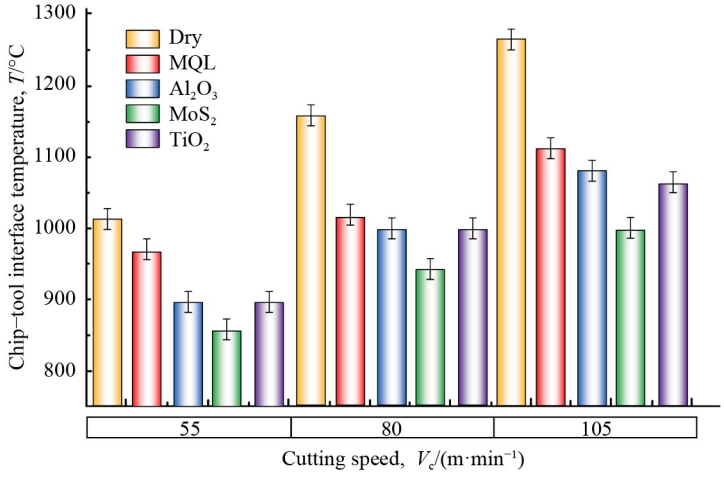

Fig. 16 Comparison of cutting temperatures at different environments. MQL: minimum quantity lubrication.

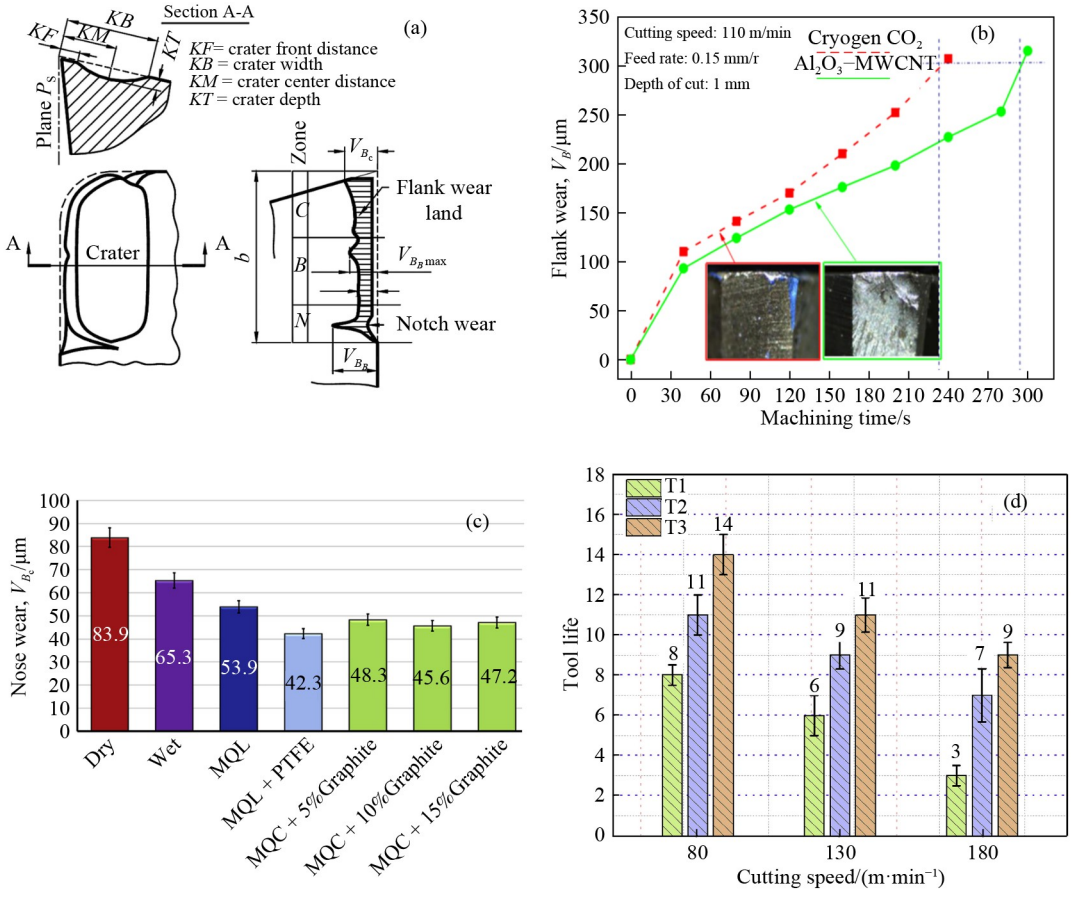

Fig. 17 (a) Tool wear types based on ISO 3685 [202], reproduced with permission from Elsevier; (b) flank wear based on machining time [192], reproduced with permission from Springer Nature; (c) tip wear V_{B_c} as an evaluation of different lubrication–cooling strategies [205], reproduced with permission from Elsevier; (d) tool life at different cutting speeds [115], reproduced with permission from Elsevier. MQL: minimum quantity lubrication; MQC: minimal quantitative cooling; PTFE: polytetrafluoroethylene.

compared with tests without any nano-enhanced phases. Therefore, using NPEC helps improve tool life under the same cutting parameters.

Gupta et al. [201] analyzed some micrographs of cutting tool tips after the machining of Ti alloy using (1) Al_2O_3, (2) MoS_2, and (3) graphite MQL, as shown in Fig. 18. Figure 18(a) depicts the major tip fracture and the final damage to the tool edge. Figure 18(b) emphasizes tool tip wear during machining with MoS_2 NPECs. During the machining of graphite NPECs, some wear marks appear on the front tool surface, as shown in Fig. 18(c). When Al_2O_3 particles impact the tool–workpiece surface, they may become tool surface crack initiators, which leads to crack expansion due to cutting forces and ultimately to the failure of the outer layer of the tool. The tool wear process was significantly reduced when graphite NPECs were used. This phenomenon is mainly due to the low viscosity of the graphite nano-enhanced phases, which allows the smooth movement of the tool edge over the working surface. The improved tribological behavior resulted in an improved tool surface. Using NPECs to reduce tool wear is better than using MQL alone. Nguyen et al. [204] investigated the effect of dry, MQL, and NPEC conditions on V_B values under different cutting parameters. The results showed that the use of MQL and the addition of 0.5 wt.% of GNP nano-enhanced phases significantly reduced flank wear by approximately 40% and 100%, respectively, compared with dry conditions. Singh et al. [200] compared and investigated the effects of dry, MQL, microtextured tools filled with GNP particles, and NPEC on tool wear when turning Ti–6Al–4V. The results showed that tool life increased by 178%–190% at different cutting speeds under NPEC conditions compared with dry conditions. Revuru et al. [207] investigated that under different cooling and lubrication conditions, when machining at high feeds and cutting speeds, tool wear was reduced by approximately 85% in graphite soybean oil-based cutting fluids compared with dry machining and by approximately 20% compared with pure cutting fluids. This finding is attributed to the lower cutting temperature of graphite NPECs than that of pure soybean oil cutting fluids. Therefore, the capability to inhibit thermal softening and chemical reaction of active elements is strong. MQL significantly reduces tool wear, which also proves the superiority of NPECs.

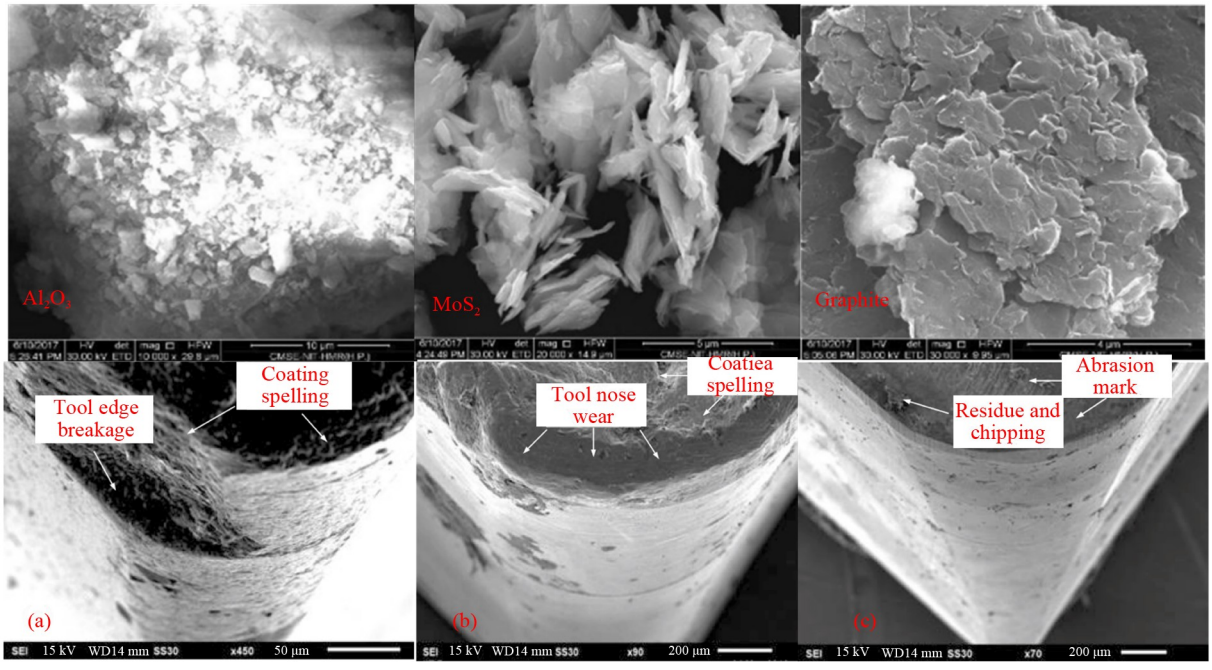

Fig. 18 Tool wear images for different NPECs [201]: (a) Al_2O_3, (b) MoS_2, and (c) graphite. Reproduced under the terms of the CC BY license.

4.1.3 Surface quality

NPECs can effectively reduce temperature, cutting forces, and tool wear, thereby improving the surface quality of the workpiece. Hegab et al. [206] found that 2 wt.% MWCNT NPECs reduced power consumption by 11.5% while improving surface quality compared with pure vegetable oil biolubricant. Sahu et al. [208] found that the surface roughness was reduced by 7% and 6.1% at 150 and 90 m/min, respectively, when turning Ti–6Al–4V workpieces using MWCNTs as NPECs. Khan et al. [209] found that turning of Ti–6Al–4V alloy using Al–GNP NPECs at four cutting speeds increased the surface finish by 15.7%, 11%, 14.7%, and 15.2%. In addition, no BUE was observed when textured tools were applied under MQL conditions. In another study, compared with dry milling and the use of pure biolubricant, the *Ra* obtained with NPEC with a volume fraction of 0.1 vol.% was reduced by 40.67% and 10.3%, respectively [210]. Thus, the use of NPECs improves the machined surface integrity and facilitates further use in turning processes.

The incorporation of nano-enhanced phases reduces the mechanical and thermal loads on the workpiece and effectively ensures the surface integrity of the machined part. Compared with the results obtained for dry cutting conditions, the surface roughness values of the workpieces obtained by Ti–6Al–4V turning increased by 40.67% and 10.3% for NPEC and MQL conditions, respectively [203]. Singh et al. [200] investigated the effect of dry, MQL, and NPEC on surface roughness when turning Ti–6Al–4V using average roughness *Ra* as a basis for determining surface quality. Figure 19(a) shows the *Ra* values for different cutting conditions. In T3 environment, *Ra* at different cutting speeds is 41%–53% and 58%–68% lower than the T2 and T1 conditions, respectively. The low *Ra* values in the NPEC (T3) environment are mainly due to the GNP NPECs providing superior cooling–lubrication, which reduces the tool adherence tendency of the chips, thus decreasing the wear of the tool and ultimately improving the quality of the machined surface. Figure 19(b) shows the variation in surface roughness at different cutting speeds for the two studied cooling environments. At lower cutting speeds (100 m/min), *Ra* in the hybrid NPEC environment was reduced by 15.49%, 12.99%, and 8.72% compared with that in the low-temperature CO_2 environment. At a high cutting speed (150 m/min), *Ra* was reduced by 26.2%, 18.18%, and 11.64%. The reduction in *Ra* may be related to the superior wetting area per unit volume of fluid on the workpiece–tool surface. In addition, the tribological properties of homogenized nanomaterials containing nano-enhanced phases (Al_2O_3–MWCNTs) acted as isolators, limiting friction at the tool–workpiece interface [192]. Figure 19(c) shows scanning electron microscope (SEM) micrographs produced by the machining of Ti alloy (grade II) under different NPEC-assisted cutting conditions [201]. In the presence of Al_2O_3 NPECs, the machined surface is not completely smooth, possibly due to the prolonged residence of nano-enhanced phases on the surface of titanium alloys. A remarkably smooth surface was observed under MoS_2 NPECs compared with Al_2O_3 NPECs. However, in the case of MoS_2 machining, tiny micro-burrs and surface pitting were observed. Considerably smooth surfaces with small micro-burrs

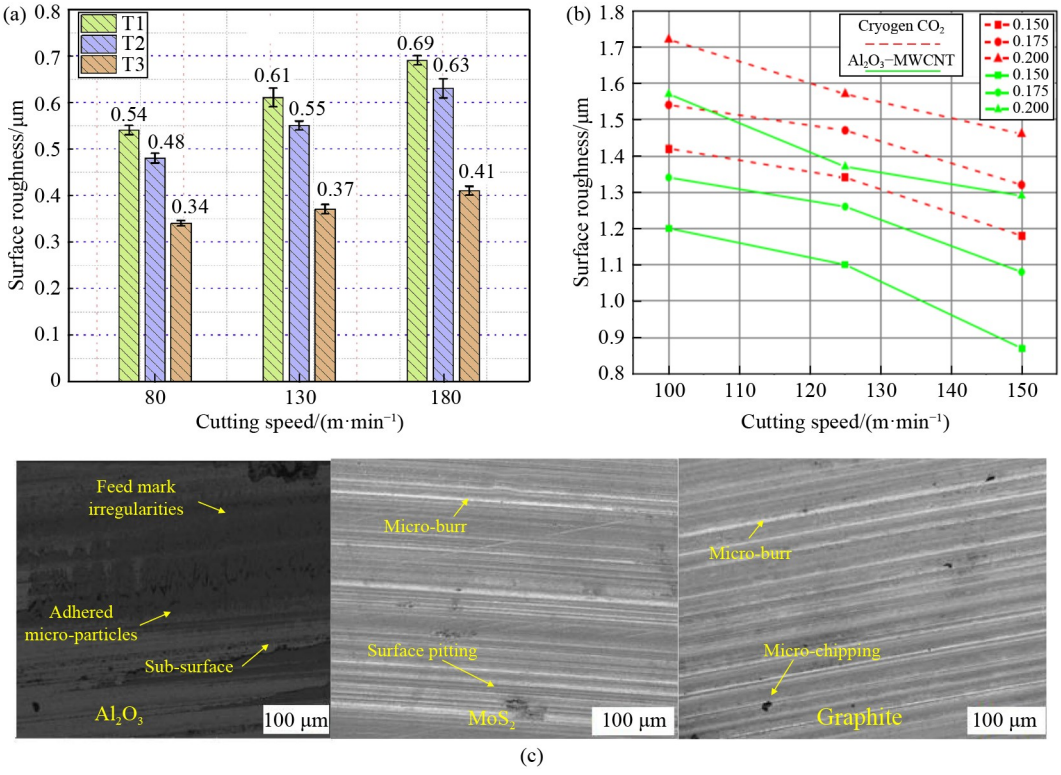

Fig. 19 (a) Variation of surface roughness *Ra* with cutting speed [110], reproduced with permission from Elsevier; (b) variation of surface roughness for two different environments at different cutting speeds [192], reproduced with permission from Springer Nature; (c) machined surfaces under different working conditions [201], reproduced under the terms of the CC BY license.

were observed for graphite NPECs under the same machining conditions. This phenomenon is mainly due to the excellent performance of the graphite NPEC as a spacer and ball bearing at the tool–workpiece contact interface. In addition, the wetting area decreases due to an increase in the contact angle between the workpiece and the NPEC. Elsheikh et al. [94] investigated the application of environmentally friendly vegetable oil NPECs in MQL turning of the AISI 4340 alloy and compared the two coolants (Al_2O_3 and CuO). CuO NPECs had high thermal conductivity and enhanced the cooling process in the cutting zone. They also demonstrated low viscosity. Thus, the low contact angle and surface tension enhance the wettability and distribution of the CuO coolant at the workpiece–tool interface compared with the Al_2O_3 NPEC, resulting in a superior surface topography. However, literature guiding the selection of nano-enhanced phases under different operating conditions is lacking. In addition to improving the integrity of the machined surface, NPECs are also effective in controlling residual stresses on the machined surface, which can be attributed to their excellent heat transfer properties.

4.2 Milling

In milling, the workpiece remains stationary relative to the milling cutter. In contrast to the continuous cutting of turning, each cutting edge of the milling cutter is processed intermittently, and the actual cutting area changes at any time. As shown in Fig. 20, for a single tool insert, the two wedge-shaped friction subsets of the chip on the front face and the workpiece on the back face are not always present but appear and disappear with some frequency [191]. Penetration of individual edges over a short time is detrimental to film formation. The strength of the lubricant film is affected by its high frequency impact. However, the cooling–lubricating media supply modes are different due to the various structures and motions of milling and turning tools, and this difference has an impact on the milling performance. Therefore, the viscosity and heat transfer characteristics of the NPEC trace lubrication must be considered. In addition, the load-bearing capacity of nano-enhanced phases and the oil film strength of NPECs are important features in the milling process.

4.2.1 Milling temperature

In metal removal, a high-speed cutting tool induces considerable plastic deformation of the workpiece material in the primary shear zone and friction in the secondary shear zone on the front tool surface and in the tertiary shear zone on the back tool surface [211]. More than 95% of the energy consumed by plastic deformation

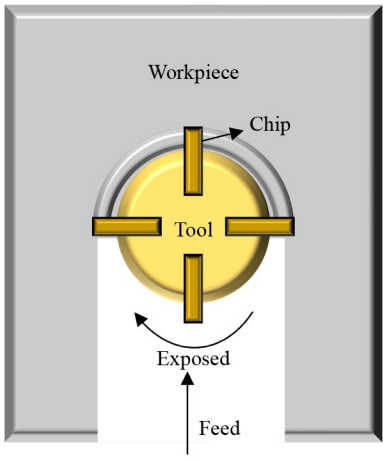

Fig. 20 Milling characteristics.

and friction losses in the machined metal is converted into heat, resulting in remarkably high temperatures in the machining zone. Therefore, milling temperatures directly affect the integrity of the workpiece surface and tool life.

Jamil et al. [212] investigated the effect of hybrid NPEC (Al_2O_3–MWCNT) on the temperature of the Ti–6Al–4V milling process. At 0.6 MPa air pressure, NPEC concentration of 0.24 wt.%, and flow rate of 120 mL/h, the maximum temperature under drying conditions was 372 °C, while the minimum temperature was 148 °C with MQL mixed NPEC. The hybrid NPEC significantly reduces the cutting temperature by minimizing the generation of shear and friction heat and simultaneously prevents direct contact between the cutting tool and the workpiece, thus reducing the cutting temperature. Kulkarni et al. [213] significantly outperformed dry milling and PMQL conditions in terms of cutting temperature when using copper-coated alumina NPECs for micro-lubricated milling of the A17075-T6 aluminum alloy plate surface. This finding proved that the addition of nano-enhanced phases to the coolant effectively reduces the tool interface temperature without affecting the milling performance characteristics. The addition of nano-enhanced phases to the selected base fluid results in Brownian motion of the particles. The continuously moving nano-enhanced phases have a large surface area, which contributes to enhanced and rapid heat transfer at the tool–workpiece interface [23]. Figure 21 shows the main effects on the maximum cutting temperatures of nickel alloy X-750 with different cooling lubrication environments and machining parameters. The lowest cutting temperature of 325 °C was obtained under HBN NPEC conditions, which reduced the maximum cutting temperature by approximately 23.1% and 27.8% for MQL and HBN coolant conditions, respectively, compared with the dry environment.

Li et al. [59] measured the surface and subsurface temperatures in a milling experiment of TC4 under four cooling–lubrication conditions. The peak surface and subsurface temperatures under dry conditions were 247.01 and 224.13 °C, respectively. The peak surface and subsurface temperatures under gas, PMQL, and graphene MQL (GMQL) conditions were (2.23% and 1.84%), (17.17% and 15.49%), and (29.91% and 26.05%) smaller than those under dry conditions, respectively. Dong et al. [214] prepared an NPEC with a volume fraction of 1.5% for milling Ti–6Al–4V using cottonseed oil as a base with six different nano-enhanced phases and 0.3 wt.% CTAB dispersant. The experimental results show that the peak temperatures of SiO_2, graphite, Al_2O_3, MOS_2, SiC, and CNT NPEC during processing are 54.9, 64.5, 65.1, 65.8, 87.2, and 294.1 °C, respectively, and the temperature of the workpiece increases in the order of SiO_2 < graphite < Al_2O_3 < MOS_2 < SiC < CNTs. The use of SiO_2 NPEC can effectively improve the cooling capacity and thus reduce the milling temperature.

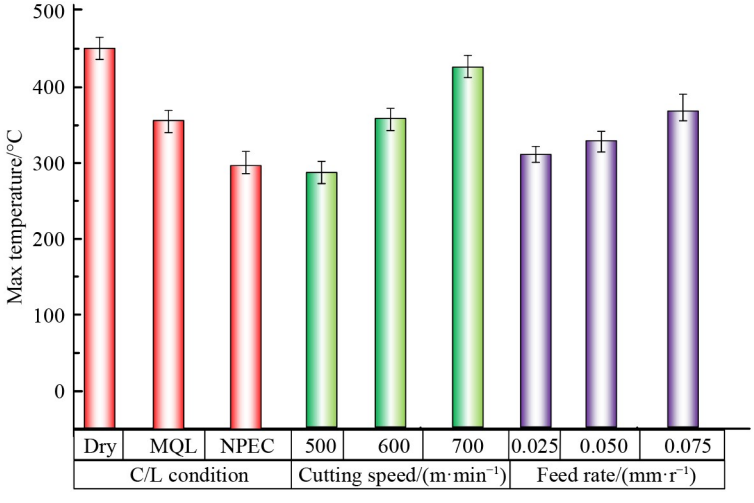

Fig. 21 Column graph showing main effects on maximum temperature in cutting zone. C/L: cooling/lubrication; MQL: minimum quantity lubrication; NPEC: nanoparticle-enhanced coolant.

4.2.2 Tool wear

As one of the key evaluation parameters in machining, tool wear depends to a large extent on the workpiece material and the cooling and lubrication conditions. Tool wear is directly related to the surface quality of the workpiece during milling. Therefore, investigating milling cutter wear under different operating conditions is crucial.

Zhou et al. [215] found a 63.3% reduction in tool wear compared with conventional cutting fluids and microtextured tools when milling Ti–6Al–4V ELI using microtextured tools and Fe_3O_4 NPECs. Roushan et al. [216] showed a significant reduction in tool wear compared with conventional cutting fluids and microtextured tools by combining CuO NPECs with PVD-coated (AlTiN/TiAlN) and uncoated WC micro end mills hybridized to extend tool life and improve surface quality. The results showed a reduction in tool wear and BUE formation at high concentrations (1 vol.%) of aqueous CuO NPECs. Jamil et al. [69] investigated the tool wear condition of Ti–6Al–4V alloy milling based on Al_2O_3–MWCNT NPECs and found that the hybrid NPEC acted similarly to a spacer, which reduced the friction of the cutting edge on the surface of the workpiece and further decreased tool wear. Kim et al. [217] observed and analyzed the tool wear of micro end mills after milling 10 flutes in each experimental case. In the case of ND NPECs with cold CO_2 gas cooling, the tool wear values were substantially lower than those in the other cases. Moreover, a low concentration (0.1 wt.%) of ND coolant was favorable for tool wear reduction. However, in the case of a high weight concentration (1.0 wt.%), the additional scraping effect due to many ND particles may lead to increased tool wear.

Li et al. [59] investigated the effect of four dry cooling–lubrication conditions on the life of milling tools made of Ti–6Al–4V alloy. Figure 22(a) compares the maximum width of the tool flank wear zone under these conditions. The maximum width of the tool flank wear zone was 187 μm in dry conditions and 175, 140, and 129 μm in gas, PMQL, and GNP NPEC conditions, respectively, which was reduced by 31.02% using GNP NPECs compared with dry conditions. Figure 22(b) shows the milling cutter wear curves. Tool wear undergoes a period of sharp increase before entering a relatively steady state and then proceeds into a phase of sharp deterioration until tool failure. GNP NPECs

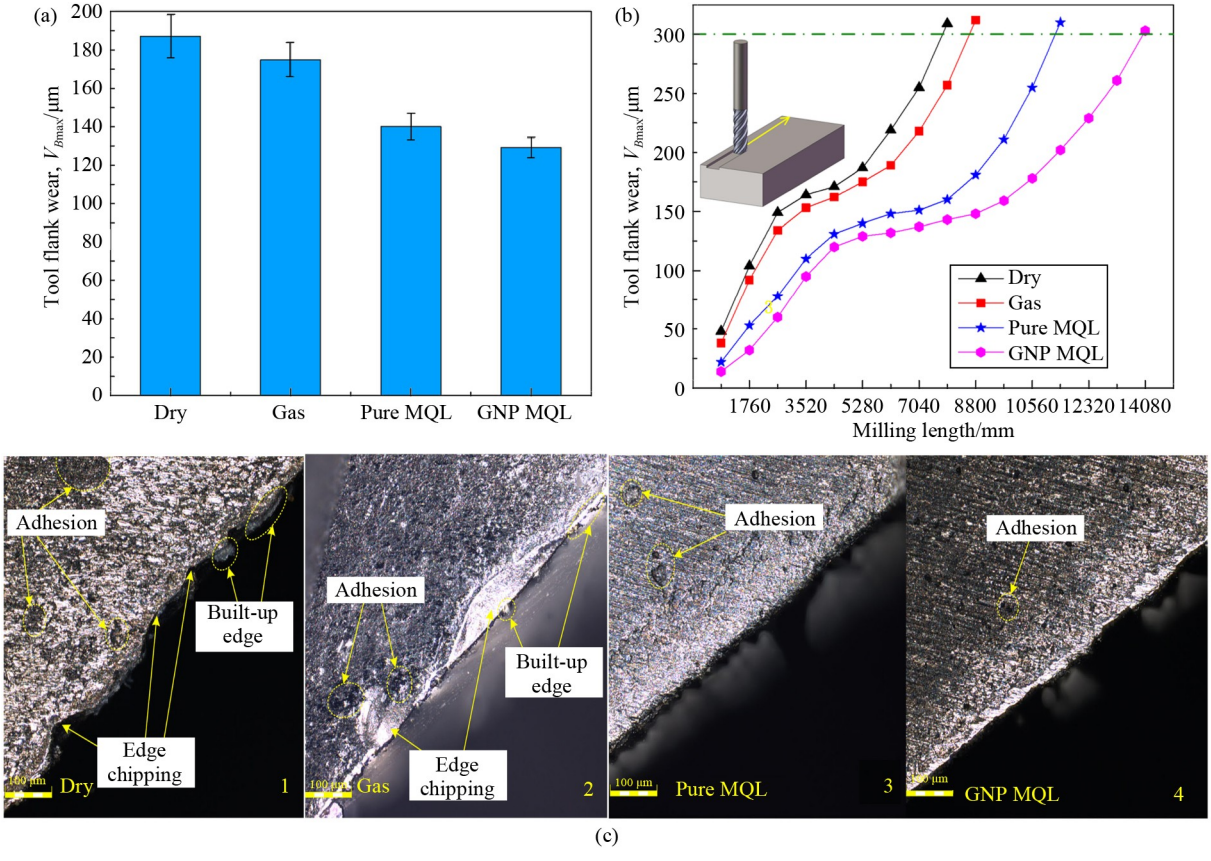

Fig. 22 Tool wear and life evolution patterns under different cooling–lubrication strategies [59]: (a) maximum width of the tool flank wear zone; (b) milling cutter wear curve; (c) cutting edge in the final stage. MQL: minimum quantity lubrication; GNP: graphene. Reproduced with permission from Springer Nature.

increased tool life by 77.78% and 33.34% compared with dry and PMQL conditions, respectively. Figure 22(c) shows the evolution of milling cutter flank wear under four conditions when the milling length reaches 5280 mm. Adhesion, edge fragmentation, and stacked edges were observed under dry and gaseous conditions. However, fewer adhesions were observed under the two other conditions. Edge fragmentation, stacking edges, and large adhesion were almost absent under PMQL and GNP NPEC conditions. GNP NPECs have significantly improved the machining performance of cutting tools.

4.2.3 Surface quality

The surface quality of the workpiece determines its performance during application, and NPEC reduces the milling temperature and tool wear, which further improves surface quality of the workpiece.

Li et al. [59] investigated the effect of dry, gas, PMQL, and GNP NPEC conditions on the surface quality of milled titanium alloys. As shown in Fig. 23(a), the surface roughness obtained a maximum value of 0.653 μm in drying conditions, and that of the workpiece was 0.647, 0.425, and 0.311 μm in the three other conditions. A minimal difference was observed between the pure gas and dry processing conditions, and the use of GNP NPECs reduced the surface roughness by 52.37% and 17.45%, respectively, compared with the drying and PMQL conditions. The lubricant film formed at the tool–workpiece contact interface under PMQL conditions reduced the milling temperature and tool wear, and the effect was further enhanced by adding GNP NPECs. High milling forces and temperatures may lead to surface craters and adhesion, and high tool wear leads to large furrows and reduced surface quality. Simultaneously, the lubricant film formed in the cutting zone separates the surface of the workpiece from the side of the cutting edge and reduces the generated adhesion, surface craters, and large grooves, as shown in Fig. 23(b). GNP NPECs further improve the surface quality of the workpiece compared with PMQL conditions because the excellent tribological properties of the GNP nano-enhanced phase improve the cooling performance of the lubricant film [218].

Roushan et al. [216,219] investigated the utilization of CuO NPECs in an MQL environment with uncoated and AlTiN-coated WC micro end mills to improve the machining performance of Ti–6Al–4V titanium alloy micro milling. Minimum average burr widths of 9.93 and 10.58 μm were obtained for up- and down-milling, respectively, with AlTiN-coated cutters under 0.25 vol.% CuO NPEC conditions. In addition, the surface roughness (*Ra*) was reduced by 81.54% when compared with that of the uncoated WC cutter under dry conditions. CuO nano-enhanced phases are spherical; thus, they can easily penetrate and embed in the fabrication of microchannels and enhance lubrication by forming a thin film between the tool and chip interface. Edelbi et al. [220] milled Ti–3Al–2.5V alloy pairs of Ti–3Al–2.5V using a two-nozzle MQL system with PVD-coated carbide. The results show that the surface roughness obtained under ZnO and Al_2O_3 NPECs is in the range of (0.312–1.032 μm) and (0.374–1.124 μm), respectively, and the ZnO NPEC is more effective than that observed under Al_2O_3 NPEC with an average *Ra* reduction of approximately 18.49%.

Yin et al. [221] investigated the effect of several typical nano-enhanced phases (Al_2O_3, MoS_2, SiO_2, CNTs, SiC, and graphite) on the surface quality of milled Ti–6Al–4V using cottonseed oil as the base. The SiO_2 NPEC treatment had the lowest surface roughness (*Ra* = 0.594 μm), which was 62.78% lower than that of the MQL treatment, followed by Al_2O_3 NPEC (*Ra* = 0.633 μm), which was 60.34% lower than that of the MQL treatment.

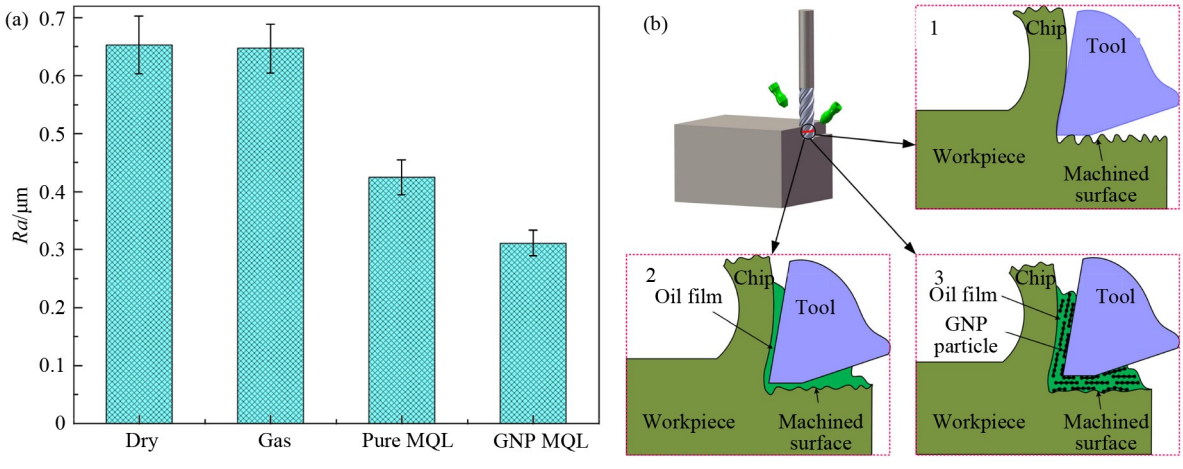

Fig. 23 (a) Surface roughness of the machined surface; (b) schematic of milling under four cooling–lubrication conditions [59]. MQL: minimum quantity lubrication; GNP: graphene. Reproduced with permission from Springer Nature.

Figure 24 shows the surface quality of the workpiece surface under different machining environments. Figure 24(d) shows that under the NPEC condition of CNTs, many scratches appeared on the surface of the workpiece. The burrs not only affect the roughness of the machined surface but also act on the tool surface, leading to additional grooves on the tool surface and exacerbating tool wear, which creates a vicious circle. Figure 24(b) shows that the workpiece surface under MoS_2 NPEC condition exhibited furrows, while that under Al_2O_3 NPEC condition revealed numerous scratches, as shown in Fig. 24(a). By contrast, the workpiece surface under SiO_2 NPEC condition has shallow scratches and the lowest surface roughness (Fig. 24(c)).

4.3 Grinding

Grinding is a basic form of machining and an important part of modern precision machining. The final accuracy and surface quality of most parts are ensured through the grinding process. The contact area of the grinding wheel with the workpiece is significantly larger than that of turning and milling, which is mainly characterized by abrasive cutting with negative rake angle, severe friction, and high specific energy [222]. Therefore, high temperatures are observed in the grinding zone, and most of the heat flows into the workpiece [223]. As the main technological bottleneck in grinding processes, heat dissipation induces a substantially short contact time between each abrasive grit and the workpiece due to the speed of the grinding wheel [224]. Simultaneously, the heat removed by the grinding debris is remarkably small. The high energy density in the grinding zone significantly affects the surface quality and performance of the workpiece. Therefore, effective measures must be taken to reduce or even eliminate the effect of grinding heat on workpiece machining accuracy and surface quality. The use of NPEC improves the heat dissipation performance. Simultaneously, the antiwear and friction reduction effects of nano-enhanced phases reduce the heat flux at the friction interface. Figure 25 shows that the NPEC can form a lubricating film with large coverage and wear resistance via self-diffusion osmosis. The lubricating film is easily bonded to the surface of the friction subsurface, which improves the stability of the oil film [225].

4.3.1 Grinding temperature

Zou et al. [226] analyzed the output response of belt grinding of titanium alloys and found that the use of MQL provided low abrasive wear and improved machined surfaces. In addition, the MQL-assisted belt grinding process resulted in good fatigue strength and compact microstructure. CNTs were applied to the grinding fluid to form a lubricant film on the surface of the grinding wheel and workpiece, reducing the generation of grinding heat to further improve the cooling effect of MQL. The addition of CNTs significantly reduced the grinding temperature by 32% and further increased the grinding rate by 48% with significant cooling effect.

Li et al. [106] measured the grinding temperature of workpiece Ti–6Al–4V under six operating conditions and presented the experimental results. Figure 26(a) shows the measurement setup for surface grinding temperatures. A type K thermocouple with a diameter of 0.30 mm was mounted in a thermocouple mounting slot with a diameter of 0.30 mm for measuring the surface grinding temperature. Figure 26(b) presents the average temperature peaks for each of the six working conditions. For grinding temperatures, the highest temperature peak of 278.932 °C was obtained under dry conditions. Under five other conditions, the T_{max} was 229.175, 203.41, 183.612, 194.914, and 200.723 °C, which were 17.838%, 27.075%, 34.173%, 30.121%, and 28.039% lower than that of the dry condition, respectively. The peak grinding

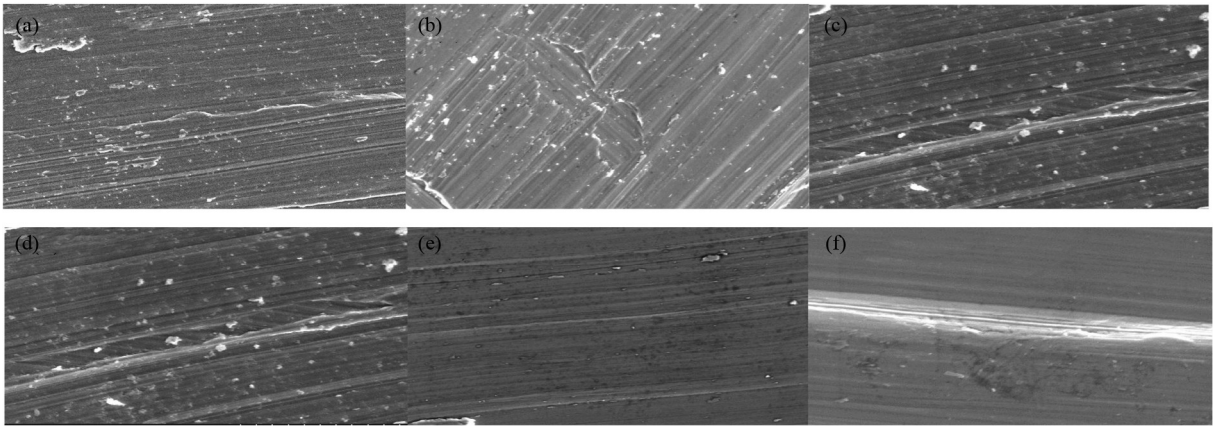

Fig. 24 Scanning electron microscope images of workpiece surface with different nanoparticle-enhanced coolants [221]: (a) Al_2O_3, (b) MoS_2, (c) SiO_2, (d) Carbon nanotubes, (e) SiC, and (f) graphite. Reproduced with permission from Springer Nature.

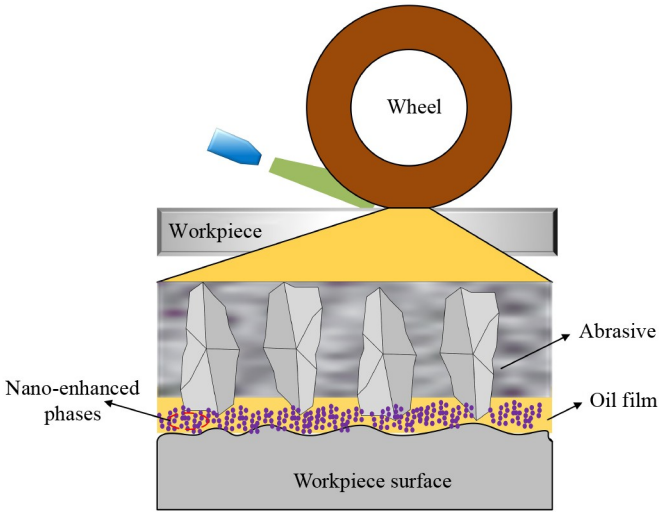

Fig. 25 Grinding mechanism.

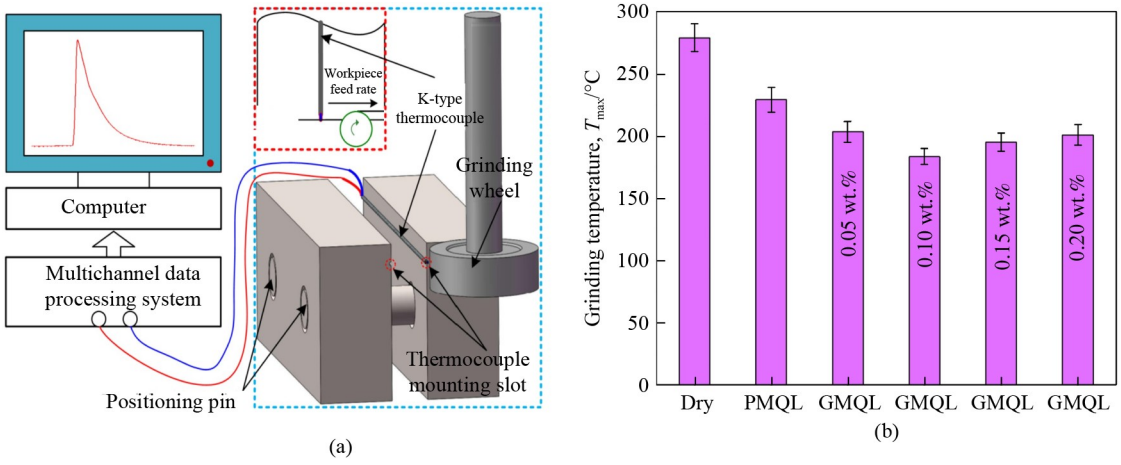

Fig. 26 (a) Measuring device for surface grinding temperature; (b) average peak temperature for six operating conditions [106]. PMQL: pure minimum quantity lubrication; GMQL: graphene minimum quantity lubrication. Reproduced with permission from Elsevier.

temperatures of PMQL, as well as four different concentrations of NPEC conditions, were significantly lower relative to the dry conditions. This finding may be due to the superior cooling capacity provided by the oil film generated by the metal saponification reaction in the grinding zone [227]. As shown in Fig. 26(b), as the concentration increased from 0.0 to 0.2 wt.%, the peak grinding temperature T_{max} first decreased and then increased, reaching a minimum at a concentration of 0.1 wt.%. This result may be attributed to the enhanced cooling capability of the oil film using a moderate amount of GNP. However, when the concentration is too low, the reinforcing effect of GNP will be reduced due to insufficient cooling. When the concentration is too high, excess GNP tends to clog the abrasive region and impedes the formation of lubricant film, thus reducing the strengthening influence of GNP due to insufficient cooling [73].

In addition, some scholars have analyzed the heat transfer behavior under the coupling of low temperature and NPECs. Zhang et al. [228] simulated the temperature field in the grinding zone under different cooling conditions. The results showed that the cooling effect of the combined process of cold air and NPEC was the best, followed by low-temperature cold air and NPECs. In addition, Zhang et al. [229] established a convective heat transfer coefficient (CHTC) model for cold air NPEC in a vortex tube based on boiling heat transfer conduction theory and numerically simulated the finite difference and temperature fields in the milling zone in a vortex tube with different cold air fractions. The simulation results show that the maximum temperature decreases and then increases with the increase of cold air fraction. The validity of the CHTC model was verified by experiments on Ti–6Al–4V.

4.3.2 Specific grinding energy

Specific grinding energy is the energy required to remove a unit volume of material and can characterize the lubrication effect at the wheel–workpiece interface [230]. Ibrahim et al. [231] prepared palm oil-based NPECs containing different percentages of GNP and evaluated the performance of Ti–6Al–4V machining using MQL. Figure 27 shows the typical values of specific cutting energy and percentage reduction for different lubrication modes. As shown in Fig. 27(a), the specific grinding energies were 193.551, 53.929, 79.709, and 75.423 J/mm^3 for dry machining, flooding, LB2000 mode, and pure palm oil–MQL lubrication modes, respectively. As shown in Fig. 27(b). The optimal value of specific energy consumption was achieved by utilizing NPEC MQL conditions with a concentration of 0.1 wt.%. GNP NPEC at a concentration of 0.1 wt.% significantly reduces specific energy by 91.87% and 80.25% compared with flood and LB2000/MQL lubrication technologies, respectively. In addition, NPEC at concentrations of 0.2, 0.3, and 0.4 wt.% saved 72.39%, 69.74%, and 66.35% of cutting energy, respectively, compared with the LB2000/MQL lubrication model. Singh et al. [50] comparatively analyzed the effect of GNP in three vegetable oils (canola, olive, and sunflower) mixed with different concentrations of GNP on the grinding force during Ti–6Al–4V grinding process. The graph in Fig. 27(d) reveals that canola oil causes a reduction in specific grinding energy by 9.72% compared with conventional cutting fluids. When GNP nano-enhanced phases were not added, the specific grinding energy was in the following order: sunflower oil < olive oil < rapeseed. However, when used with GNP nano-enhanced phases, the same order of performance was changed to olive < sunflower oil < rapeseed. A GNP concentration of 1.5 wt.% resulted in a relative reduction of 33.83% in grinding energy compared with conventional cutting fluids.

Li et al. [106] evaluated the effect of GMQL on specific grinding energy through grinding experiments. Figure 27(c) shows the specific grinding energies for six operating conditions (dry, PMQL, and four GMQLs). For specific grinding energy, a maximum of 598.384 J/mm^3 was obtained under dry conditions. In the five other conditions, the specific grinding energy was reduced by 42.978%, 59.606%, 67.375%, 62.039%, and 57.912%,

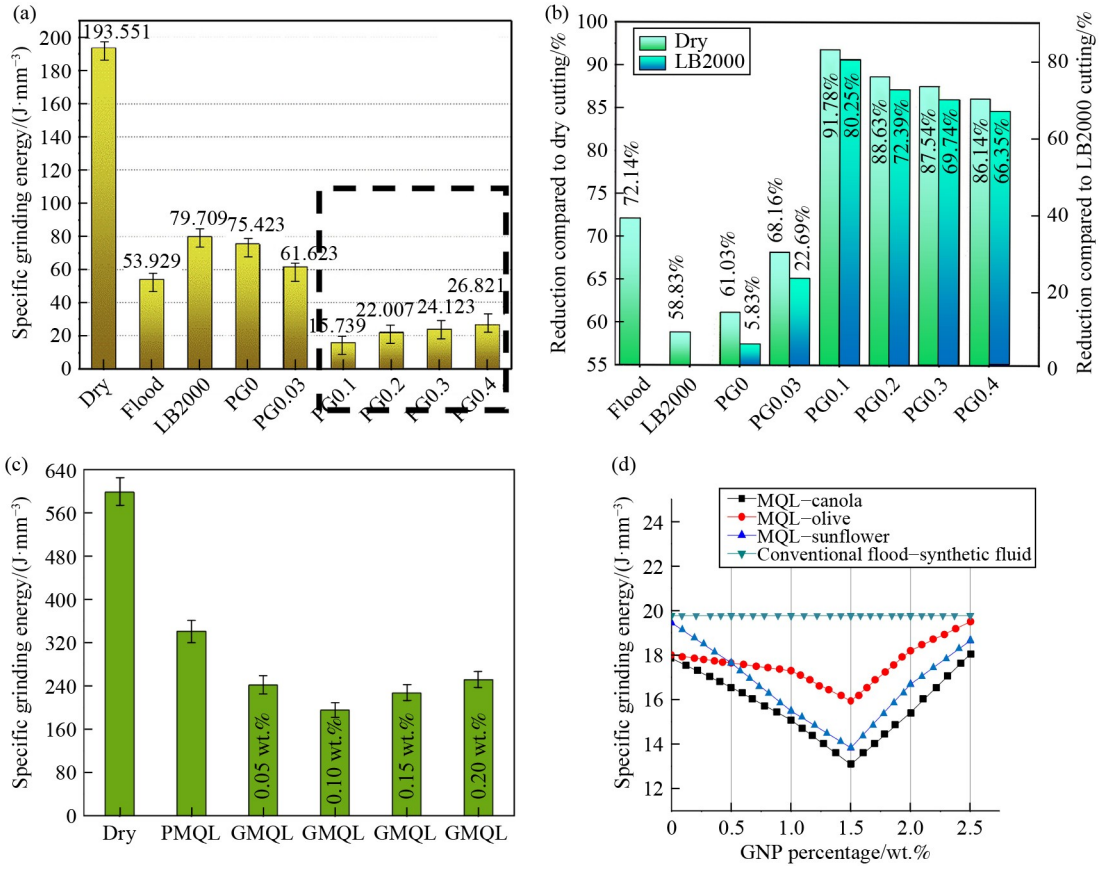

Fig. 27 (a) Effect of each lubrication method on specific grinding energy; (b) percentage reduction in specific grinding energy [231]; (c) specific grinding energy at six operating conditions [106]; (d) variation in specific grinding energy with different concentrations of graphene (GNP) in different vegetable oils [50]. MQL: minimum quantity lubrication; PMQL: pure MQL; GMQL: graphene MQL. Reproduced with permissions from Refs. [50,106,231] from Elsevier.

respectively, considering the dry condition. The oil film exhibited excellent lubrication properties after the addition of GNP nano-enhanced phases, which improved the lubrication condition in the cutting area and reduced the cutting force and COF, thus decreasing the specific grinding energy. As the concentration of NPEC increases, the specific grinding energy first decreased and then increased, reaching the minimum value at a concentration of 0.1 wt.%. This phenomenon is due to the enhanced oil film lubrication performance, which is attributed to the moderate GNP. However, when the concentration is too low, the reinforcing effect of GNP is weakened due to insufficient lubrication in the grinding area. However, when the concentration is too high, excess GNP tends to clog the grinding area and impedes the formation of the lubricant film, reducing the strengthening effect of GNP due to insufficient lubrication.

4.3.3 Surface quality

Ibrahim et al. [231] prepared palm oil-based NPEC containing different percentages of GNPs and evaluated the performance of Ti–6Al–4V processing using MQL. Under dry conditions, severe delamination can be observed on the contact surfaces due to lack of lubrication and heat dissipation in the contact zone. By contrast, under LB2000 MQL lubrication conditions, relatively smooth surfaces and minimal surface damage can be observed due to the lubricating effect of the LB2000 droplets and the effective cooling characteristics. Palm oil can provide adequate lubrication because it has highly polar molecules that adhere tightly to the contact surfaces and are used as an anti-friction layer [232]. The synergistic interaction between the GNP nano-enhanced phase and the molecular layer of palm oil yielded the best results at GNP 0.1 wt.%. In addition, GNP exhibits self-healing and crack bridging effects. Increasing GNP to 0.4 wt.% leads to an increase in the contact angle of the lubricant droplets, which reduces the wettability of the NPEC. In addition, high GNP concentrations result in high viscosity, which limits aerosol penetration into the cutting zone. Zhang et al. [130] investigated the lubrication properties of MoS_2 nano-enhanced phase palm oil-based NPEC under MQL conditions. When 2% nano-enhanced phase jet MQL milling was performed with paraffin and palm oil liquids, the corresponding *Ra* and R_z values perpendicular to the direction of the milled particles were (50.0% and 61.1%) and (41.1% and 48.2%) lower than that of dry milling, respectively. Compared with the MQL of paraffin and palm oil liquids without nano-enhanced phases, *Ra* was reduced by 25% and 30%, and R_z by 15.4% and 23.7%, respectively. This reduction is due to the strong absorption capacity and high film-forming strength of MoS_2, which increases the difficulty in breaking the oil film. MoS_2 nanofibers have minimal effect on the wear resistance of the nanofibers because they mainly wear on the surface of the friction partner to form a lubricating film. Figure 28(a) shows the surface roughness measured under the six operating conditions; in terms of surface quality, significant adhesion, grinding burns, and large furrows were observed under dry conditions. Under the PMQL and the four NPEC MQL conditions, almost no grinding burns were observed, and adhesion was significantly reduced. Especially under the NPEC condition (0.1 wt.%), almost no adhesion phenomenon was also observed. For surface roughness, the surface roughness *Ra* was reduced by 51.797% under the optimum condition of NPEC compared with the dry condition [106].

Setti et al. [233] investigated the grinding properties of Ti–6Al–4V, where Al_2O_3 NPEC improved the surface quality of Ti–6Al–4V by reducing the friction and temperature generation between the contacting surfaces. Figure 29 reveals the difference in surface morphology due to pure rapeseed oil and rapeseed oil with GNP additives. In the case of pure rapeseed oil, rough surfaces and sticky debris due to lack of heat transfer were observed on the specimen surfaces. However, in the case of rapeseed oil-based MQL, the GNP additive produced a remarkably fine and defect-free surface. The GNP additive significantly improved the tribological properties of vegetable oil. Relatively rough surfaces were observed on specimens cooled by overflow based on synthetic cutting fluids. The surface quality of the specimens was worst under dry conditions, and major surface defects such as surface burns were observed. Thus, multilayer graphene nanosheets have superior tribological potential as additives for green tribological vegetable oils [50]. Another study revealed that the best cooling lubrication was achieved at 0.1 wt.% GNP NPEC with 51.797% reduction in *Ra* compared with dry conditions. This finding may be attributed to the improved lubrication and cooling status of the grinding zone due to the oil film, thus reducing the cutting heat, COF, and cutting force and improving the surface quality. The results show that moderate GNP can enhance the lubrication and cooling capability of the oil film, which enhances the surface quality and reduces the surface roughness. In addition, the grinding process produces the work-hardening phenomenon due to the extrusion and friction of the grinding wheel and the workpiece, which accelerates the tool wear and thus reduces the surface processing quality [234]. The high temperatures generated in the grinding zone reduce work hardening but are not conducive to machining [224]. The introduction of NPECs reduces the grinding heat, while the synergistic effect of the nano-enhanced phases and the biolubricant reduces the friction and extrusion phenomena at the contact interface of the grinding wheel workpiece, avoiding the generation of work-hardening phenomena [106].

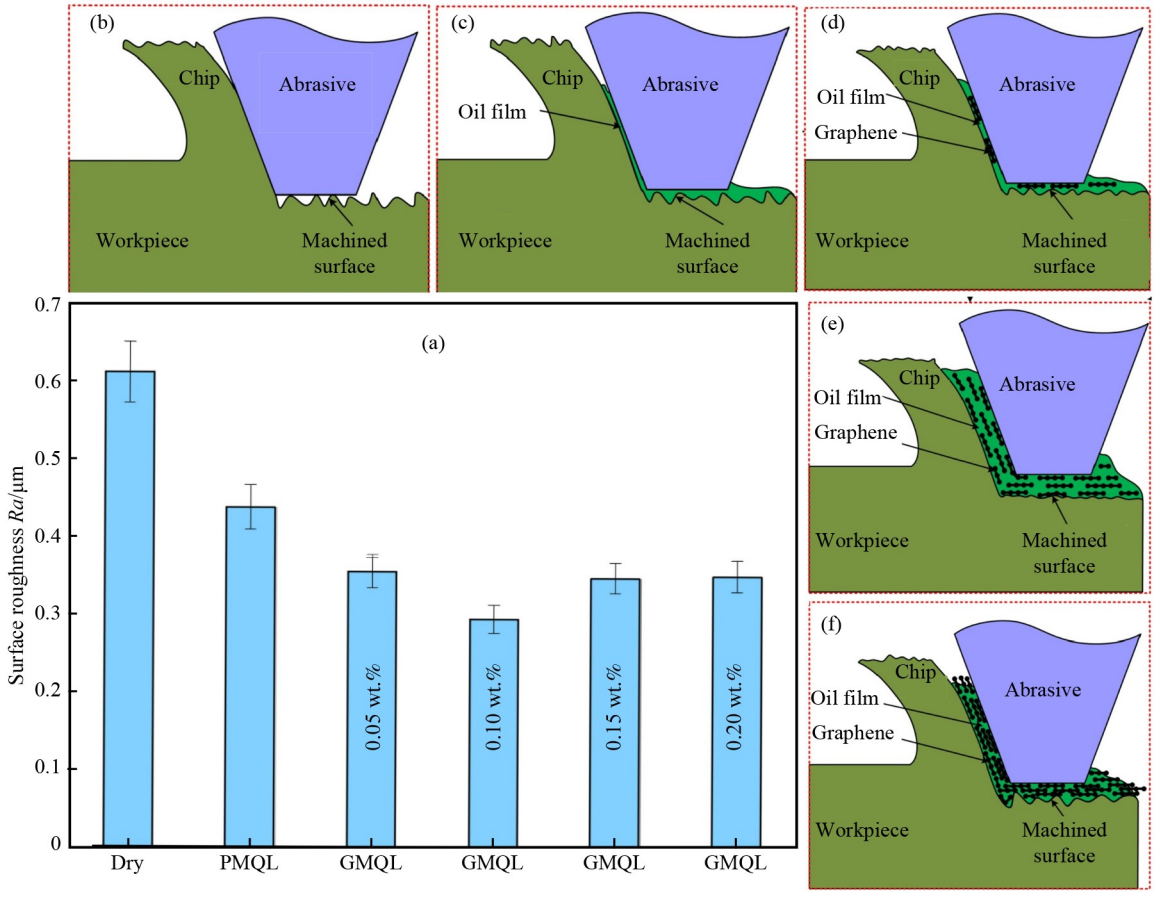

Fig. 28 (a) Surface roughness for six operating conditions; (b) dry, (c) PMQL, (d) GMQL with lower cutting fluid concentration, (e) GMQL with appropriate cutting fluid concentration, (f) GMQL with higher cutting fluid concentration [106]. GMQL: graphene minimum quantity lubrication; PMQL: pure minimum quantity lubrication. Reproduced with permission from Elsevier.

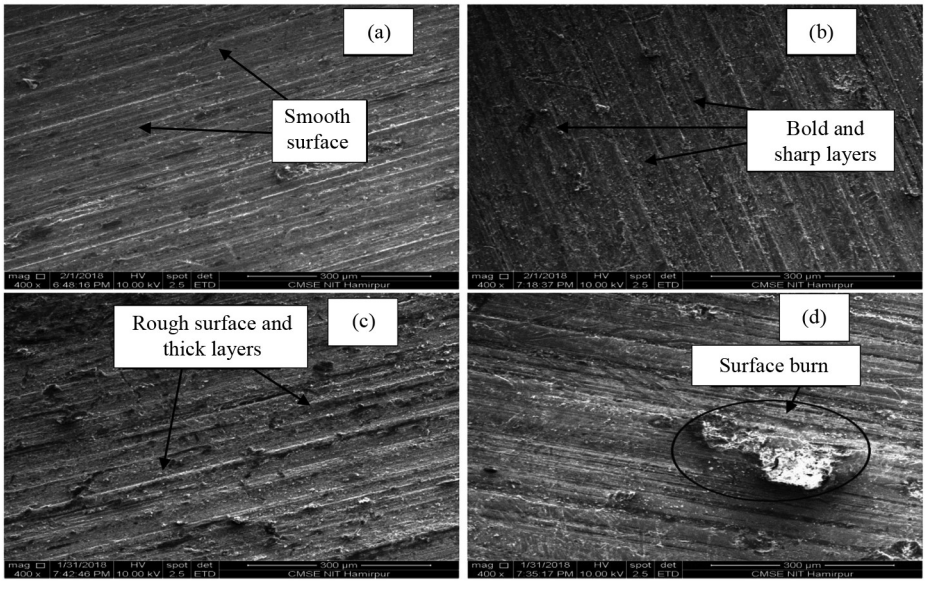

Fig. 29 Scanning electron microscope images of the surface of specimens processed under different conditions [50]: (a) graphene nanoparticle-enhanced coolant, (b) cooling based on synthetic cutting fluid, (c) pure rapeseed oil-based minimum quantity lubrication, and (d) dry grinding. Reproduced with permission from Elsevier.

4.4 Application effects

1) Turning

Overall, the application of NPEC MQL in turning achieves the desired cutting performance, and the end result is superior to the single application of pure vegetable oil-based biolubricant MQL. The NPEC in turning titanium alloys can reduce the cutting temperature by 31%–42%, increase the tool life by 178%–190%, and improve the surface quality by 58%–68% relative to dry machining. However, the application of NPEC in the turning process should still focus on the following points.

First, an optimal solution for matching the selection of different NPECs with the cutting parameters exists. Under specific NPEC conditions, additional heat is generated at the tool–workpiece contact interface when the cutting speed is high, leading to surface integrity deterioration. In this case, nano-enhanced phases with strong heat transfer properties, such as GNPs, should be selected to effectively reduce the above evaluation indexes and obtain the ideal surface quality of the workpiece. Therefore, the machining quality will be improved according to the corresponding level of cutting parameter evaluation indexes by choosing a reasonable cooling medium and its flow parameters to establish a quantitative correspondence. Second, the application of NPEC should be comprehensively explored, and the addition of hybrid nano-enhanced phases or the use of low-temperature media coordinated with textured tools can effectively enhance cutting performance and show superior results. However, if a single NPEC can obtain the workpiece surface quality required to address engineering applications, then the addition of multiple nano-enhanced phases will result in resource wastage and increased cost. Therefore, the nano-enhanced phase is accordingly rationalized for MQL-assisted machining.

2) Milling

Overall, the application of NPEC in milling achieved the desired cutting performance. The cutting temperature was reduced by 26.05%–29.91% relative to dry machining. Tool life and surface quality were increased by 31.02%–77.78% and 52.37%–81.54%, respectively. Similar to turning, milling also suffers from vegetable oil biolubricant and nano-enhanced phase selectivity. Therefore, further research is necessary to investigate the optimal combination of different vegetable oils and nano-enhanced phases under various machining parameters. Internal jet supply is gradually becoming mainstream based on the special characteristics of milling equipment, such as the structure and motion forms of tools and tool holders, but this method is mainly applicable to end mills. In addition, the use of cryogenic gases such as LN_2 can further improve the cooling effect and machining quality. However, the use of cryogenic media is highly demanding for milling cutter manufacturing and the supply system with NPEC, which increases the cost outlay. Research on the use of hybrid nano-enhanced phases for milling titanium alloys is still relatively small, but the hybrid nano-enhanced phases can synthesize their excellent properties to play a crucial role in coordination with each other.

3) Grinding

The heat generated by the same workpiece material is substantially higher than that generated by turning and milling due to the special characteristics of the grinding wheels. Surface burns still exist due to the low thermal conductivity of titanium and nickel-based alloys. Compared with dry machining, NPECs can reduce the cutting temperature by 17.8%–32% and improve the surface quality by 50.0%–61.1%. Scholars have focused on increasing the cooling capacity of cutting fluids to reduce the proportion of energy flowing into the workpiece. The use of NPEC addresses heat buildup in difficult-to-machine materials, thereby reducing surface burns and thermal softening of the workpiece. Recommended biolubricants should have high viscosity and fatty acid saturation and contain polar groups and other properties (e.g., palm and castor oils) that favor the formation of strongly adsorbed lubricant films. Nano-enhanced phases have correspondingly high hardness and spherical properties (e.g., Al_2O_3), providing excellent rolling friction reduction and anti-wear in high-pressure grinding interfaces. However, efficient matching of the grinding parameters to the type of nano-enhanced phase is also required for optimal results. Table 5 summarizes the performance of the MQL with NPEC during machining.

Overall, GNP NPECs exhibit extraordinary machining performance in turning, milling, and grinding. However, optimal volume fractions for different machining environments are lacking. In addition, the application of hybrid nano-enhanced phases can compensate for some of the cooling and lubrication capacity deficiencies that exist under the conditions of the use of single nano-enhanced phases. Meanwhile, coupling with a low-temperature medium and a multi-energy field can further improve the processing performance. However, the current research is still relatively small and should be further explored in the future.

5 Conclusions and prospects

5.1 Conclusions

The excellent heat transfer and film-forming properties of NPECs can improve direct tool–workpiece contact, reduce machining temperatures and tool wear, and improve surface quality, thereby conforming to the contemporary concept of green manufacturing for sustainable development. The following conclusions were

Table 5 NPEC processing properties

References	Cutting fluid	Working condition	Conclusion (compared with MQL)
[115,200]	Canola oil + GNP	Turning	COF: ↓ 16%–39%, *Ra*: ↓ 41%–53%, cutting temperature: ↓ 50.53 °C
[206]	Vegetable oil + MWCNTs	Turning	Energy consumption: ↓ 11.5%, tool wear: ↓ 45%
[204]	Canola oil + GNP	Turning	Tool life: ↑ 50%, tool wear: ↓ 60%
[209]	Vegetable oil + Al–GNP	Turning	Energy consumption: ↓ 1.5%, surface quality: ↑ 11%–15.7%
[192]	Distilled water + Al_2O_3–CNT	Turning	*Ra*: ↓ 8.72%, tool life: ↑ 23%
[207]	Soybean + GNP	Turning	Tool wear: ↓ 20%
[205]	Vegetable oil + GNP	Turning	Surface quality: ↑ 36%
[210]	Jojoba oil + MoS_2	Turning	*Ra*: ↓ 34.56%, tool wear: ↓ 16%
[235]	Cottonseed oil + Al_2O_3 etc.	Milling	*Ra*: Al_2O_3 < SiO_2< MoS_2 < CNTs < graphite < SiC
[236]	Vegetable oil + CuO/GNP	Milling	(CuO) *Ra*: ↓ 14.7%, (GNP) *Ra*: ↓ 21.96%
[59,218]	Vegetable oil + GNP	Milling	*Ra*: ↓ 17.45%, tool wear: ↓ 5.9%
[214]	Cottonseed oil + Al_2O_3	Milling	*Ra*: ↓ 66.7%
[215]	Olive oil + Fe_3O_4	Milling	*Ra*: ↓27.75%, tool wear: ↓ 63.3%
[35]	Distilled water + Al_2O_3	Milling	COF: ↓ 53.9%
[208]	Water + MWCNTs	Milling	*Ra*: ↓ 27%, tool wear: ↓ 34%
[171]	Vegetable oil + carbon onion	Milling	*Ra*: ↓ 46.32%
[237]	Cottonseed oil + Al_2O_3	Milling	*Ra*: ↓ 48.12%
[238]	Vegetable oil + HBN	Milling	*Ra*: ↓ 8.2%, milling temperature: ↓ 4.7%, tool wear: ↓ 5.4%
[50]	Canola oil + GNP	Grinding	*Ra*: ↓ 16.9%, specific grinding energy: ↓ 33.83%
[129]	Palm oil + GNP	Grinding	COF: ↓ 71.2%
[226]	Castor oil + CNT	Grinding	Cutting temperature: ↓ 32°C
[239]	Canola oil + GNP	Grinding	Specific grinding energy: ↓ 15.7%, *Ra*: ↓ 36.4%, COF: ↓ 40.9%
[106]	Vegetable oil + GNP	Grinding	Grinding temperature: ↓ 16.3%, specific grinding energy: ↓ 24.4%, *Ra*: ↓ 23.4%
[233]	Water + Al_2O_3−CuO	Grinding	*Ra*: ↓ 18%
[231]	Palm oil + GNP	Grinding	Specific grinding energy: ↓ 80.3%
[208]	Water + MWCNTs	Grinding	Tool wear: ↓ 34%

drawn by revealing the thermophysical properties of NPEC for MQL and their mechanism of action and verifying the effectiveness of NPEC in machining.

1) High fatty acid saturation and polar groups are key properties of vegetable oil-based fluids that improve the lubricant film adsorption capacity and strength in the cutting zone. The base fluid can be water- or vegetable oil-based depending on the cooling process and lubrication guidance. Hard or nano-enhanced phases with a layered structure can be selected depending on the interfacial load. One- and two-step methods for the preparation of NPEC have advantages and disadvantages. Thus, the two-step method is recommended for the preparation of NPECs in the industrial field. The stability of NPECs is an important bottleneck that limits their use in machining, and their stability can be achieved by physically/chemically dispersing and modulating the nano-enhanced phase in the base fluid.

2) Compared with traditional cutting fluids, the Brownian motion and heat transfer channels of NPECs markedly improve the high-temperature environment in the cutting zone. The infiltration film-forming properties of droplets are affected by surface tension and viscosity; a small surface tension leads to the high utilization and permeability of NPECs and extends the thermal boundary layer to improve heat transfer performance. NPECs with fast droplet penetration rate should be selected in the turning process, while those with large droplet diffusion area and high viscosity should be selected in the milling process.

3) NPEC is a high-performance cooling lubricant medium with cutting fluid reduction supply. The friction performance of the cutting interface is dramatically improved, with the COF reduced by 34.3% under GNP NPEC lubrication compared with palm oil lubrication, resulting in enhanced tool life and surface integrity. Compared with conventional MQL, this technology reduces cutting temperatures by approximately 26.05%–42%, increases tool life by approximately 17.8%–190%, improves tool wear by approximately 25%–42.4%, and enhances machined surface quality, including *Ra* reduction, by approximately 50.0%–81.54%.

5.2 Prospects

NPEC technology is an environmentally friendly alternative to traditional cutting fluid-flooded machining. Future development trends should focus on the following points.

1) NPECs show excellent processing performance. However, the oxidization problem of vegetable oil biolubricants in the cutting zone at non-cold temperatures limits its promotion. Considerable potential for chemical modifications, such as epoxidation, esterification, and hydrogenation, currently exists. Thus, these modifications may also be an important area of research in the future.

2) A hybrid NPEC lubrication method is proposed and validated for the coordination of cooling and lubrication properties during the machining of difficult-to-machine materials. Excellent tribological and heat transfer properties are guaranteed to improve the surface quality of the workpiece and tool wear. However, the synergistic mechanism of the particle size ratio and the proportioning concentration of the hybridized nano-enhanced phases for heat dissipation from anti-friction must be further analyzed. Simultaneously, the sustainable assessment of processing must be further improved by creating a database of NPEC and different materials and processes to provide guidance for sustainable processing in the future.

3) As the most commonly used atomization method for MQL, pneumatic atomization has several limitations. The multi-energy field atomization intelligent supply system will be a key to solving the bottleneck of the current atomization technology. The NPEC technology can then be further improved in terms of processing performance. The current experimental research and equipment development in this area still have room for improvement.

4) The current application mechanism of ultrasonic vibration, textured tool, and magnetic field empowerment-assisted NPEC needs further in-depth study. Simultaneously, the key technology of intelligent supply should be combined to establish the mapping relationship between machining and optimal empowerment parameters, which can realize the large-scale application of intelligent technology in industrialization at an early date.

Nomenclature

BUE	Built-up edge
CBN	Cubic boron nitride
CHTC	Convective heat transfer coefficient
CNT	Carbon nanotube
COF	Coefficient of friction
CTAB	Cetyltrimethylammonium bromide
EG	Ethylene glycol
GA	Gum Arabic
GMQL	Graphene minimum quantity lubrication
GNP	Graphene
Grad$T$	Temperature gradient
HBN	Hexagonal boron nitride
MQL	Minimum quantity lubrication
MWCNT	Multi-walled carbon nanotube
ND	Diamond
NPEC	Nanoparticle-enhanced coolant
PCD	Polycrystalline diamond
PMQL	Pure minimum quantity lubrication
PTFE	Polytetrafluoroethylene
SDBS	Sodium dodecylbenzene sulfonate
SDS	Sodium dodecyl sulfate
SEM	Scanning electron microscope
TCIT	Tool–chip interface

Acknowledgements This study was financially supported by the National Key R&D Program of China (Grant No. 2020YFB2010500), the National Natural Science Foundation of China (Grant Nos. 52105457 and 51975305), the Special Fund of Taishan Scholars Project, China (Grant No. tsqn202211179), the Youth Talent Promotion Project in Shandong, China (Grant No. SDAST2021qt12), and the Natural Science Foundation of Shandong Province, China (Grant Nos. ZR2023QE057, ZR2022QE028, ZR2021QE116, and ZR2020KE027).

Conflict of Interest The authors declare that they have no conflict of interest.

References

1. Kim J H, Kim E J, Lee C M. A study on the heat affected zone and machining characteristics of difficult-to-cut materials in laser and induction assisted machining. Journal of Manufacturing Processes, 2020, 57: 499–508
2. Gao T, Li C H, Wang Y Q, Liu X S, An Q L, Li H N, Zhang Y B, Cao H J, Liu B, Wang D Z, Said Z, Debnath S, Jamil M, Ali H M, Sharma S. Carbon fiber reinforced polymer in drilling: from damage mechanisms to suppression. Composite Structures, 2022, 286: 115232
3. Wu S J, Wei L, Guo G Q, Zhang S Q, Li C H, Chen M, Wang D Z. Study on the mechanism of AL2024-T351/Ti–6Al–4V

laminated materials by ultrasonic vibration drilling. Archives of Civil and Mechanical Engineering, 2022, 22(4): 161

4. Liu M Z, Li C H, Cao H J, Zhang S, Chen Y, Liu B, Zhang N Q, Zhou Z M. Research progresses and applications of CMQL machining technology. China Mechanical Engineering, 2022, 33(5): 529–550 (in Chinese)
5. Zhou S, Wang D Z, Wu S J, Gu G Q, Dong G J, An Q L, Guo H, Li C H. Minimum quantity lubrication machining nickel base alloy: a comprehensive review. The International Journal of Advanced Manufacturing Technology, 2023 (in press)
6. Duan Z J, Li C H, Zhang Y B, Dong L, Bai X F, Yang M, Jia D Z, Li R Z, Cao H J, Xu X F. Milling surface roughness for 7050 aluminum alloy cavity influenced by nozzle position of nanofluid minimum quantity lubrication. Chinese Journal of Aeronautics, 2021, 34(6): 33–53
7. Duan Z J, Li C H, Zhang Y B, Yang M, Gao T, Liu X, Li R Z, Said Z, Debnath S, Sharma S. Mechanical behavior and semiempirical force model of aerospace aluminum alloy milling using nano biological lubricant. Frontiers of Mechanical Engineering, 2023, 18(1): 4
8. Yin Q G, Li C H, Dong L, Bai X F, Zhang Y B, Yang M, Jia D Z, Li R Z, Liu Z Q. Effects of physicochemical properties of different base oils on friction coefficient and surface roughness in MQL milling AISI 1045. International Journal of Precision Engineering and Manufacturing-Green Technology, 2021, 8(6): 1629–1647
9. Zhu L B, Cao H J, Huang H H, Liu Z F. Air cooling system thermodynamic analysis and thermal balance control of dry cutting machine tool. Journal of Mechanical Engineerin, 2019, 55(5): 204–211
10. Wang X M, Li C H, Zhang Y B, Yang M. Zhou Z M, Chen Y, Liu B, Wang D Z. Research progress on key technology of enabled atomization and supply system of minimum quantity lubrication. Surface Technology, 2022, 51(9): 1–14
11. Gao T, Li C H, Zhang Y B, Yang M, Cao H J, Wang D Z, Liu X, Zhou Z M, Liu B. Mechanical behavior of material removal and predictive force model for CFRP grinding using nano reinforced biological lubricant. Journal of Mechanical Engineering, 2023, 59(13): 325–342 (in Chinese)
12. Bai X F, Zhou F M, Li C H, Dong L, Lv X J, Yin Q G. Physicochemical properties of degradable vegetable-based oils on minimum quantity lubrication milling. The International Journal of Advanced Manufacturing Technology, 2020, 106(9–10): 4143–4155
13. Gupta M K, Khan A M, Song Q H, Liu Z Q, Khalid Q S, Jamil M, Kuntoğlu M, Usca Ü A, Sarıkaya M, Pimenov D Y. A review on conventional and advanced minimum quantity lubrication approaches on performance measures of grinding process. The International Journal of Advanced Manufacturing Technology, 2021, 117(3–4): 729–750
14. Osman K A, Ünver H Ö, Şeker U. Application of minimum quantity lubrication techniques in machining process of titanium alloy for sustainability: a review. The International Journal of Advanced Manufacturing Technology, 2019, 100(9–12): 2311–2332
15. Pervaiz S, Anwar S, Qureshi I, Ahmed N. Recent advances in the machining of titanium alloys using minimum quantity lubrication (MQL) based techniques. International Journal of Precision Engineering and Manufacturing-Green Technology, 2019, 6(1): 133–145
16. Sarikaya M, Gupta M K, Tomaz I, Danish M, Mia M, Rubaiee S, Jamil M, Pimenov D Y, Khanna N. Cooling techniques to improve the machinability and sustainability of light-weight alloys: a state-of-the-art review. Journal of Manufacturing Processes, 2021, 62: 179–201
17. Singh G, Gupta M K, Hegab H, Khan A M, Song Q H, Liu Z Q, Mia M, Jamil M, Sharma V S, Sarikaya M, Pruncu C I. Progress for sustainability in the mist assisted cooling techniques: a critical review. The International Journal of Advanced Manufacturing Technology, 2020, 109(1–2): 345–376
18. Jia D Z, Li C H, Liu J H, Zhang Y B, Yang M, Gao T, Said Z, Sharma S. Prediction model of volume average diameter and analysis of atomization characteristics in electrostatic atomization minimum quantity lubrication. Friction, 2023, 11(11): 2107–2131
19. Cui X, Li C H, Ding W F, Chen Y, Mao C, Xu X F, Liu B, Wang D Z, Li H N, Zhang Y B, Said Z, Debnath S, Jamil M, Ali H M, Sharma S. Minimum quantity lubrication machining of aeronautical materials using carbon group nanolubricant: from mechanisms to application. Chinese Journal of Aeronautics, 2022, 35(11): 85–112
20. Jia D Z, Zhang N Q, Liu B, Zhou Z M, Wang X P, Zhang Y B, Mao C, Li C H. Particle size distribution characteristics of electrostatic minimum quantity lubrication and grinding surface quality evaluation. Diamond & Abrasives Engineering, 2021, 41(3): 89–95
21. Said Z, Sundar L S, Tiwari A K, Ali H M, Sheikholeslami M, Bellos E, Babar H. Recent advances on the fundamental physical phenomena behind stability, dynamic motion, thermophysical properties, heat transport, applications, and challenges of nanofluids. Physics Reports, 2022, 946: 1–94
22. Sharma A K, Tiwari A K, Dixit A R. Effects of minimum quantity lubrication (MQL) in machining processes using conventional and nanofluid based cutting fluids: a comprehensive review. Journal of Cleaner Production, 2016, 127: 1–18
23. Sharma A K, Tiwari A K, Dixit A R. Progress of nanofluid application in machining: a review. Materials and Manufacturing Processes, 2015, 30(7): 813–828
24. Sidik N A C, Samion S, Ghaderian J, Yazid M N A W M. Recent progress on the application of nanofluids in minimum quantity lubrication machining: a review. International Journal of Heat and Mass Transfer, 2017, 108: 79–89
25. Said Z, Gupta M, Hegab H, Arora N, Khan A M, Jamil M, Bellos E. A comprehensive review on minimum quantity lubrication (MQL) in machining processes using nano-cutting fluids. The International Journal of Advanced Manufacturing Technology, 2019, 105(5–6): 2057–2086
26. Sen B, Mia M, Krolczyk G M, Mandal U K, Mondal S P. Eco-friendly cutting fluids in minimum quantity lubrication assisted machining: a review on the perception of sustainable manufacturing. International Journal of Precision Engineering and Manufacturing-Green Technology, 2021, 8(1): 249–280
27. Wickramasinghe K C, Sasahara H, Rahim E A, Perera G I P.

Green metalworking fluids for sustainable machining applications: a review. Journal of Cleaner Production, 2020, 257: 120552
28. Wang X M, Li C H, Zhang Y B, Ding W F, Yang M, Gao T, Cao H J, Xu X F, Wang D Z, Said Z, Debnath S, Jamil M, Ali H M. Vegetable oil-based nanofluid minimum quantity lubrication turning: academic review and perspectives. Journal of Manufacturing Processes, 2020, 59: 76–97
29. Chinchanikar S, Kore S S, Hujare P. A review on nanofluids in minimum quantity lubrication machining. Journal of Manufacturing Processes, 2021, 68: 56–70
30. Kulkarni P, Chinchanikar S. A review on machining of nickel-based superalloys using nanofluids under minimum quantity lubrication (NFMQL). Journal of the Institution of Engineers: Series C, 2023, 104(1): 183–199
31. Baldin V, da Silva L R R, Machado A R, Houck C F. State of the art of biodegradable nanofluids application in machining processes. International Journal of Precision Engineering and Manufacturing-Green Technology, 2023, 10(5): 1299–1336
32. Zhang Y B, Li H N, Li C H, Huang C Z, Ali H M, Xu X F, Mao C, Ding W F, Cui X, Yang M, Yu T B, Jamil M, Gupta M K, Jia D Z, Said Z. Nano-enhanced biolubricant in sustainable manufacturing: from processability to mechanisms. Friction, 2023, 11(5): 836–837
33. Liu M Z, Li C H, Zhang Y B, An Q L, Yang M, Gao T, Mao C, Liu B, Cao H J, Xu X F, Said Z, Debnath S, Jamil M, Ali H M, Sharma S. Cryogenic minimum quantity lubrication machining: from mechanism to application. Frontiers of Mechanical Engineering, 2021, 16(4): 649–697
34. Cui X, Li C H, Zhang Y B, Ding W F, An Q L, Liu B, Li H N, Said Z, Sharma S, Li R Z, Debnath S. Comparative assessment of force, temperature, and wheel wear in sustainable grinding aerospace alloy using biolubricant. Frontiers of Mechanical Engineering, 2023, 18(1): 3
35. Kumar A S, Deb S, Paul S. Tribological characteristics and micromilling performance of nanoparticle enhanced water based cutting fluids in minimum quantity lubrication. Journal of Manufacturing Processes, 2020, 56: 766–776
36. Mao C, Zhang J, Huang Y, Zou H F, Huang X M, Zhou Z X. Investigation on the effect of nanofluid parameters on MQL grinding. Materials and Manufacturing Processes, 2013, 28(4–6): 436–442
37. Tang L Z, Zhang Y B, Li C H, Zhou Z M, Nie X L, Chen Y, Cao H J, Liu B, Zhang N Q, Said Z, Debnath S, Jamil M, Ali H M, Sharma S. Biological stability of water-based cutting fluids: progress and application. Chinese Journal of Mechanical Engineering, 2022, 35(1): 3
38. Najiha M S, Rahman M M, Yusoff A R. Flank wear characterization in aluminum alloy (6061 T6) with nanofluid minimum quantity lubrication environment using an uncoated carbide tool. Journal of Manufacturing Science and Engineering, 2015, 137(6): 061004
39. Liu N C, Zou X, Yuan J, Wu S H, Chen Y. Performance evaluation of castor oil-ethanol blended coolant under minimum quantity lubrication turning of difficult-to-machine materials. Journal of Manufacturing Processes, 2020, 58: 1–10
40. Yıldırım Ç V, Kıvak T, Sarıkaya M, Erzincanlı F. Determination of MQL parameters contributing to sustainable machining in the milling of nickel-base superalloy Waspaloy. Arabian Journal for Science and Engineering, 2017, 42(11): 4667–4681
41. R S, N R J H, J S K, Krolczyk G M. A comprehensive review on research developments of vegetable-oil based cutting fluids for sustainable machining challenges. Journal of Manufacturing Processes, 2021, 67: 286–313
42. Kui G W A, Islam S, Reddy M M, Khandoker N, Chen V L C. Recent progress and evolution of coolant usages in conventional machining methods: a comprehensive review. The International Journal of Advanced Manufacturing Technology, 2022, 119(1–2): 3–40
43. Tawakoli T, Hadad M J, Sadeghi M H, Daneshi A, Stöckert S, Rasifard A. An experimental investigation of the effects of workpiece and grinding parameters on minimum quantity lubrication—MQL grinding. International Journal of Machine Tools and Manufacture, 2009, 49(12–13): 924–932
44. Ejaz A, Babar H, Ali H M, Jamil F, Janjua M M, Fattah I M R, Said Z, Li C H. Concentrated photovoltaics as light harvesters: outlook, recent progress, and challenges. Sustainable Energy Technologies and Assessments, 2021, 46: 101199
45. Rodriguez R L, Lopes J C, Garcia M V, Fonteque Ribeiro F S, Diniz A E, Eduardo de Ângelo Sanchez L, José de Mello H, Roberto de Aguiar P, Bianchi E C. Application of hybrid eco-friendly MQL+WCJ technique in AISI 4340 steel grinding for cleaner and greener production. Journal of Cleaner Production, 2021, 283: 124670
46. Xavior M A, Adithan M. Determining the influence of cutting fluids on tool wear and surface roughness during turning of AISI 304 austenitic stainless steel. Journal of Materials Processing Technology, 2009, 209(2): 900–909
47. Khan M M A, Mithu M A H, Dhar N R. Effects of minimum quantity lubrication on turning AISI 9310 alloy steel using vegetable oil-based cutting fluid. Journal of Materials Processing Technology, 2009, 209(15–16): 5573–5583
48. Wang Y G, Li C H, Zhang Y B, Yang M, Li B K, Jia D Z, Hou Y L, Mao C. Experimental evaluation of the lubrication properties of the wheel/workpiece interface in minimum quantity lubrication (MQL) grinding using different types of vegetable oils. Journal of Cleaner Production, 2016, 127: 487–499
49. Ojolo S J, Bamgboye A I, Ogunsina B S, Oke S A. Analytical approach for predicting biogas generation in a municipal solid waste anaerobic digester. Iranian Journal of Environmental Health Sciences & Engineering, 2008, 5(3): 179–186
50. Singh H, Sharma V S, Dogra M. Exploration of graphene assisted vegetables oil based minimum quantity lubrication for surface grinding of TI–6AL–4V-ELI. Tribology International, 2020, 144: 106113
51. Dong L, Li C H, Zhou F M, Bai X F, Gao W, Duan Z J, Li X P, Lv X J, Zhang F B. Temperature of the 45 steel in the minimum quantity lubricant milling with different biolubricants. The International Journal of Advanced Manufacturing Technology, 2021, 113(9–10): 2779–2790
52. Guo S M, Li C H, Zhang Y B, Wang Y G, Li B K, Yang M, Zhang X P, Liu G T. Experimental evaluation of the lubrication performance of mixtures of castor oil with other vegetable oils in

MQL grinding of nickel-based alloy. Journal of Cleaner Production, 2017, 140: 1060–1076

53. Guo S M, Li C H, Zhang Y B, Yang M, Jia D Z, Zhang X P, Liu G T, Li R Z, Bing Z R, Ji H J. Analysis of volume ratio of castor/soybean oil mixture on minimum quantity lubrication grinding performance and microstructure evaluation by fractal dimension. Industrial Crops and Products, 2018, 111: 494–505
54. Jia D Z, Li C H, Zhang Y B, Yang M, Wang Y G, Guo S M, Cao H J. Specific energy and surface roughness of minimum quantity lubrication grinding Ni-based alloy with mixed vegetable oil-based nanofluids. Precision Engineering, 2017, 50: 248–262
55. Ozcelik B, Kuram E, Cetin M H, Demirbas E. Experimental investigations of vegetable based cutting fluids with extreme pressure during turning of AISI 304L. Tribology International, 2011, 44(12): 1864–1871
56. Sani A S A, Rahim E A, Sharif S, Sasahara H. Machining performance of vegetable oil with phosphonium- and ammonium-based ionic liquids via MQL technique. Journal of Cleaner Production, 2019, 209: 947–964
57. Padmini R, Krishna P V, Rao G K M. Effectiveness of vegetable oil based nanofluids as potential cutting fluids in turning AISI 1040 steel. Tribology International, 2016, 94: 490–501
58. Wang Y G, Li C H, Zhang Y B, Yang M, Li B K, Dong L, Wang J. Processing characteristics of vegetable oil-based nanofluid MQL for grinding different workpiece materials. International Journal of Precision Engineering and Manufacturing-Green Technology, 2018, 5(2): 327–339
59. Li M, Yu T B, Zhang R C, Yang L, Li H Y, Wang W S. MQL milling of TC4 alloy by dispersing graphene into vegetable oil-based cutting fluid. The International Journal of Advanced Manufacturing Technology, 2018, 99(5–8): 1735–1753
60. Rahmati B, Sarhan A A D, Sayuti M. Morphology of surface generated by end milling AL6061-T6 using molybdenum disulfide (MoS_2) nanolubrication in end milling machining. Journal of Cleaner Production, 2014, 66: 685–691
61. Sayuti M, Sarhan A A D, Hamdi M. An investigation of optimum SiO_2 nanolubrication parameters in end milling of aerospace Al6061-T6 alloy. The International Journal of Advanced Manufacturing Technology, 2013, 67(1–4): 833–849
62. Paturi U M R, Maddu Y R, Maruri R R, Reddy Narala S K. Measurement and analysis of surface roughness in WS_2 solid lubricant assisted minimum quantity lubrication (MQL) turning of Inconel 718. Procedia CIRP, 2016, 40: 138–143
63. Yıldırım Ç V, Kıvak T, Erzincanlı F. Tool wear and surface roughness analysis in milling with ceramic tools of Waspaloy: a comparison of machining performance with different cooling methods. Journal of the Brazilian Society of Mechanical Sciences and Engineering, 2019, 41(2): 83
64. Yıldırım Ç V, Sarıkaya M, Kıvak T, Şirin Ş. The effect of addition of HBN nanoparticles to nanofluid-MQL on tool wear patterns, tool life, roughness and temperature in turning of Ni-based Inconel 625. Tribology International, 2019, 134: 443–456
65. Tevet O, Von-Huth P, Popovitz-Biro R, Rosentsveig R, Wagner H D, Tenne R. Friction mechanism of individual multilayered nanoparticles. Proceedings of the National Academy of Sciences of the United States of America, 2011, 108(50): 19901–19906
66. Choudhary A, Naskar A, Paul S. An investigation on application of nano-fluids in high speed grinding of sintered alumina. Journal of Manufacturing Processes, 2018, 35: 624–633
67. Musavi S H, Davoodi B, Niknam S A. Effects of reinforced nanoparticles with surfactant on surface quality and chip formation morphology in MQL-turning of superalloys. Journal of Manufacturing Processes, 2019, 40: 128–139
68. Kao M J, Lin C R. Evaluating the role of spherical titanium oxide nanoparticles in reducing friction between two pieces of cast iron. Journal of Alloys and Compounds, 2009, 483(1–2): 456–459
69. Jamil M, Khan A M, Hegab H, Gupta M K, Mia M, He N, Zhao G L, Song Q H, Liu Z Q. Milling of Ti–6Al–4V under hybrid Al_2O_3-MWCNT nanofluids considering energy consumption, surface quality, and tool wear: a sustainable machining. The International Journal of Advanced Manufacturing Technology, 2020, 107(9–10): 4141–4157
70. He T, Liu N C, Xia H Z, Wu L, Zhang Y, Li D G, Chen Y. Progress and trend of minimum quantity lubrication (MQL): a comprehensive review. Journal of Cleaner Production, 2023, 386: 135809
71. Dubey V, Sharma A K, Pimenov D Y. Prediction of surface roughness using machine learning approach in MQL turning of AISI 304 steel by varying nanoparticle size in the cutting fluid. Lubricants, 2022, 10(5): 81
72. Khajehzadeh M, Moradpour J, Razfar M R. Influence of nanolubricant particles' size on flank wear in hard turning. Materials and Manufacturing Processes, 2019, 34(5): 494–501
73. Lee P H, Kim J W, Lee S W. Experimental characterization on eco-friendly micro-grinding process of titanium alloy using air flow assisted electrospray lubrication with nanofluid. Journal of Cleaner Production, 2018, 201: 452–462
74. Yuan S M, Hou X B, Wang L, Chen B C. Experimental investigation on the compatibility of nanoparticles with vegetable oils for nanofluid minimum quantity lubrication machining. Tribology Letters, 2018, 66(3): 106
75. Talib N, Sasahara H, Rahim E A. Evaluation of modified jatropha-based oil with hexagonal boron nitride particle as a biolubricant in orthogonal cutting process. The International Journal of Advanced Manufacturing Technology, 2017, 92(1–4): 371–391
76. Pal A, Chatha S S, Sidhu H S. Performance evaluation of various vegetable oils and distilled water as base fluids using eco-friendly MQL technique in drilling of AISI 321 stainless steel. International Journal of Precision Engineering and Manufacturing-Green Technology, 2022, 9(3): 745–764
77. Bai X F, Jiang J, Li C H, Dong L, Ali H M, Sharma S. Tribological performance of different concentrations of Al_2O_3 nanofluids on minimum quantity lubrication milling. Chinese Journal of Mechanical Engineering, 2023, 36(1): 11
78. Sen B, Mia M, Gupta M K, Rahman M A, Mandal U K, Mondal S P. Influence of Al_2O_3 and palm oil-mixed nano-fluid on machining performances of Inconel-690: IF-THEN rules-based FIS model in eco-benign milling. The International Journal of Advanced Manufacturing Technology, 2019, 103(9–12): 3389–3403
79. Wang Y G, Li C H, Zhang Y B, Yang M, Zhang X P, Zhang N Q, Dai J J. Experimental evaluation on tribological performance of

the wheel/workpiece interface in minimum quantity lubrication grinding with different concentrations of Al_2O_3 nanofluids. Journal of Cleaner Production, 2017, 142: 3571–3583

80. Ali H M, Babar H, Shah T R, Sajid M U, Qasim M A, Javed S. Preparation techniques of TiO_2 nanofluids and challenges: a review. Applied Sciences, 2018, 8(4): 587
81. Kıvak T, Sarıkaya M, Yıldırım Ç V, Şirin Ş. Study on turning performance of PVD TiN coated Al_2O_3+TiCN ceramic tool under cutting fluid reinforced by nano-sized solid particles. Journal of Manufacturing Processes, 2020, 56: 522–539
82. Judran H K, Al-Hasnawi A G T, Al Zubaidi F N, Al-Maliki W A K, Alobaid F, Epple B. A high thermal conductivity of MgO−H_2O nanofluid prepared by two-step technique. Applied Sciences, 2022, 12(5): 2655
83. Sharma B, Sharma S K, Gupta S M, Kumar A. Modified two-step method to prepare long-term stable CNT nanofluids for heat transfer applications. Arabian Journal for Science and Engineering, 2018, 43(11): 6155–6163
84. Singh K, Sharma S K, Gupta S M. Preparation of long duration stable CNT nanofluid using SDS. Integrated Ferroelectrics, 2020, 204(1): 11–22
85. Chen Z X, Shahsavar A, Al-Rashed A A A A, Afrand M. The impact of sonication and stirring durations on the thermal conductivity of alumina−liquid paraffin nanofluid: an experimental assessment. Powder Technology, 2020, 360: 1134–1142
86. Babita, Sharma S K, Gupta S M. Preparation and evaluation of stable nanofluids for heat transfer application: a review. Experimental Thermal and Fluid Science, 2016, 79: 202–212
87. Dhinesh Kumar D, Valan Arasu A. A comprehensive review of preparation, characterization, properties and stability of hybrid nanofluids. Renewable & Sustainable Energy Reviews, 2018, 81: 1669–1689
88. Chakraborty S, Sarkar I, Haldar K, Pal S K, Chakraborty S. Synthesis of Cu−Al layered double hydroxide nanofluid and characterization of its thermal properties. Applied Clay Science, 2015, 107: 98–108
89. Chakraborty S, Sarkar I, Ashok A, Sengupta I, Pal S K, Chakraborty S. Thermo-physical properties of Cu-Zn-Al LDH nanofluid and its application in spray cooling. Applied Thermal Engineering, 2018, 141: 339–351
90. Mansour D E A, Elsaeed A M, Izzularab M A. The role of interfacial zone in dielectric properties of transformer oil-based nanofluids. IEEE Transactions on Dielectrics and Electrical Insulation, 2016, 23(6): 3364–3372
91. Nguyen V S, Rouxel D, Hadji R, Vincent B, Fort Y. Effect of ultrasonication and dispersion stability on the cluster size of alumina nanoscale particles in aqueous solutions. Ultrasonics Sonochemistry, 2011, 18(1): 382–388
92. Sadeghi R, Etemad S G, Keshavarzi E, Haghshenasfard M. Investigation of alumina nanofluid stability by UV-Vis spectrum. Microfluidics and Nanofluidics, 2015, 18(5–6): 1023–1030
93. Shahsavar A, Salimpour M R, Saghafian M, Shafii M B. An experimental study on the effect of ultrasonication on thermal conductivity of ferrofluid loaded with carbon nanotubes. Thermochimica Acta, 2015, 617: 102–110
94. Elsheikh A H, Elaziz M A, Das S R, Muthuramalingam T, Lu S F. A new optimized predictive model based on political optimizer for eco-friendly MQL-turning of AISI 4340 alloy with nano-lubricants. Journal of Manufacturing Processes, 2021, 67: 562–578
95. Vatanparast H, Shahabi F, Bahramian A, Javadi A, Miller R. The role of electrostatic repulsion on increasing surface activity of anionic surfactants in the presence of hydrophilic silica nanoparticles. Scientific Reports, 2018, 8(1): 7251
96. Mao C, Zou H F, Zhou X, Huang Y, Gan H Y, Zhou Z X. Analysis of suspension stability for nanofluid applied in minimum quantity lubricant grinding. The International Journal of Advanced Manufacturing Technology, 2014, 71(9–12): 2073–2081
97. Behera B C, Chetan, Setti D, Ghosh S, Rao P V. Spreadability studies of metal working fluids on tool surface and its impact on minimum amount cooling and lubrication turning. Journal of Materials Processing Technology, 2017, 244: 1–16
98. Shukla R, Tiwari A K, Agarawal S. Effects of surfactant and MoO_3 nanofluid on tribological and machining characteristics in minimum quantity lubrication (MQL)-turning of AISI 304 steel. Proceedings of the Institution of Mechanical Engineers, Part E: Journal of Process Mechanical Engineering, 2022
99. Şirin E, Kıvak T, Yıldırım Ç V. Effects of mono/hybrid nanofluid strategies and surfactants on machining performance in the drilling of Hastelloy X. Tribology International, 2021, 157: 106894
100. Amiri A, Naraghi M, Ahmadi G, Soleymaniha M, Shanbedi M. A review on liquid-phase exfoliation for scalable production of pure graphene, wrinkled, crumpled and functionalized graphene and challenges. FlatChem, 2018, 8: 40–71
101. Koca H D, Doganay S, Turgut A, Tavman I H, Saidur R, Mahbubul I M. Effect of particle size on the viscosity of nanofluids: a review. Renewable & Sustainable Energy Reviews, 2018, 82: 1664–1674
102. Baldin V, da Silva L R R, Gelamo R V, Iglesias A B, da Silva R B, Khanna N, Rocha Machado A. Influence of graphene nanosheets on thermo-physical and tribological properties of sustainable cutting fluids for MQL application in machining processes. Lubricants, 2022, 10(8): 193
103. Gajrani K K, Suvin P S, Kailas S V, Sankar M R. Thermal, rheological, wettability and hard machining performance of MoS_2 and CaF_2 based minimum quantity hybrid nano-green cutting fluids. Journal of Materials Processing Technology, 2019, 266: 125–139
104. Li B K, Li C H, Zhang Y B, Wang Y G, Jia D Z, Yang M, Zhang N Q, Wu Q D, Han Z G, Sun K. Heat transfer performance of MQL grinding with different nanofluids for Ni-based alloys using vegetable oil. Journal of Cleaner Production, 2017, 154: 1–11
105. Wang J H, Zhuang W P, Liang W F, Yan T T, Li T, Zhang L X, Li S. Inorganic nanomaterial lubricant additives for base fluids, to improve tribological performance: recent developments. Friction, 2022, 10(5): 645–676
106. Li M, Yu T B, Zhang R C, Yang L, Ma Z L, Li B C, Wang X Z, Wang W S, Zhao J. Experimental evaluation of an eco-friendly grinding process combining minimum quantity lubrication and

graphene-enhanced plant-oil-based cutting fluid. Journal of Cleaner Production, 2020, 244: 118747

107. Yang M, Li C H, Zhang Y B, Wang Y G, Li B K, Hou Y L. Experimental research on microscale grinding temperature under different nanoparticle jet minimum quantity cooling. Materials and Manufacturing Processes, 2017, 32(6): 589–597
108. Pavan R B, Venu Gopal A, Amrita M, Goriparthi B K. Experimental investigation of graphene nanoplatelets-based minimum quantity lubrication in grinding Inconel 718. Proceedings of the Institution of Mechanical Engineers, Part B: Journal of Engineering Manufacture, 2019, 233(2): 400–410
109. Singh R K, Sharma A K, Dixit A R, Tiwari A K, Pramanik A, Mandal A. Performance evaluation of alumina-graphene hybrid nano-cutting fluid in hard turning. Journal of Cleaner Production, 2017, 162: 830–845
110. Singh R, Dureja J S, Dogra M, Gupta M K, Mia M, Song Q H. Wear behavior of textured tools under graphene-assisted minimum quantity lubrication system in machining Ti–6Al–4V alloy. Tribology International, 2020, 145: 106183
111. Ramya M, Nideep T K, Nampoori V P N, Kailasnath M. Shape dependent heat transfer and nonlinear optical limiting characteristics of water stable ZnO nanofluid. Surfaces and Interfaces, 2021, 26: 101345
112. Duangthongsuk W, Wongwises S. An experimental study on the heat transfer performance and pressure drop of TiO_2−water nanofluids flowing under a turbulent flow regime. International Journal of Heat and Mass Transfer, 2010, 53(1–3): 334–344
113. Kole M, Dey T K. Role of interfacial layer and clustering on the effective thermal conductivity of CuO−gear oil nanofluids. Experimental Thermal and Fluid Science, 2011, 35(7): 1490–1495
114. Saeedinia M, Akhavan-Behabadi M A, Razi P. Thermal and rheological characteristics of CuO-base oil nanofluid flow inside a circular tube. International Communications in Heat and Mass Transfer, 2012, 39(1): 152–159
115. Wang B G, Wang X B, Lou W J, Hao J C. Thermal conductivity and rheological properties of graphite/oil nanofluids. Colloids and Surfaces A: Physicochemical and Engineering Aspects, 2012, 414: 125–131
116. Simpson S, Schelfhout A, Golden C, Vafaei S. Nanofluid thermal conductivity and effective parameters. Applied Sciences, 2019, 9(1): 87
117. Sharifpur M, Tshimanga N, Meyer J P, Manca O. Experimental investigation and model development for thermal conductivity of α-Al_2O_3−glycerol nanofluids. International Communications in Heat and Mass Transfer, 2017, 85: 12–22
118. Teng T P, Hung Y H, Teng T C, Mo H E, Hsu H G. The effect of alumina/water nanofluid particle size on thermal conductivity. Applied Thermal Engineering, 2010, 30(14–15): 2213–2218
119. Mehta B, Subhedar D, Panchal H, Said Z. Synthesis, stability, thermophysical properties and heat transfer applications of nanofluid—a review. Journal of Molecular Liquids, 2022, 364: 120034
120. Xie H Q, Wang J C, Xi T G, Liu Y, Ai F, Wu Q R. Thermal conductivity enhancement of suspensions containing nanosized alumina particles. Journal of Applied Physics, 2002, 91(7): 4568–4572
121. Wei B J, Zou C J, Li X K. Experimental investigation on stability and thermal conductivity of diathermic oil based TiO_2 nanofluids. International Journal of Heat and Mass Transfer, 2017, 104: 537–543
122. Maheshwary P B, Handa C C, Nemade K R. A comprehensive study of effect of concentration, particle size and particle shape on thermal conductivity of titania/water based nanofluid. Applied Thermal Engineering, 2017, 119: 79–88
123. Afrand M, Toghraie D, Sina N. Experimental study on thermal conductivity of water-based Fe_3O_4 nanofluid: development of a new correlation and modeled by artificial neural network. International Communications in Heat and Mass Transfer, 2016, 75: 262–269
124. Toghraie D, Chaharsoghi V A, Afrand M. Measurement of thermal conductivity of ZnO−TiO_2/EG hybrid nanofluid. Journal of Thermal Analysis and Calorimetry, 2016, 125(1): 527–535
125. Johari M N I, Zakaria I A, Azmi W H, Mohamed W A N W. Green bio glycol Al_2O_3−SiO_2 hybrid nanofluids for PEMFC: the thermal-electrical-hydraulic perspectives. International Communications in Heat and Mass Transfer, 2022, 131: 105870
126. Yang L, Du K. A comprehensive review on heat transfer characteristics of TiO_2 nanofluids. International Journal of Heat and Mass Transfer, 2017, 108: 11–31
127. Pang C W, Jung J Y, Lee J W, Kang Y T. Thermal conductivity measurement of methanol-based nanofluids with Al_2O_3 and SiO_2 nanoparticles. International Journal of Heat and Mass Transfer, 2012, 55(21–22): 5597–5602
128. Xie H Q, Yu W, Chen W. MgO nanofluids: higher thermal conductivity and lower viscosity among ethylene glycol-based nanofluids containing oxide nanoparticles. Journal of Experimental Nanoscience, 2010, 5(5): 463–472
129. Cui X, Li C H, Zhang Y B, Jia D Z, Zhao Y J, Li R Z, Cao H J. Tribological properties under the grinding wheel and workpiece interface by using graphene nanofluid lubricant. The International Journal of Advanced Manufacturing Technology, 2019, 104(9–12): 3943–3958
130. Zhang Y B, Li C H, Jia D Z, Zhang D K, Zhang X W. Experimental evaluation of MoS_2 nanoparticles in jet MQL grinding with different types of vegetable oil as base oil. Journal of Cleaner Production, 2015, 87: 930–940
131. Lee K, Hwang Y, Cheong S, Choi Y, Kwon L, Lee J, Kim S H. Understanding the role of nanoparticles in nano-oil lubrication. Tribology Letters, 2009, 35(2): 127–131
132. Zhang Y B, Li C H, Jia D Z, Li B K, Wang Y G, Yang M, Hou Y L, Zhang X W. Experimental study on the effect of nanoparticle concentration on the lubricating property of nanofluids for MQL grinding of Ni-based alloy. Journal of Materials Processing Technology, 2016, 232: 100–115
133. Asadi A, Aberoumand S, Moradikazerouni A, Pourfattah F, Żyła G, Estellé P, Mahian O, Wongwises S, Nguyen H M, Arabkoohsar A. Recent advances in preparation methods and thermophysical properties of oil-based nanofluids: a state-of-the-art review. Powder Technology, 2019, 352: 209–226
134. Saeedi A H, Akbari M, Toghraie D. An experimental study on rheological behavior of a nanofluid containing oxide nanoparticle

and proposing a new correlation. Physica E: Low-dimensional Systems and Nanostructures, 2018, 99: 285–293

135. Krishnakumar T S, Viswanath S P, Varghese S M, Jose Prakash M. Experimental studies on thermal and rheological properties of Al_2O_3−ethylene glycol nanofluid. International Journal of Refrigeration, 2018, 89: 122–130
136. Duangthongsuk W, Wongwises S. Measurement of temperature-dependent thermal conductivity and viscosity of TiO_2−water nanofluids. Experimental Thermal and Fluid Science, 2009, 33(4): 706–714
137. Huminic G, Huminic A. Hybrid nanofluids for heat transfer applications—a state-of-the-art review. International Journal of Heat and Mass Transfer, 2018, 125: 82–103
138. Şirin Ş, Kıvak T. Performances of different eco-friendly nanofluid lubricants in the milling of Inconel X-750 superalloy. Tribology International, 2019, 137: 180–192
139. Soltani O, Akbari M. Effects of temperature and particles concentration on the dynamic viscosity of MgO–MWCNT/ethylene glycol hybrid nanofluid: experimental study. Physica E: Low-dimensional Systems and Nanostructures, 2016, 84: 564–570
140. Asadi A, Asadi M, Rezaei M, Siahmargoi M, Asadi F. The effect of temperature and solid concentration on dynamic viscosity of MWCNT/MgO (20−80)−SAE50 hybrid nano-lubricant and proposing a new correlation: an experimental study. International Communications in Heat and Mass Transfer, 2016, 78: 48–53
141. Elias M M, Mahbubul I M, Saidur R, Sohel M R, Shahrul I M, Khaleduzzaman S S, Sadeghipour S. Experimental investigation on the thermo-physical properties of Al_2O_3 nanoparticles suspended in car radiator coolant. International Communications in Heat and Mass Transfer, 2014, 54: 48–53
142. Hu X C, Yin D S, Chen X, Xiang G J. Experimental investigation and mechanism analysis: effect of nanoparticle size on viscosity of nanofluids. Journal of Molecular Liquids, 2020, 314: 113604
143. Minakov A V, Rudyak V Y, Pryazhnikov M I. Systematic experimental study of the viscosity of nanofluids. Heat Transfer Engineering, 2021, 42(12): 1024–1040
144. Khan A I, Valan Arasu A. A review of influence of nanoparticle synthesis and geometrical parameters on thermophysical properties and stability of nanofluids. Thermal Science and Engineering Progress, 2019, 11: 334–364
145. Nithiyanantham U, Zaki A, Grosu Y, González-Fernández L, Anagnostopoulos A, Navarro M E, Ding Y, Igartua J M, Faik A. Effect of silica nanoparticle size on the stability and thermophysical properties of molten salts based nanofluids for thermal energy storage applications at concentrated solar power plants. Journal of Energy Storage, 2022, 51: 104276
146. Ajeeb W, Thieleke da Silva R R S, Murshed S M S. Experimental investigation of heat transfer performance of Al_2O_3 nanofluids in a compact plate heat exchanger. Applied Thermal Engineering, 2023, 218: 119321
147. Abdelhalim M A K, Mady M M, Ghannam M M. Rheological and dielectric properties of different gold nanoparticle sizes. Lipids in Health and Disease, 2011, 10(1): 208
148. Rudyak V Y, Minakov A V, Pryazhnikov M I. Preparation, characterization, and viscosity studding the single-walled carbon nanotube nanofluids. Journal of Molecular Liquids, 2021, 329: 115517
149. Heidarshenas A, Azizi Z, Peyghambarzadeh S M, Sayyahi S. Experimental investigation of the particle size effect on heat transfer coefficient of Al_2O_3 nanofluid in a cylindrical microchannel heat sink. Journal of Thermal Analysis and Calorimetry, 2020, 141(2): 957–967
150. Meriläinen A, Seppälä A, Saari K, Seitsonen J, Ruokolainen J, Puisto S, Rostedt N, Ala-Nissila T. Influence of particle size and shape on turbulent heat transfer characteristics and pressure losses in water-based nanofluids. International Journal of Heat and Mass Transfer, 2013, 61: 439–448
151. Li X K, Zou C J, Qi A H. Experimental study on the thermo-physical properties of car engine coolant (water/ethylene glycol mixture type) based SiC nanofluids. International Communications in Heat and Mass Transfer, 2016, 77: 159–164
152. Timofeeva E V, Routbort J L, Singh D. Particle shape effects on thermophysical properties of alumina nanofluids. Journal of Applied Physics, 2009, 106(1): 014304
153. Bhattad A, Sarkar J. Effects of nanoparticle shape and size on the thermohydraulic performance of plate evaporator using hybrid nanofluids. Journal of Thermal Analysis and Calorimetry, 2021, 143(1): 767–779
154. Ferrouillat S, Bontemps A, Poncelet O, Soriano O, Gruss J A. Influence of nanoparticle shape factor on convective heat transfer and energetic performance of water-based SiO_2 and ZnO nanofluids. Applied Thermal Engineering, 2013, 51(1–2): 839–851
155. Bertolini R, Ghiotti A, Bruschi S. Graphene nanoplatelets as additives to MQL for improving tool life in machining Inconel 718 alloy. Wear, 2021, 476: 203656
156. Golubovic M N, Hettiarachchi H D M, Worek W M, Minkowycz W J. Nanofluids and critical heat flux, experimental and analytical study. Applied Thermal Engineering, 2009, 29(7): 1281–1288
157. Zhang Y B, Li C H, Yang M, Jia D Z, Wang Y G, Li B K, Hou Y L, Zhang N Q, Wu Q D. Experimental evaluation of cooling performance by friction coefficient and specific friction energy in nanofluid minimum quantity lubrication grinding with different types of vegetable oil. Journal of Cleaner Production, 2016, 139: 685–705
158. Jia D Z, Zhang Y B, Li C H, Yang M, Gao T, Said Z, Sharma S. Lubrication-enhanced mechanisms of titanium alloy grinding using lecithin biolubricant. Tribology International, 2022, 169: 107461
159. Zhang Y B, Li C H, Jia D Z, Zhang D K, Zhang X W. Experimental evaluation of the lubrication performance of MoS_2/CNT nanofluid for minimal quantity lubrication in Ni-based alloy grinding. International Journal of Machine Tools and Manufacture, 2015, 99: 19–33
160. Dang J Q, An Q L, Lian G H, Zuo Z Y, Li Y G, Wang H W, Chen M. Surface modification and its effect on the tensile and fatigue properties of 300M steel subjected to ultrasonic surface rolling process. Surface and Coatings Technology, 2021, 422: 127566
161. Dang J Q, Zhang H, An Q L, Lian G H, Li Y G, Wang H W,

Chen M. Surface integrity and wear behavior of 300M steel subjected to ultrasonic surface rolling process. Surface and Coatings Technology, 2021, 421: 127380

162. Dang J Q, Wang C G, Wang H H, An Q L, Wei J, Gao B, Li Z M, Chen M. Deformation behavior and microstructure evolution of 300M ultrahigh strength steel subjected to high strain rate: an analytical approach. Journal of Materials Research and Technology, 2023, 25: 812–831
163. Dang J Q, Zhang H, An Q L, Ming W W, Chen M. On the microstructural evolution pattern of 300M steel subjected to surface cryogenic grinding treatment. Journal of Manufacturing Processes, 2021, 68: 169–185
164. Dang J Q, Zhang H, An Q L, Ming W W, Chen M. Surface modification of ultrahigh strength 300M steel under supercritical carbon dioxide ($scCO_2$)-assisted grinding process. Journal of Manufacturing Processes, 2021, 61: 1–14
165. Dang J Q, Zang H, An Q L, Ming W W, Chen M. Feasibility study of creep feed grinding of 300M steel with zirconium corundum wheel. Chinese Journal of Aeronautics, 2022, 35(3): 565–578
166. Wang D X, Zhang Y, Zhao Q L, Jiang J L, Liu G L, Li C H. Tribological mechanism of graphene and ionic liquid mixed fluid on grinding interface under nanofluid minimum quantity lubrication. Chinese Journal of Mechanical Engineering, 2023, 36(1): 78
167. Wang D X, Zhang Y, Zhao Q L, Jiang J L, Liu G L, Li C H. Tribological mechanism of carbon group nanofluids on grinding interface under minimum quantity lubrication based on molecular dynamic simulation. Frontiers of Mechanical Engineering, 2023, 18(1): 17
168. Ross N S, Srinivasan N, Amutha P, Gupta M K, Korkmaz M E. Thermo-physical, tribological and machining characteristics of Hastelloy C276 under sustainable cooling/lubrication conditions. Journal of Manufacturing Processes, 2022, 80: 397–413
169. Sikdar S, Rahman M H, Menezes P L. Synergistic study of solid lubricant nano-additives incorporated in canola oil for enhancing energy efficiency and sustainability. Sustainability, 2022, 14(1): 290
170. Sayuti M, Erh O M, Sarhan A A D, Hamdi M. Investigation on the morphology of the machined surface in end milling of aerospace AL6061-T6 for novel uses of SiO_2 nanolubrication system. Journal of Cleaner Production, 2014, 66: 655–663
171. Sayuti M, Sarhan A A D, Tanaka T, Hamdi M, Saito Y. Cutting force reduction and surface quality improvement in machining of aerospace duralumin AL-2017-T4 using carbon onion nanolubrication system. The International Journal of Advanced Manufacturing Technology, 2013, 65(9–12): 1493–1500
172. Yang Y Y, Yang M, Li C H, Li R Z, Said Z, Ali H M, Sharma S. Machinability of ultrasonic vibration-assisted micro-grinding in biological bone using nanolubricant. Frontiers of Mechanical Engineering, 2023, 18(1): 1
173. Ouyang T C, Tang W T, Pan M M, Tang J, Huang H Z. Friction-reducing and anti-wear properties of 3D hierarchical porous graphene/multi-walled carbon nanotube in castor oil under severe condition: experimental investigation and mechanism study. Wear, 2022, 498–499: 204302
174. Samuel J, Rafiee J, Dhiman P, Yu Z Z, Koratkar N. Graphene colloidal suspensions as high performance semi-synthetic metal-working fluids. The Journal of Physical Chemistry C, 2011, 115(8): 3410–3415
175. Gulzar M, Masjuki H H, Kalam M A, Varman M, Zulkifli N W M, Mufti R A, Zahid R. Tribological performance of nanoparticles as lubricating oil additives. Journal of Nanoparticle Research, 2016, 18(8): 223
176. Ali M K A, Hou X J, Mai L Q, Cai Q P, Turkson R F, Chen B C. Improving the tribological characteristics of piston ring assembly in automotive engines using Al_2O_3 and TiO_2 nanomaterials as nano-lubricant additives. Tribology International, 2016, 103: 540–554
177. Peña-Parás L, Rodríguez-Villalobos M, Maldonado-Cortés D, Guajardo M, Rico-Medina C S, Elizondo G, Quintanilla D I. Study of hybrid nanofluids of TiO_2 and montmorillonite clay nanoparticles for milling of AISI 4340 steel. Wear, 2021, 477: 203805
178. Talib N, Nasir R M, Rahim E A. Tribological behaviour of modified jatropha oil by mixing hexagonal boron nitride nanoparticles as a bio-based lubricant for machining processes. Journal of Cleaner Production, 2017, 147: 360–378
179. Alves S M, Barros B S, Trajano M F, Ribeiro K S B, Moura E. Tribological behavior of vegetable oil-based lubricants with nanoparticles of oxides in boundary lubrication conditions. Tribology International, 2013, 65: 28–36
180. Kumar G, Garg H C, Gijawara A. Experimental investigation of tribological effect on vegetable oil with CuO nanoparticles and ZDDP additives. Industrial Lubrication and Tribology, 2019, 71(3): 499–508
181. Azman S S N, Zulkifli N W M, Masjuki H, Gulzar M, Zahid R. Study of tribological properties of lubricating oil blend added with graphene nanoplatelets. Journal of Materials Research, 2016, 31(13): 1932–1938
182. Ramanan K V, Ramesh Babu S, Jebaraj M, Nimel Sworna Ross K. Face turning of incoloy 800 under MQL and nano-MQL environments. Materials and Manufacturing Processes, 2021, 36(15): 1769–1780
183. Wu X F, Xu W H, Ma H, Zhou Z M, Liu B, Cui X, Li C H. Mechanism of electrostatic atomization and surface quality evaluation of 7075 aluminum alloy under electrostatic minimum quantity lubrication milling. Surface Technology, 2023, 52(6): 337–350
184. Rahman S S, Ashraf M Z I, Amin A N, Bashar M S, Ashik M F K, Kamruzzaman M. Tuning nanofluids for improved lubrication performance in turning biomedical grade titanium alloy. Journal of Cleaner Production, 2019, 206: 180–196
185. Nabil M F, Azmi W H, Abdul Hamid K K, Mamat R, Hagos F Y. An experimental study on the thermal conductivity and dynamic viscosity of TiO_2–SiO_2 nanofluids in water: ethylene glycol mixture. International Communications in Heat and Mass Transfer, 2017, 86: 181–189
186. Kalita P, Malshe A P, Arun Kumar S, Yoganath V G, Gurumurthy T. Study of specific energy and friction coefficient in minimum quantity lubrication grinding using oil-based nanolubricants. Journal of Manufacturing Processes, 2012, 14(2):

160–166

187. Ulutan D, Ozel T. Machining induced surface integrity in titanium and nickel alloys: a review. International Journal of Machine Tools and Manufacture, 2011, 51(3): 250–280
188. Hu D Y, Wang X Y, Mao J X, Wang R Q. Creep-fatigue crack growth behavior in GH4169 superalloy. Frontiers of Mechanical Engineering, 2019, 14(3): 369–376
189. Gao T, Zhang Y B, Li C H, Wang Y Q, An Q L, Liu B, Said Z, Sharma S. Grindability of carbon fiber reinforced polymer using CNT biological lubricant. Scientific Reports, 2021, 11(1): 22535
190. Duan Z J, Li C H, Ding W F, Zhang Y B, Yang M, Gao T, Cao H J, Xu X F, Wang D Z, Mao C, Li H N, Kumar G M, Said Z, Debnath S, Jamil M, Ali H M. Milling force model for aviation aluminum alloy: academic insight and perspective analysis. Chinese Journal of Mechanical Engineering, 2021, 34(1): 18
191. Yang Y Y, Gong Y D, Li C H, Wen X L, Sun J Y. Mechanical performance of 316 L stainless steel by hybrid directed energy deposition and thermal milling process. Journal of Materials Processing Technology, 2021, 291: 117023
192. Jamil M, Khan A M, Hegab H, Gong L, Mia M, Gupta M K, He N. Effects of hybrid Al_2O_3–CNT nanofluids and cryogenic cooling on machining of Ti–6Al–4V. The International Journal of Advanced Manufacturing Technology, 2019, 102(9–12): 3895–3909
193. Hosokawa A, Kosugi K, Ueda T. Turning characteristics of titanium alloy Ti–6Al–4V with high-pressure cutting fluid. CIRP Annals, 2022, 71(1): 81–84
194. Wang X M, Song Y X, Li C H, Zhang Y B, Ali H M, Sharma S, Li R Z, Yang M, Gao T, Liu M Z, Cui X, Said Z, Zhou Z M. Nanofluids application in machining: a comprehensive review. The International Journal of Advanced Manufacturing Technology, 2023 (in press)
195. Artozoul J, Lescalier C, Dudzinski D. Experimental and analytical combined thermal approach for local tribological understanding in metal cutting. Applied Thermal Engineering, 2015, 89: 394–404
196. Wu S J, Chen F Y, Wang D Z, Wang G Q, Li C H, Lu J Z. Machining mechanism and stress model in cutting Ti6Al4V. The International Journal of Advanced Manufacturing Technology, 2023 (in press)
197. Sharma A K, Katiyar J K, Bhaumik S, Roy S. Influence of alumina/MWCNT hybrid nanoparticle additives on tribological properties of lubricants in turning operations. Friction, 2019, 7(2): 153–168
198. Schultheiss F, Fallqvist M, M'Saoubi R, Olsson M, Ståhl J E. Influence of the tool surface micro topography on the tribological characteristics in metal cutting—Part II theoretical calculations of contact conditions. Wear, 2013, 298–299: 23–31
199. Yi S, Li N, Solanki S, Mo J, Ding S L. Effects of graphene oxide nanofluids on cutting temperature and force in machining Ti–6Al–4V. The International Journal of Advanced Manufacturing Technology, 2019, 103(1–4): 1481–1495
200. Singh R, Dureja J S, Dogra M, Gupta M K, Mia M. Influence of graphene-enriched nanofluids and textured tool on machining behavior of Ti–6Al–4V alloy. The International Journal of Advanced Manufacturing Technology, 2019, 105(1–4): 1685–1697
201. Gupta M K, Mia M, Pruncu C I, Khan A M, Azizur Rahman M, Jamil M, Sharma V S. Modeling and performance evaluation of Al_2O_3, MoS_2 and graphite nanoparticle-assisted MQL in turning titanium alloy: an intelligent approach. Journal of the Brazilian Society of Mechanical Sciences and Engineering, 2020, 42(4): 207
202. Gupta M K, Song Q H, Liu Z Q, Sarikaya M, Jamil M, Mia M, Khanna N, Krolczyk G M. Experimental characterisation of the performance of hybrid cryo-lubrication assisted turning of Ti–6Al–4V alloy. Tribology International, 2021, 153: 106582
203. Moura R R, da Silva M B, Machado Á R, Sales W F. The effect of application of cutting fluid with solid lubricant in suspension during cutting of Ti–6Al–4V alloy. Wear, 2015, 332–333: 762–771
204. Nguyen D, Lee P H, Guo Y, Park K H, Kwon P. Wear performance evaluation of minimum quantity lubrication with exfoliated graphite nanoplatelets in turning titanium alloy. Journal of Manufacturing Science and Engineering, 2019, 141(8): 081006
205. Sartori S, Ghiotti A, Bruschi S. Solid lubricant-assisted minimum quantity lubrication and cooling strategies to improve Ti6Al4V machinability in finishing turning. Tribology International, 2018, 118: 287–294
206. Hegab H, Umer U, Deiab I, Kishawy H. Performance evaluation of Ti–6Al–4V machining using nano-cutting fluids under minimum quantity lubrication. The International Journal of Advanced Manufacturing Technology, 2018, 95(9–12): 4229–4241
207. Revuru R S, Zhang J Z, Posinasetti N R, Kidd T. Optimization of titanium alloys turning operation in varied cutting fluid conditions with multiple machining performance characteristics. The International Journal of Advanced Manufacturing Technology, 2018, 95(1–4): 1451–1463
208. Sahu N K, Andhare A B, Raju R A. Evaluation of performance of nanofluid using multiwalled carbon nanotubes for machining of Ti–6Al–4V. Machining Science and Technology, 2018, 22(3): 476–492
209. Khan A M, Hussain G, Alkahtani M, Alzabidi A, Abidi M H, He N. Holistic sustainability assessment of hybrid Al–GNP-enriched nanofluids and textured tool in machining of Ti–6Al–4V alloy. The International Journal of Advanced Manufacturing Technology, 2021, 112(3–4): 731–743
210. Gaurav G, Sharma A, Dangayach G S, Meena M L. Assessment of jojoba as a pure and nano-fluid base oil in minimum quantity lubrication (MQL) hard-turning of Ti–6Al–4V: a step towards sustainable machining. Journal of Cleaner Production, 2020, 272: 122553
211. Wang B, Liu Z Q, Cai Y K, Luo X C, Ma H F, Song Q H, Xiong Z H. Advancements in material removal mechanism and surface integrity of high speed metal cutting: a review. International Journal of Machine Tools and Manufacture, 2021, 166: 103744
212. Jamil M, He N, Zhao W, Khan A M, Laghari R A. Tribology and machinability performance of hybrid Al_2O_3–MWCNTs nanofluids-assisted MQL for milling Ti–6Al–4V. The International Journal of Advanced Manufacturing Technology, 2022, 119(3–4): 2127–2144

213. Kulkarni H B, Nadakatti M M, Kulkarni S C, Kulkarni R M. Investigations on effect of nanofluid based minimum quantity lubrication technique for surface milling of Al7075-T6 aerospace alloy. Materials Today: Proceedings, 2020, 27: 251–256
214. Dong L, Li C H, Bai X F, Zhai M G, Qi Q, Yin Q A, Lv X J, Li L F. Analysis of the cooling performance of Ti–6Al–4V in minimum quantity lubricant milling with different nanoparticles. The International Journal of Advanced Manufacturing Technology, 2019, 103(5–8): 2197–2206
215. Zhou C C, Guo X H, Zhang K D, Cheng L, Wu Y Q. The coupling effect of micro-groove textures and nanofluids on cutting performance of uncoated cemented carbide tools in milling Ti–6Al–4V. Journal of Materials Processing Technology, 2019, 271: 36–45
216. Roushan A, Rao U S, Patra K, Sahoo P. Performance evaluation of tool coatings and nanofluid MQL on the micro-machinability of Ti–6Al–4V. Journal of Manufacturing Processes, 2022, 73: 595–610
217. Kim J S, Kim J W, Lee S W. Experimental characterization on micro-end milling of titanium alloy using nanofluid minimum quantity lubrication with chilly gas. The International Journal of Advanced Manufacturing Technology, 2017, 91(5–8): 2741–2749
218. Li M, Yu T B, Yang L, Li H Y, Zhang R C, Wang W S. Parameter optimization during minimum quantity lubrication milling of TC4 alloy with graphene-dispersed vegetable-oil-based cutting fluid. Journal of Cleaner Production, 2019, 209: 1508–1522
219. Roushan A, Rao U S, Sahoo P, Patra K. Performance study of uncoated and AlTiN-coated tungsten carbide tools in micromilling of Ti6Al4V using nano-MQL. Journal of the Brazilian Society of Mechanical Sciences and Engineering, 2023, 45(1): 63
220. Edelbi A, Kumar R, Sahoo A K, Pandey A. Comparative machining performance investigation of dual-nozzle MQL-assisted ZnO and Al_2O_3 nanofluids in face milling of Ti−3Al−2.5V alloys. Arabian Journal for Science and Engineering, 2023, 48(3): 2969–2993
221. Yin Q A, Li C H, Dong L, Bai X F, Zhang Y B, Yang M, Jia D Z, Hou Y L, Liu Y H, Li R Z. Effects of the physicochemical properties of different nanoparticles on lubrication performance and experimental evaluation in the NMQL milling of Ti–6Al–4V. The International Journal of Advanced Manufacturing Technology, 2018, 99(9–12): 3091–3109
222. Liu M Z. Li C H, Zhang Y B, Yang M, Gao T, Cui X, Wang X M, Xu W H, Zhou Z M, Liu B, Said Z, Li R Z, Sharma S. Analysis of grinding mechanics and improved grinding force model based on randomized grain geometric characteristics. Chinese Journal of Aeronautics, 2023, 36(7): 160–193
223. Yang M, Li C H, Zhang Y B, Jia D Z, Li R Z, Hou Y L, Cao H J, Wang J. Predictive model for minimum chip thickness and size effect in single diamond grain grinding of zirconia ceramics under different lubricating conditions. Ceramics International, 2019, 45(12): 14908–14920
224. Huang B T, Zhang Y B, Wang X M, Chen Y, Cao H J, Liu B, Nie X L, Li C H. Experimental evaluation of wear mechanism and grinding performance of SG wheel in machining nickel-based alloy GH4169. Surface Technology, 2021, 50(12): 62–70
225. Yang M, Li C H, Luo L, Li R Z, Long Y Z. Predictive model of convective heat transfer coefficient in bone micro-grinding using nanofluid aerosol cooling. International Communications in Heat and Mass Transfer, 2021, 125: 105317
226. Zou L, Li H, Yang Y G, Huang Y. Feasibility study of minimum quantity lubrication assisted belt grinding of titanium alloys. Materials and Manufacturing Processes, 2020, 35(9): 961–968
227. Gao T, Zhang Y B, Li C H, Wang Y Q, Chen Y, An Q L, Zhang S, Li H N, Cao H J, Ali H M, Zhou Z M, Sharma S. Fiber-reinforced composites in milling and grinding: machining bottlenecks and advanced strategies. Frontiers of Mechanical Engineering, 2022, 17(2): 24
228. Zhang J C, Li C H, Zhang Y B, Yang M, Jia D Z, Hou Y L, Li R Z. Temperature field model and experimental verification on cryogenic air nanofluid minimum quantity lubrication grinding. The International Journal of Advanced Manufacturing Technology, 2018, 97(1–4): 209–228
229. Zhang J C, Wu W T, Li C H, Yang M, Zhang Y B, Jia D Z, Hou Y L, Li R Z, Cao H J, Ali H M. Convective heat transfer coefficient model under nanofluid minimum quantity lubrication coupled with cryogenic air grinding Ti–6Al–4V. International Journal of Precision Engineering and Manufacturing-Green Technology, 2021, 8(4): 1113–1135
230. Sinha M K, Ghosh S, Paruchuri V R. Modelling of specific grinding energy for Inconel 718 superalloy. Proceedings of the Institution of Mechanical Engineers, Part B: Journal of Engineering Manufacture, 2019, 233(2): 443–460
231. Ibrahim A M M, Li W, Xiao H, Zeng Z X, Ren Y H, Alsoufi M S. Energy conservation and environmental sustainability during grinding operation of Ti–6Al–4V alloys via eco-friendly oil/graphene nano additive and minimum quantity lubrication. Tribology International, 2020, 150: 106387
232. Holtzman B K, Kendall J M. Organized melt, seismic anisotropy, and plate boundary lubrication. Geochemistry, Geophysics, Geosystems, 2010, 11(12): Q0AB06
233. Setti D, Sinha M K, Ghosh S, Rao P V. Performance evaluation of Ti–6Al–4V grinding using chip formation and coefficient of friction under the influence of nanofluids. International Journal of Machine Tools and Manufacture, 2015, 88: 237–248
234. Jia D Z, Li C H, Zhang Y B, Yang M, Cao H J, Liu B, Zhou Z M. Grinding performance and surface morphology evaluation of titanium alloy using electric traction bio micro lubricant. Journal of Mechanical Engineering, 2022, 58(5): 198–211
235. Bai X F, Li C H, Dong L, Yin Q A. Experimental evaluation of the lubrication performances of different nanofluids for minimum quantity lubrication (MQL) in milling Ti–6Al–4V. The International Journal of Advanced Manufacturing Technology, 2019, 101(9–12): 2621–2632
236. Yuan S, Hou X, Zhu G, Amin M. A novel approach of applying copper nanoparticles in minimum quantity lubrication for milling of Ti–6Al–4V. Advances in Production Engineering & Management, 2017, 12(2): 139–150
237. Duan Z J, Yin Q A, Li C H, Dong L, Bai X F, Zhang Y B, Yang M, Jia D Z, Li R Z, Liu Z Q. Milling force and surface morphology of 45 steel under different Al_2O_3 nanofluid

concentrations. The International Journal of Advanced Manufacturing Technology, 2020, 107(3–4): 1277–1296

238. Şirin Ş, Sarıkaya M, Yıldırım Ç V, Kıvak T. Machinability performance of nickel alloy X-750 with SiAlON ceramic cutting tool under dry, MQL and HBN mixed nanofluid-MQL. Tribology International, 2021, 153: 106673
239. Singh H, Sharma V S, Singh S, Dogra M. Nanofluids assisted environmental friendly lubricating strategies for the surface grinding of titanium alloy: Ti6Al4V-ELI. Journal of Manufacturing Processes, 2019, 39: 241–249